AD706751

*Final Report*

**DASA 2409**

# STEP FREQUENCY RADAR STUDY OF SECEDE III BARIUM RELEASE

D D C
JUN 3 1970
B

*By:* HOWARD F. BATES

*Prepared for:*

DIRECTOR
DEFENSE ATOMIC SUPPORT AGENCY
WASHINGTON, D.C. 20305

CONTRACT DASA01-69-C-0032-P001

STANFORD RESEARCH INSTITUTE

SRI

Reproduced by the
CLEARINGHOUSE
for Federal Scientific & Technical
Information Springfield Va. 22151

*Final Report*

**DASA 2409**

*December 1969*

# STEP FREQUENCY RADAR STUDY OF SECEDE III BARIUM RELEASE

*By:* HOWARD F. BATES

*Prepared for:*

DIRECTOR
DEFENSE ATOMIC SUPPORT AGENCY
WASHINGTON, D.C. 20305

CONTRACT DASA01-69-C-0032-P001

SRI Project 7784

This research has been sponsored by the Defense Atomic Support Agency under NWET Subtask L43 AAX HX 607.

*Approved by:*

DAVID A. JOHNSON, *Director*
*Radio Physics Laboratory*

RAY L. LEADABRAND, *Executive Director*
*Electronics and Radio Sciences*

*Copy No.* 16

## ABSTRACT

Step-frequency radars were installed near Kodiak and Homer, Alaska to view the barium releases made into the lower F region near Fairbanks in March 1969. Echoes were obtained from four of the six releases; good echoes were obtained from two, but quantitative results can only be obtained from one. Backscatter cross sections of $10^4$ $km^2$ were found at early times for two of the releases, whereas photographs indicate cloud sizes were less than $10^2$ $km^2$. The echo amplitudes observed at Homer (line-of-sight 725-km range and $5^\circ$ off-perpendicular from magnetic field at cloud) were 10 to 15 dB less than those at Kodiak (925 km and $3^\circ$). The frequency range covered by the Kodiak echoes was higher than that at Homer. These factors taken together indicate that the echoes were produced by highly aspect-sensitive field-aligned irregularities; the aspect sensitivity is estimated to be about 10 to 20 dB per degree of off-perpendicularity. Strong, persistent echoes observed near 18 MHz at Kodiak and 13 MHz at Homer during the one release for which quantitative data can be computed are interpreted as resulting from exact normality between RF wave and magnetic field; the aspect sensitivity of these echoes was about 20 dB per degree. The backscatter cross section apparently had a maximum near 30 MHz; this is interpreted as showing that the irregularities in the cloud had a dominant transverse size near 5 m. A diffraction argument utilizing the observed aspect sensitivity indicates that the length of the structure before striation was of the order of a kilometer. At the onset of pronounced striations the aspect sensitivity abruptly decreased, indicating that the length of the irregularities decreased, or, alternatively, the angular spectrum of the irregularity distribution increased in width. With the exception of this change, no correspondence between optical and radio effects could be found,

suggesting that the changes observed by the radars were invisible changes within the cloud. All of the results of the various radio experiments suggest that the ion cloud was either (1) an overdense ball of field-aligned irregularities, or (2) a smooth, overdense ball immersed within a field-aligned cloud of weak-scattering irregularities. The second appears the most likely at this point. Further experimental work is needed to clarify this problem.

CONTENTS


ABSTRACT . . . . . i

LIST OF ILLUSTRATIONS. . . . . v

ACKNOWLEDGMENTS. . . . . vii

INTRODUCTION . . . . . 1

II SCATTERING THEORY. . . . . 3

III BARIUM-CLOUD PHOTOGRAPHS . . . . . 7

IV EQUIPMENT. . . . . 11

V DATA REDUCTION . . . . . 15

VI BACKSCATTER FROM THE BARIUM CLOUDS . . . . . 17

VII BACKSCATTER CROSS SECTION. . . . . 25

VIII DISCUSSION . . . . . 41

IX CONCLUSIONS. . . . . 53

REFERENCES . . . . . 57

Appendix A--POWER-VS.-FREQUENCY PLOTS. . . . . A-1

Appendix B--AVERAGE-POWER-VS.-TIME PLOTS . . . . . B-1

DISTRIBUTION LIST. . . . . D-1

DD Form 1473

## ILLUSTRATIONS


Figure 1 Photographs of HEMLOCK made from Fort Yukon TV Monitor Film . 8

Figure 2 Photographs of HEMLOCK made from Fort Yukon TV Monitor Film . 9

Figure 3 Frequency Extent Versus Time of Backscatter Echoes Observed at Homer and Kodiak from HEMLOCK. . . . . 18

Figure 4 Frequency Extent Versus Time of Backscatter Observed at Homer and Kodiak from GUM . . . . . 18

Figure 5 Maximum Received Echo Power--HEMLOCK Release. . . . . 22

Figure 6 Maximum Received Echo Power--GUM Release. . . . . 23

Figure 7 Geometry Used for Raypath Computations. . . . . 28

Figure 8 Computed Frequency Versus Incidence Angle at Cloud. . . . . 29

Figure 9 Vertical-Incidence Ionograms Obtained During GUM and HEMLOCK Releases at College . . . . . 30

Figure 10 Comparison of Experimental Data with Computed Retardation from the Linear and Constant Models of the Lower Ionosphere . 34

## ACKNOWLEDGMENTS

I wish to especially acknowledge the invaluable discussions of George Oetzel and Edward Fremouw pertaining to the results described in this report. Many thanks are also due Donald Neilson and John Lomax for the use of the Kodiak data, and to John Lomax and DASA for the loan of the sounder used at Homer. Donald Alves kept the Homer sounder running and was of inestimable help in making sure everything went smoothly during data runs. Thanks are due Bruce Craig who programmed the computer to read the analog tapes. Many thanks are due Anne Hessing for devising the data-analysis program and making it work.

The research was supported by Defense Atomic Support Agency under Contract DASA-69-C-0032-P001.

## INTRODUCTION

The purpose of this project was to determine the behavior of the backscatter cross section in the HF to low VHF region from barium clouds in the lower F layer. The hope was that these data would provide a basis for understanding the mechanism of radio-wave scatter from barium clouds.

It is believed that the results of this study have indeed led to a better understanding of the scattering processes involved, although in the course of the study as many new questions were raised as were answered. An unfortunate combination of circumstances from the standpoint of our radar experiment led to the result that usable amplitude data were obtained from only one release, making the general applicability of some of the results open to question.

The project involved multifrequency HF radars installed near Homer and Kodiak, Alaska for use during the SECEDE III barium releases made just north of Fairbanks in March 1969. Six barium releases were made, as follows:

| Event | Date (March) | Time (UT) | Height (km) | Barium (kg) |
|---|---|---|---|---|
| JUNIPER | 5 | 0431:50 | 140 | 6 |
| | | 0432:24 | 170 | 2.4 |
| ELM | 6 | 0432:02 | 140 | 12 |
| | | 0432:47 | 170 | 12 |
| IRONWOOD | | 1409:42 | 128 | 12 |
| | | 1410:47 | 186 | 12 |
| FIR | 15 | 0508:15 | 165 | 48 |
| GUM | 19 | 0519:15 | 168 | 48 |
| HEMLOCK | 20 | 0539:10 | 176 | 96 |

All were evening releases except IRONWOOD, which was made into an aurora an hour or so before F-layer sunrise to test the hypotheses that the barium would be ionized by the auroral precipitation. No echoes were obtained from this release, and there is apparently some question as to whether an ion cloud formed.

The FIR release was made into an aurora; an ion cloud formed, but it apparently moved westward very rapidly. No recognizable echoes were obtained from that release.

Echoes were obtained at Homer and Kodiak for the remainder of the releases. The JUNIPER and ELM releases were rather small, however, and the echoes were low in amplitude and frequency range, making them difficult to analyze. The results of these two events will be largely ignored, because it was not possible to get reliable echo-amplitude data from them. This report is therefore confined to a discussion of primarily the HEMLOCK release and to some extent the GUM release.

This report is organized as follows. Section II contains a brief review of the theory of weak scatter. Section III contains a representative sample of photographs of the HEMLOCK release and a discussion of the behavior of barium clouds. The radars are described in Section IV and the data-analysis procedure in Section V. A general discussion of the backscatter results is contained in Section VI. Section VII contains a discussion of the backscatter cross-section and Section VIII discusses the implications of these findings with respect to the formation of the barium ion clouds. The conclusions are summarized in Section IX. Appendices A and B contain the complete set of records reduced by the computer analysis program.

## II SCATTERING THEORY

H. G. Booker [1956] presented an elegant weak-scatter theory based on the Born approximation--i.e., the wave amplitude is not diminished by scatter, or, alternatively, multiple scatter can be ignored. While it can be argued that weak-scatter theory does not apply to the barium ion cloud, particularly at early times, Booker's theory provides considerable insight into the mechanism of backscatter from irregularities in an ionized plasma.

In the case of an irregularly ionized plasma, the irregularities can be considered to exist in the permittivity of the medium. Booker's main result is contained in his Eq. 17, from which we obtain the following relation:

$$\sigma \sim \overline{\left|\frac{\Delta\epsilon}{\epsilon}\right|^2} \; P(\vec{k}_i - \vec{k}_s) \tag{1}$$

where

$\sigma$ = Cross-section for scatter

$\epsilon$ = Permittivity of the medium

P = Power spectrum of the permittivity in the medium

$k = 2\pi\lambda^{-1}$, the propagation vector of the RF waves

i = Incident wave

s = Scattered wave.

The power spectrum of the permittivity is the squared amplitude of the spatial Fourier transform of the fractional change of the permittivity, or,

$$P(k_p) = \frac{1}{\pi} \left| \int_r \frac{\Delta\epsilon(\vec{r})}{\epsilon} \; e^{-i\,\vec{k}_p \cdot \vec{r}} \, \vec{dr} \right|^2 \tag{2}$$

where

$\vec{r}$ = Spatial vector

$k_p$ = "Propagation constant" of the spatial Fourier components of the medium.

Booker showed that the amplitude of the scattered signal was proportional to the amplitude of that component of the Fourier spectrum whose propagation vector is given by

$$\vec{k}_i - \vec{k}_s = \vec{k}_p \quad . \tag{3}$$

If we define the wavelength of the Fourier components in the medium in the same manner as the RF wavelength is defined in Eq. (1) and note that the incident and scattered RF waves have the same wavelength, Eq. (3) reduces to the Bragg scattering law:

$$\lambda_i = 2\lambda_p \text{ Sin } \beta/2 \tag{4}$$

where $\beta$ is the angle between the incident and scattered wave normals.

For the case of backscatter, the angle $\beta$ is $180^\circ$ and Eq. (4) reduces to

$$\lambda_i = 2\lambda_p \quad . \tag{5}$$

Thus, Booker's scattering theory says that the backscattered amplitude on a given frequency is linearly related to the amplitude of that spatial Fourier component of the irregular medium whose wavelength is precisely one-half that of the incident RF wave. This is a very powerful concept because it allows one to visualize the mechanism of scatter. In essence, a radar wave Fourier transforms the medium by picking out a particular wavelength component in the irregularity spectrum.

Since the signal amplitude varies linearly with the spatial Fourier transform of the medium, the inverse Fourier transform (i.e., from the frequency to the spatial domain) of the backscattered signal yields a

measure of the spatial distribution of irregularities; irregularity shapes cannot be deduced because phase information needed in the Fourier transform is missing when only signal amplitude is available.

As noted above, this scattering theory is strictly true only for Born-approximation scatter, but the notion is very useful when considering some types of strong-scatter problems. In the case of scatter from overdense irregularities the concept breaks down because the linear superposition of solutions (i.e., Fourier transformation) no longer yields valid solutions to Maxwell's equations. Superposition is possible for weak scatter because perturbations in the permittivity of the medium can be approximated in terms of linear variations in the electron density. When the plasma frequency approaches the radar frequency, however, this linear relationship does not hold, and Fourier transformation of the irregularities, a linear process, no longer leads to correct solutions of Maxwell's equations.

## III BARIUM-CLOUD PHOTOGRAPHS

A detailed discussion of the formation of the barium ion clouds is beyond the scope of this report. In this section, however, a brief description of the development of the HEMLOCK and GUM ion clouds will be given.

The cloud photographs in Figures 1 and 2 are enlargements of the 16-mm monitor-scope films from the TV system operated by the University of Alaska. The photos shown were taken from Fort Yukon, Alaska; the College TV records could not be used because of clouds. The quality of the film leaves something to be desired for a detailed analysis, but the prints are adequate for our purposes.

The ion cloud from the HEMLOCK release separated from the neutral cloud rather quickly. The ion cloud began to separate within 25 s after the release, and by 45 s (Figure 1), the ion cloud can be seen clearly as a bulge at the lower right-hand corner of the round neutral cloud. The ion cloud developed into a triangular form whose apex was away from the neutral cloud; the photo at 85 s illustrates this behavior. No fine structure is visible yet in the ion cloud; the quality of the individual prints is low, but no structure is evident in the ion cloud when the film is viewed as a motion picture.

As time progressed, the wedge shape of the cloud became more pronounced, and the brightness of the face of the wedge toward the neutral cloud increased with respect to that of the apex. At 155 s the flatness of the side of the ion cloud toward the neutral cloud is clearly evident; this behavior suggests strongly that the side toward the neutral cloud is aligned along the magnetic field.

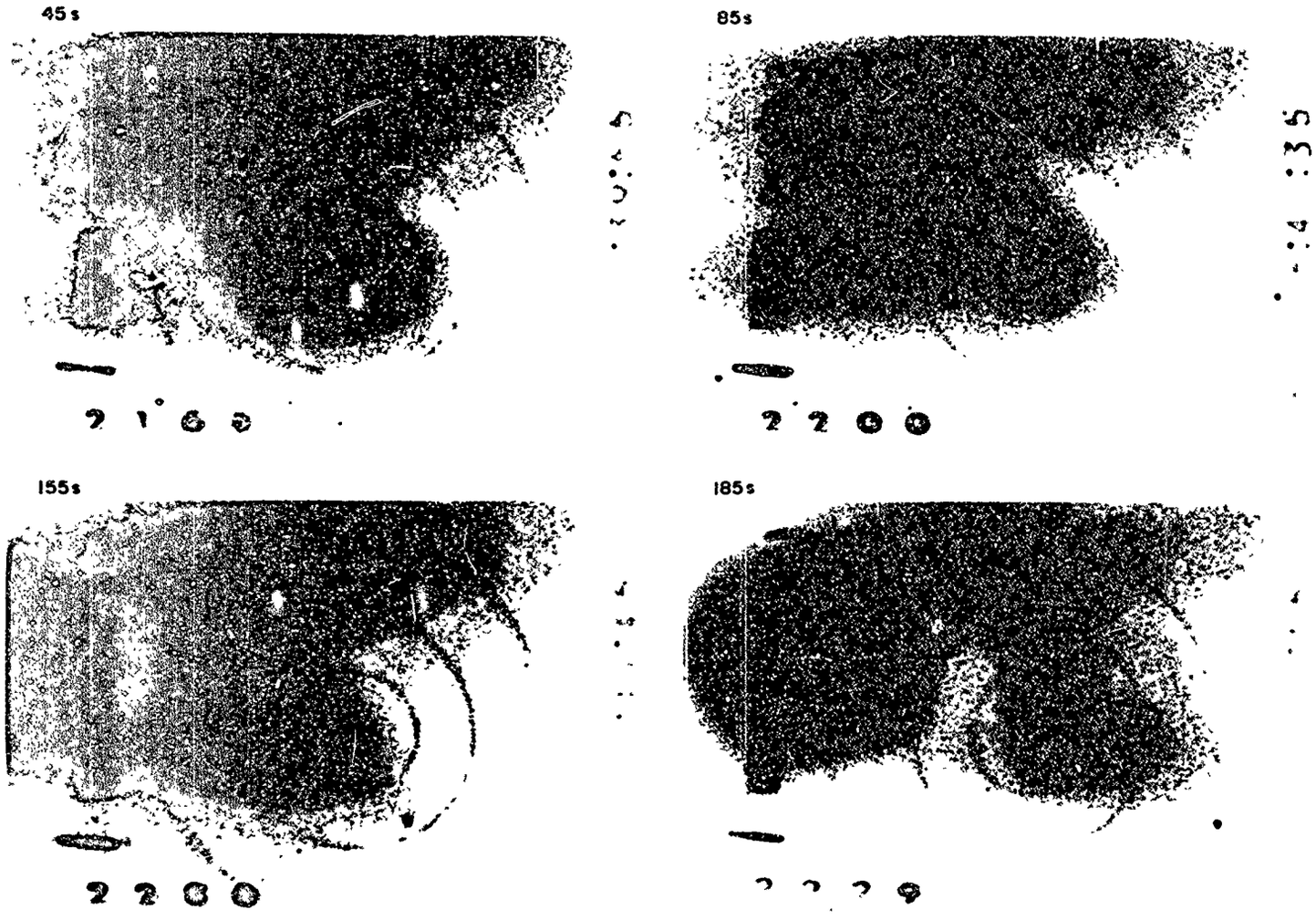


FIGURE 1 PHOTOGRAPHS OF HEMLOCK MADE FROM FORT YUKON TV MONITOR FILM. Time listed is after release. Graticule rings are 1, 3, 6, and 10° in diameter.

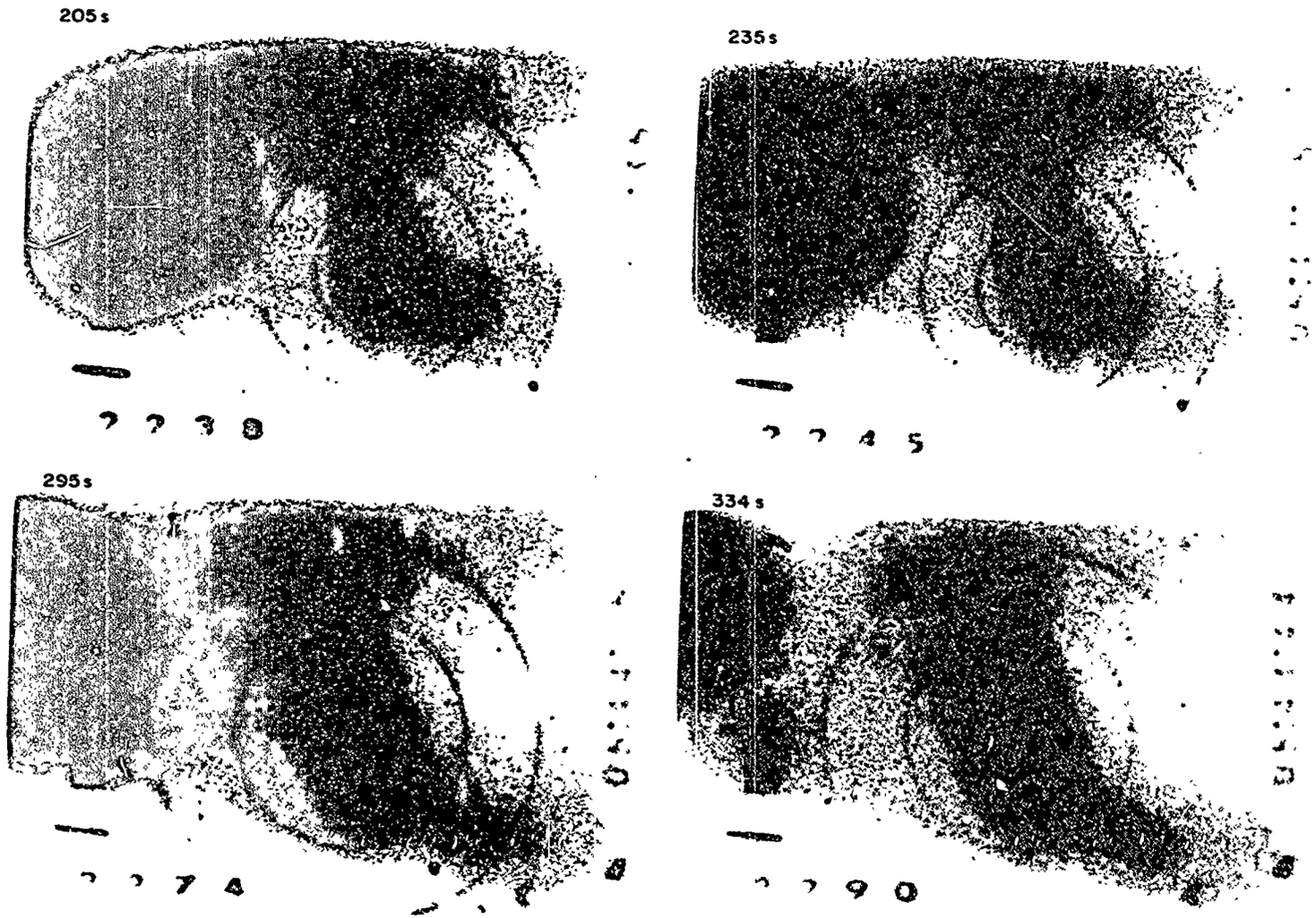


FIGURE 2 PHOTOGRAPHS OF HEMLOCK MADE FROM FORT YUKON TV MONITOR FILM. Time listed is after release. Graticule rings are 1, 3, 6, and 10° in diameter.

There is a hint of fine structure in the cloud after 125 s, and by 175 s fine structure (striae) can be seen. Striation is clearly evident in the 185-s photo in Figure 1.

After the onset of visible striation at approximately 170 s, fine structure in the form of long rays appeared and grew rapidly. An estimate of the size of the striae can be made from the photos; the circles have a diameter of 1, 3, 6, and $10^{\circ}$ respectively. Since the cloud was in the neighborhood of 200 km from Fort Yukon at this time, the diameter of the innermost circle is roughly 3.5 km.

After striation, the TV monitor photos indicate that the cloud tended to lose its triangular shape; slides taken from another vantage point by the University of Alaska show, however, that the cloud remains somewhat wedge-shaped. The remaining photos in Figure 2 show that the cloud structure continues to grow in overall size, but the scale of the fine structure remains small; the individual striae are much less than a kilometer in diameter.

When viewed in a motion picture, the striae are relatively fixed in the cloud over periods of tens of seconds. This suggests that a stria is a column of ionization or a fold viewed edge-on in a thin structure. Photographs viewing the cloud along the magnetic field are needed to resolve this problem. The stationarity of the striae indicates that the striations are probably not the result of a wavelike disturbance, such as a standing wave from a plasma instability within the cloud; it is difficult to see how the striations could remain fixed for tens of seconds if they were the result of waves propagating within the changing cloud.

## IV EQUIPMENT

The radars used at Homer and Kodiak were Granger step-sounders modified to sound on 640 channels between 4 and 64 MHz. Granger 4-to-64-MHz vertical-monopole log-periodic antennas were used. The power output was nominally 30 kW; 200-μs pulses were used at a repetition rate of 75 $s^{-1}$. Backscatter ionograms, taking approximately 8.5 seconds to complete, were begun every 10 seconds on the zero second. Time was set relative to time marks transmitted by WWV in Colorado.

The data were recorded on film and magnetic tape. Two types of film recording were made--ionograms and ampligrams. The ionograms were made by using the detected video to modulate the cathode-ray-tube (CRT) trace intensity as the film was advanced during the sweep. Ampligrams were made by displaying the amplitude of each scan of every fourth frequency channel on a CRT and moving the film in the camera rapidly enough to display each scan separately.

Analog tape recordings were made of each scan of each channel; various additional sounder outputs were recorded so that later computer analysis would be facilitated.

The receiver was calibrated in 10-dB steps at the center frequency of each band before each event. This calibration was put on both film and tape. (It is emphasized that this calibration applies only to the receiver; variations due to the antenna and the transmitter power amplifier were not measured and are unknown.) The video amplifier system had been modified such that the video signal was direct-coupled from the detector to the recording devices; the zero-level was therefore a fixed reference for amplitude measurements. In this experiment the

zero-level of the receiver (including the TR switch) was approximately 1 to 5 μV input voltage at 50 ohms; 0 dB is therefore defined as 1 μV at the antenna terminals.

The Homer and Kodiak sounders were synchronized to obtain bistatic backscatter between the sites. This part of the experiment failed, and the reason is not completely clear. Synchronization of the radars was accomplished by recording the F-layer signals propagating from one radar to the other; these forward-oblique signals were recorded all during the HEMLOCK release, but no bistatic echoes were received from the barium cloud. Subsequent analysis of the Homer and Kodiak records shows that the Homer ionograms contained 640 frequency channels while the Kodiak records apparently had 641. Since the forward-oblique signal was recorded in the 4-to-8-MHz band, the sounders must have lost synchronization somewhere above 8 MHz, probably during a band change. Although we know what must have happened, we have not yet located the precise cause of the trouble nor when it occurred in each sweep.

Because the equipment strongly affects the data, a brief description of the Granger backscatter system is in order. The sounder is essentially composed of four separate units, beginning at 4 MHz, and each covering an octave in frequency. Some elements are common to the system--for example, the distributed power amplifiers in the transmitter--but most are not. Since each of these four units is relatively independent of the rest, each unit must be adjusted separately for a balanced response over the entire frequency range. A number of factors make it impossible to get a constant response or even a constant average response over the frequency range, making it necessary to achieve a compromise response.

Probably the most important such effect is the receiver response near the edge of each octave frequency band. Image-rejection considerations make it necessary to design the receiver response to be 5 dB down at the band edges. Thus, signals near the band edge are discriminated against by the sounder, and this effect is important when considering the records. If the frequency-synthesizing units are not

all adjusted for optimum performance, the overall system sensitivity (including transmitter output) can be additionally affected near the band edges. Unfortunately, we did not have sufficient time before shipment of the vans to Alaska to align these units for optimum operation, so the degradation near the band edges probably exceeded the 5-dB figure for the receiver alone. Another receiver problem of the sounder is that the overall receiver sensitivity changes markedly from band to band; the sensitivity decreases with frequency.

Thus, the disappearance or appearance of a backscatter echo near a band edge (8, 16, or 32 MHz) is probably more an equipmental problem than a characteristic of the scattering medium. This effect is present in the Homer and Kodiak records; for example, in Figure 4 (Section VI) the band edge effects are clearly visible, particularly in the Kodiak data. Such effects will be noted throughout the report wherever equipment effects are important to the results.

An examination of the Kodiak records indicates that the Kodiak sounder did not operate properly in the 8-to-16-MHz band. The ampligrams and ionograms show that the barium cloud echo generally began at the band edge above 16 MHz; the sudden appearance was not entirely a band-edge problem because the echoes just above 16 MHz were frequently 30 dB above the threshold while just below 16 MHz no echoes were recorded.

In an attempt to locate the trouble after the fact, the background records were examined. In some of the records obtained March 18, auroral and ground-scatter echoes extending through the 8-to-16-MHz band show a sudden drop in amplitude at about 10 MHz, and there was a tendency for the echoes to disappear between 14 and 16 MHz and then reappear strongly at 16 MHz. Thus, it appears that the overall system sensitivity decreased markedly from about 12 to 16 MHz. At 10 MHz the decrease appears to exceed 20 dB. The magnitude of this drop cannot be checked now because amplitude records were not taken at Kodiak during the background runs.

## V DATA REDUCTION

One of the major problems in this study was reducing the data to usable and compact form. The technique finally employed was to convert the GUM and HEMLOCK analog magnetic-tape records to digital data. This was done in the following manner.

First, the ionogram films were examined for the GUM and HEMLOCK events to determine the approximate slant range of the barium cloud echo as a function of time. Next, these range data were used to set a 200-km sampling window for the analog-to-digital converter. The analog data in this window were divided into 45 segments and the maximum of the signal in each segment digitized, yielding one digital value approximately every 5 km. Since the transmitted pulse length was 30 km, the wanted signal extended over at least six sampling segments, thereby ensuring that the digital data were dense enough to represent the analog data.

Near the end of each scan of each channel, 15 additional samples spaced 5 km apart were taken; these data, read beyond the range where any backscatter echoes were received, provided a measure of the noise amplitude on each channel. The calibration on the beginning of the first HEMLOCK tape was digitized to obtain the absolute echo amplitude.

The data were plotted, and the precise range to the echo was scaled as a function of time after the release; the maximum signal amplitude was then read in a 20-km window centered on this range. These data were converted to power in decibels (0 dB = 1 $\mu$V at the antenna) and recorded on a second digital tape. The average noise level was also recorded on the new tape. The final plots, shown in Appendix A, were obtained by excluding all signal maxima for average noise levels above approximately 20 dB and requiring that the wanted signal maximum

exceed the average noise of about 3 dB. In the Kodiak plots in Appendix A, all data below 15 dB were discarded. The average signal power in Appendix B (the average was computed in power, not in log power) was computed in 2-MHz segments centered on the frequency shown in each graph as a function of time.

## VI BACKSCATTER FROM THE BARIUM CLOUDS

The purpose of this section is to review briefly the data generated under this study and included in the appendices.

While backscatter was observed at Homer and Kodiak from most of the releases, this report is primarily confined to discussing the results from HEMLOCK. GUM results will be brought in occasionally, but they will not be discussed to a great extent. Although the GUM records have not been analyzed as fully as those from HEMLOCK, nothing in the GUM records has been found to contradict the results derived from the HEMLOCK records. Ionospheric conditions were somewhat different for the two events, and most of the differences between the events are believed to be attributable to ionospheric differences.

Figures 3 and 4 illustrate the frequency range of the backscatter echoes as scaled from the ionograms recorded at Kodiak and Homer. In general the trend is similar at each site, but the values are quite different. The sudden jump in frequency extent corresponded to the appearance of pronounced striation, a rapid occurrence for HEMLOCK.

Both figures show the effect of the drop in sensitivity at the band edges at 16 and 32 MHz. Thus, the beginning of the Kodiak echo at 16 MHz, and the ending of the Homer HEMLOCK echo at 32 MHz, are an artifact of the equipment.

The jumping of the Kodiak GUM echo from 32 to 48 MHz some 700 to 800 seconds after the release is only partly a band-edge problem. The 740-s record in Appendix A shows that a 30-to-40-dB echo appeared suddenly between 40 and 45 MHz and lasted about one-half minute. While the hole between 30 and 40 MHz was partly equipmental, much of it must have been real, indicating that the backscattering cross section varied widely in frequency and time.

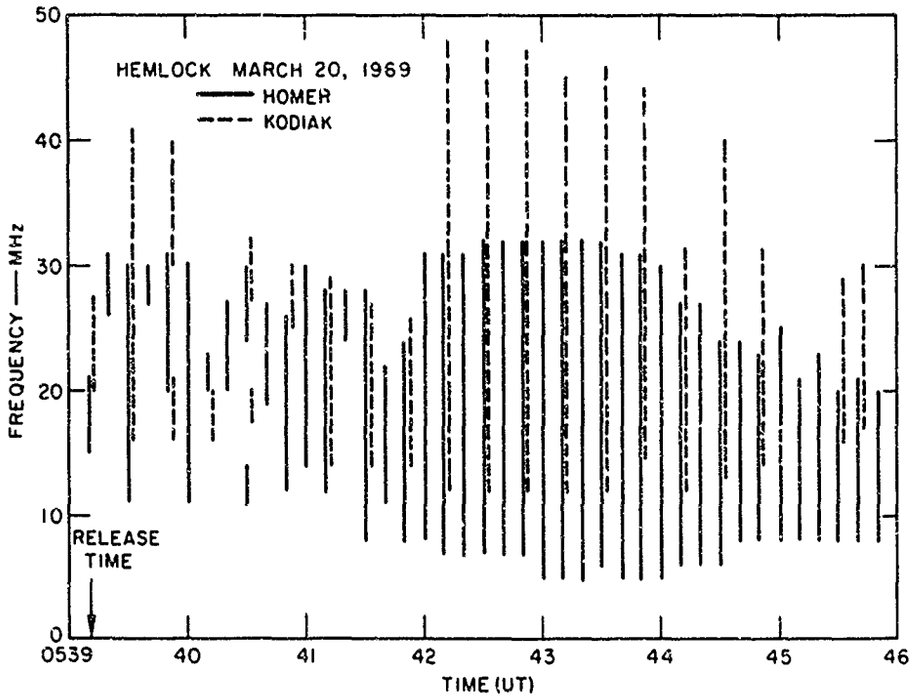


FIGURE 3 FREQUENCY EXTENT VERSUS TIME OF BACKSCATTER ECHOES OBSERVED AT HOMER AND KODIAK FROM HEMLOCK

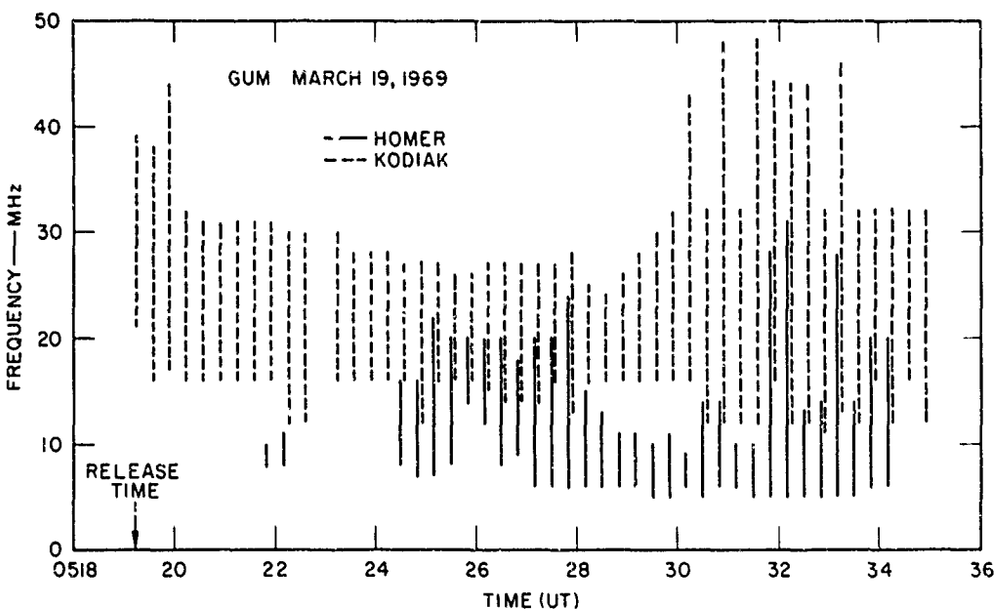


FIGURE 4 FREQUENCY EXTENT VERSUS TIME OF BACKSCATTER OBSERVED AT HOMER AND KODIAK FROM GUM

Appendix A contains the records reduced by computer from approximately zero to seven minutes after the HEMLOCK release, and 8 to 18 minutes after GUM. The power level was found by fitting a quadratic calibration equation to the recorded calibration points. For Homer the curve was fitted to the 20-, 30-, and 40-dB points, and for Kodiak the 20-, 40-, and 50-dB points. The amplitude of the sounder output was nearly logarthmic, so the output was nearly linear in decibels; the quadratic calibration curve was used to correct for the small amount of curvature in the experimental calibration data. Below 20 dB the calibrated amplitude is unreliable.

As shown by the cloud photographs in Appendix B, visible striations in the ion cloud began approximately three minutes after the release. The oblique ionograms taken approximately 180 to 190 seconds after the release show a sudden jump in frequency extent and echo amplitude. Similarly, the GUM echoes show an enhancement at approximately the time optical striations became pronounced. It is therefore concluded that the appearance of pronounced striation is accompanied by a marked increase in the echo frequency extent.

The TV monitor films for both GUM and HEMLOCK were examined in detail for changes corresponding to those observed in the Homer and Kodiak backscatter records, but no correspondences other than that noted above were found. Thus, it appears that the changes observed in the backscatter records were caused primarily by invisible changes in the clouds.

In the following paragraphs the HEMLOCK and GUM backscatter records in Appendices A and B are discussed. The times noted refer to the approximate end time of each sweep relative to the approximate release time of 0519:10 UT; each sweep lasted 8:54 seconds. Thus, the Kodiak 10-s record actually began at the release time and ended 8.5 s afterward.

Before striation the records show a periodic amplitude versus frequency structure; some of this periodic variation may have been produced by interference between the ordinary and extraordinary magneto-

ionic components--i.e., Faraday fading. At this point, however, it is not clear how much of the variation was caused by Faraday fading and how much was caused by a variation in the backscatter cross section. One characteristic of the records is a strong maximum in amplitude near 18 MHz for Kodiak and near 13 MHz for Homer.

The periodic nature of the backscatter amplitude before striation is more pronounced in the Kodiak HEMLOCK records than in the Homer records. One reason is that signal levels were considerably higher at Kodiak than at Homer, despite the increased distance to Kodiak. This periodic variation is also clearly present in the Kodiak GUM records before striation (these records are not shown). The Homer GUM echo is in the interference band and it is hard to determine whether it also shows the periodicity.

At the onset of pronounced striation, the echo amplitude increased greatly at high frequencies. The Kodiak records for HEMLOCK show this behavior clearly. The increase is not so marked in the Homer records.

After striation, the echoes slowly died away. The HEMLOCK and GUM echoes lasted longer than indicated in Appendix A, but the records not shown contain no new behavior and are therefore not included.

One characteristic of the barium-cloud echoes after striation is their rapid decrease in amplitude beyond some frequency. The fact that the Homer and Kodiak echoes did not show the decrease at the same frequency indicates that much of the rapid decrease was caused by aspect sensitivity.

The records for the GUM release beginning 500 s after the release are shown in Appendix A. Before that time a tape recorder problem caused a wide variation in the zero level, and amplitudes could not be obtained by machine-processing the records.

The GUM records included show considerable variation from frequency to frequency and record to record. In particular, at 740 s a strong echo appeared between 40 and 50 MHz and lasted half a minute. The 810-s record illustrates the periodic variation with frequency that is included in many of the records from both events.

Appendix B contains computer plots of the average echo power as a function of time. The data were obtained by averaging the signal power (not log-power) over a 2-MHz band centered on the frequency listed for each plot.

The HEMLOCK plots above 16 MHz for Homer and 20 MHz for Kodiak show a different behavior from those below; those above show a strong increase in echo amplitude after striation, while in those below, the increase is less pronounced.

Finally, Figures 5 and 6 contain the maximum amplitude in each ionogram as a function of time and the associated frequency at which the maximum occurred. For HEMLOCK, the frequency range was split into two parts so as to take into account the different types of echoes in the records.

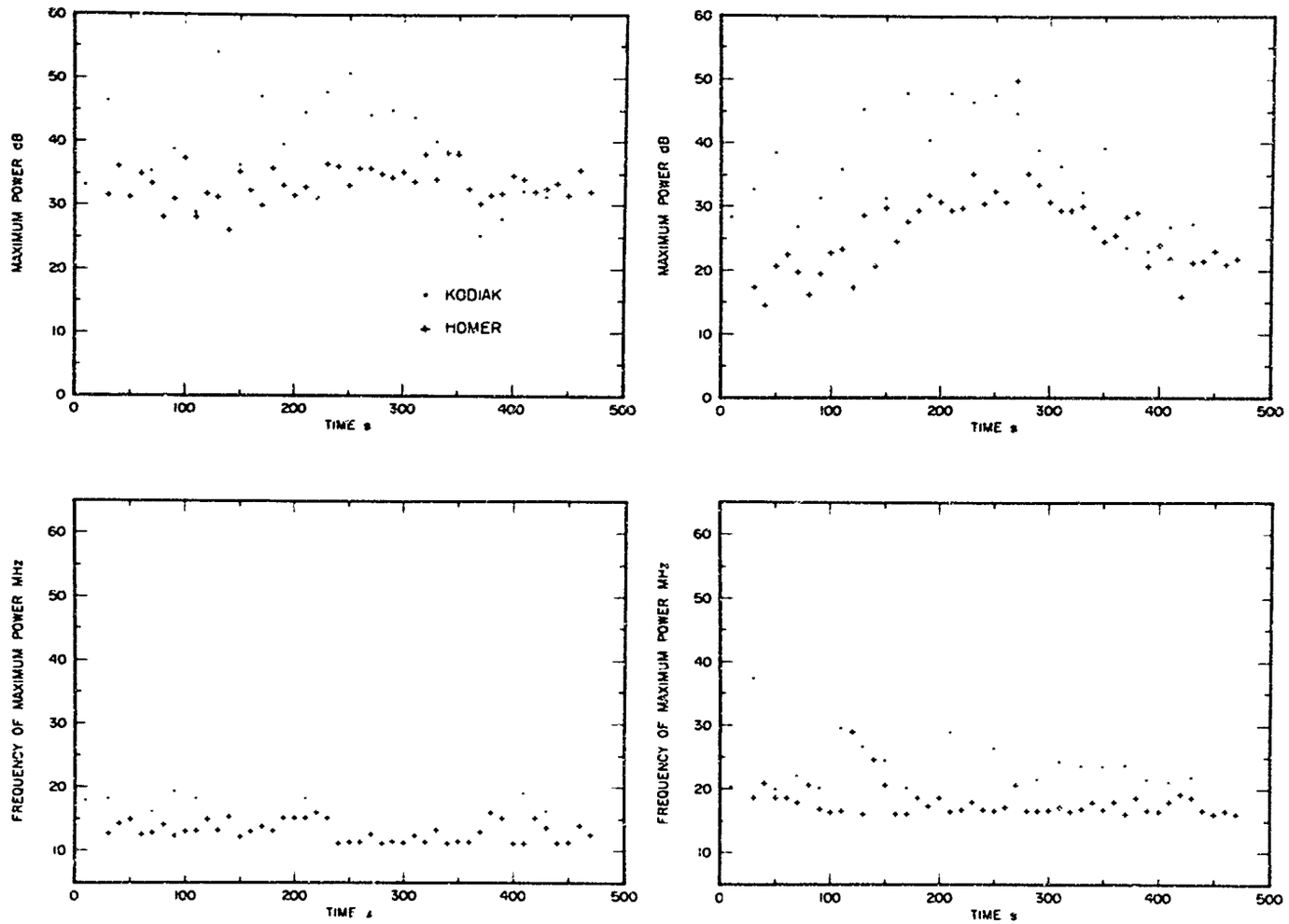


FIGURE 5 MAXIMUM RECEIVED ECHO POWER — HEMLOCK RELEASE. The upper plots show the maximum received echo power, and the lower plots show the frequency of that maximum, versus time for the HEMLOCK release. The left-hand records were obtained from a window located between 10 and 16 MHz for Homer, and 16 and 20 MHz for Kodiak; the window for the right-hand records was all frequencies above 16 for Home and 20 for Kodiak.

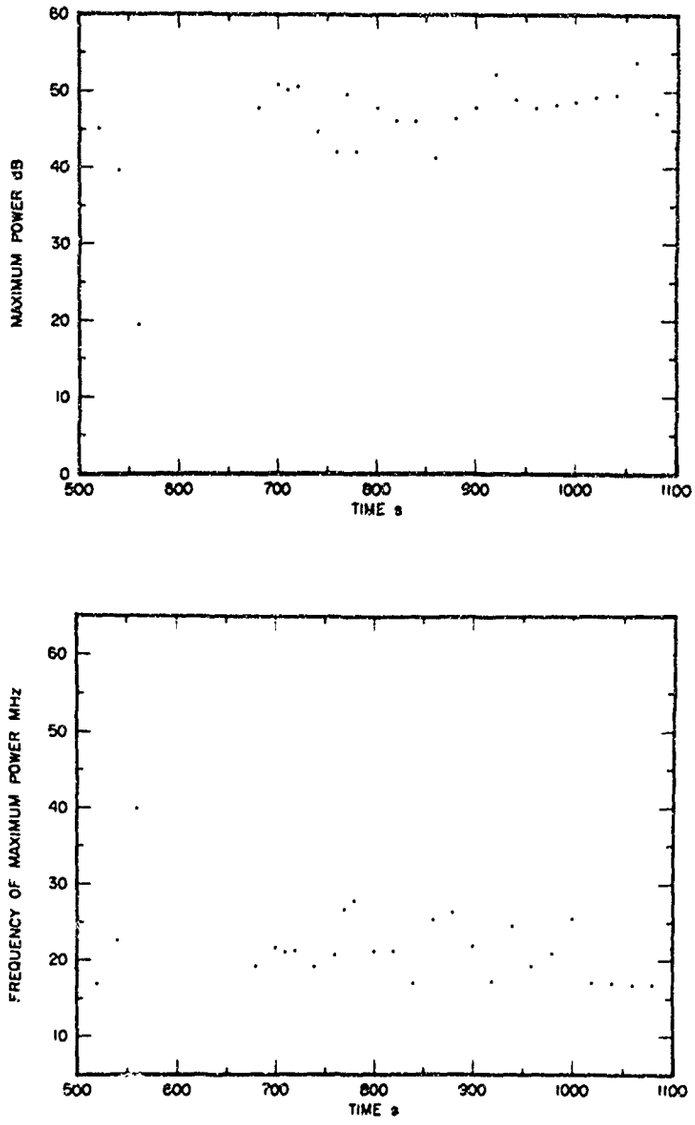


FIGURE 6 MAXIMUM RECEIVED ECHO POWER — GUM RELEASE. The upper plot shows the maximum received echo power above 16 MHz, and the lower the frequency of that maximum, versus time for the Kodiak data obtained from the GUM release.

## VII BACKSCATTER CROSS SECTION

The aim of the project was to determine the HF backscatter cross section of the barium clouds. In this section it will be shown that the backscatter cross section is strongly dependent upon frequency and aspect angle to the magnetic field.

Most of the Homer and Kodiak records, shown in Appendix A, contain a strong echo at about 13 and 18 MHz, respectively, which remains relatively fixed in frequency throughout the event. All other strong echoes come and go or vary in frequency. The behavior of these fixed echoes suggests that they were produced by exact normality between RF wave and magnetic field in the cloud; that this hypothesis appears to be correct is shown in the following pages.

First, however, let us digress and show that some sort of focusing mechanism such as aspect sensitivity is necessary to explain the great backscatter cross sections observed.

The scattering cross section $\sigma$ for isotropic volume scatter from a target is given by the <u>radar equation</u>:

$$\sigma = \frac{P_r}{P_o} \left( \frac{4\pi R^2}{G \lambda} \right)^2 \qquad (6)$$

where

$P_r$ = Received power

$P_o$ = Transmitted power

$R$ = Distance to the scattering volume

$G$ = Gain of the receiving/transmitting antenna

$\lambda$ = Radar wavelength.

A 0-dB signal has been taken in this report to be 1 $\mu$V at the antenna terminals; for the 50-$\Omega$ system the absolute power corresponding to the 0-dB relative power level was $2 \times 10^{-14}$ W. The transmitter power was 30 kW, the antenna gain about 5, and the distance was approximately 725 km for Homer and 925 km for Kodiak. Substituting these values into Eq. (6), we find that the backscatter cross section for a 0-dB echo at 20 MHz was 0.065 $km^2$ for Homer and 0.17 $km^2$ for Kodiak.

The maximum signals recorded at Kodiak and Homer were of the order of 40 to 50 dB, implying backscattering cross sections in excess of $10^3$ $km^2$. Cloud photographs show that the projected cloud area was of the order of 10 to 100 $km^2$, one or two orders of magnitude smaller than the backscatter cross section. Such a discrepancy can only mean that the barium cloud did not scatter isotropically but that scatter was confined to a limited range of solid angle--i.e., the scatter was directive.

The neutral barium cloud at early times appears to be a sphere; if we assume that the ion cloud is a conducting sphere, the scattering cross section equals the projected area, 100 $km^2$. As noted above, this is too small, so the cloud must appear to be more like a plane than a sphere. If we take as an upper limit a representation of the cloud as a plane conductor whose diameter equals one Fresnel zone (roughly 5 km), echoes of the order of 70 dB would be obtained; such a value would yield an effective backscatter cross section of the order of $10^6$ $km^2$, more than enough to explain the observations.

It is therefore concluded that the cloud appears to an HF radar as a field-aligned plane conductor. While this notion might appear to be physically unreasonable, it is, on the contrary, quite reasonable, because a field-aligned cloud of field-aligned irregularities is well approximated by a finite plane with a backscattering coefficient of less than unity. For example, if we use the results computed for the plane above, a cloud of field-aligned irregularities with an area of 10 $km^2$ and a scattering coefficient of 0.001 to 0.01 would yield the 40-to-50-dB echoes observed at Homer and Kodiak. Thus, the observed data are consistent with the notion that the echoes observed at Kodiak

and Homer were highly aspect-sensitive and were produced by field-aligned irregularities associated with the clouds.

Direct backscatter from ionospheric irregularities is quite aspect sensitive in the HF band. Bates and Albee [1969, 1970] reported that the backscattering cross section for E- and F-layer irregularities decreased of the order of 5 dB per degree of off-perpendicularity to the magnetic field.

In the HF band, refraction in the normal ionosphere strongly influences the production of aspect-sensitive echoes. For example, any ray that undergoes reflection is normal to the high-latitude magnetic field somewhere in the ionosphere along the path of the ray. Thus, a study of aspect sensitivity at HF requires that ionospheric refraction be taken into account quantitatively. In general, ray-tracing techniques are required, but a useful method for approximating the effect of refraction is outlined below.

In the technique presented here the ionosphere below the cloud is removed by assuming that the cloud is embedded in the lower edge of a slab whose index of refraction equals that of the ionosphere at the cloud. Snell's law is then solved at the interface, yielding the amount of bending the ray undergoes at any given frequency. This procedure is equivalent to replacing the ionosphere by a thin shell, a technique that has been shown to give good results for HF propagation [Smith 1939, Davies, 1965].

The geometry of the problem is illustrated in Figure 7. Spherical geometry is used, but the use of a thin layer eliminates the necessity of using the spherical form of Snell's Law (Bouger's Rule). Thus,

$$\sin \psi_o = \mu \sin \psi \quad . \tag{7}$$

If we neglect the magnetic field, the phase index of refraction for a propagating radio wave in a plasma is

$$\mu = \left(1 - \frac{f_p^2}{f^2}\right)^{\frac{1}{2}} \tag{8}$$

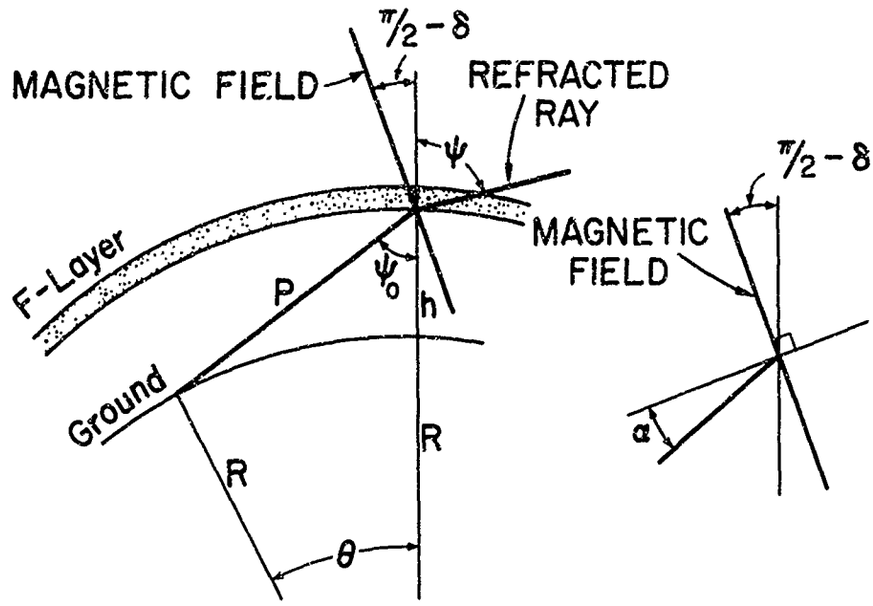


FIGURE 7 GEOMETRY USED FOR RAYPATH COMPUTATIONS

where $f_p$ is the plasma frequency of the refracting medium, and f is the operating radio frequency.

To compute the angle $\alpha$ between the refracted wave and the perpendicular to the magnetic field, we note that

$$\psi = \delta - \alpha \tag{9}$$

where $\delta$ is the dip angle of the magnetic field.

Solving Eqs. (7), (8), and (9) together, we find that

$$\frac{f}{f_p} = \left[ 1 - \frac{R^2 \operatorname{Sin}^2 \theta}{P^2 \operatorname{Sin}^2(\delta - \alpha)} \right]^{-\frac{1}{2}} . \tag{10}$$

Equation (10) provides the frequency that meets the magnetic field at an angle $\alpha$ from normality.

The slant ranges of the barium releases were approximately 725 and 925 km, respectively, from Homer and Kodiak. The release altitude for HEMLOCK was 175 km. When these values are substituted into Eq. (10), the plots in Figure 8 result for two values of the plasma frequency.

The magnetic dip angle of 77.8° at the cloud was obtained from the harmonic expansion for the magnetic field of Cain et al. [1965]; this value should be taken as approximate because the high-latitude field is not known to the accuracy necessary to compute the precise value.

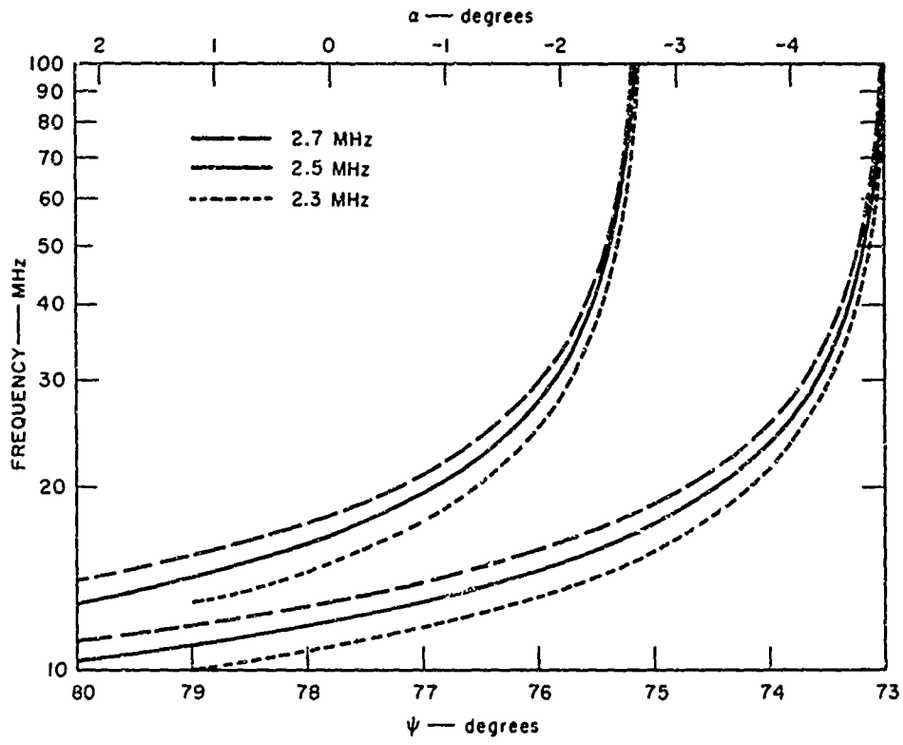


FIGURE 8 COMPUTED FREQUENCY VERSUS INCIDENCE ANGLE AT CLOUD. The off-perpendicular angle is based upon a computed 77.8° dip angle at the release point.

The method outlined above is an approximate one, but its results are probably quite close to those that would be obtained from a more exact analysis. It is believed that the results of this simple model are sufficient for our purposes. Refraction inside the cloud is ignored, and this may be a serious shortcoming of the method.

The plasma frequency at the cloud must be found if a quantitative value for the aspect sensitivity of the echoes is to be deduced. Fortunately, the College ionosonde detected the HEMLOCK release [Oetzel and Chang, 1969], and from these records (Figure 9) we can obtain a

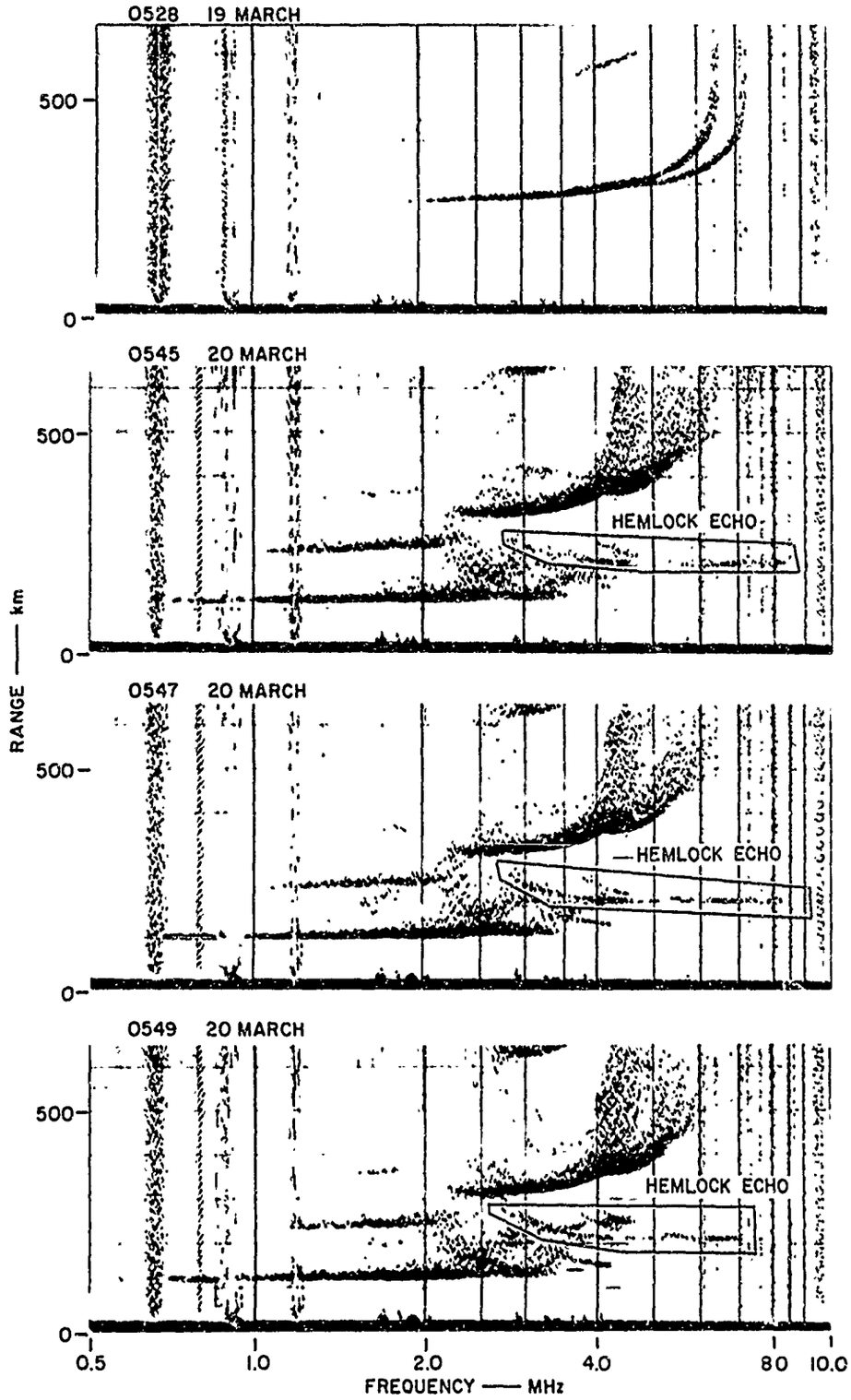


FIGURE 9 VERTICAL-INCIDENCE IONOGRAMS OBTAINED DURING GUM AND HEMLOCK RELEASES AT COLLEGE

good estimate of the electron density at the cloud. The barium-cloud echo shows retardation and magnetoionic splitting at the low-frequency end. An approximate method will be used to put limits on the plasma frequency at the release point; ray tracings would be best for this purpose, but since the electron-density profile of the ionosphere below the release point cannot be deduced from the ionograms, the simplified computation is sufficiently close to establish limits on the electron density.

Let us take two limiting cases: (1) the electron density below the release point was constant at the E-layer value, and (2) the electron density increased linearly from the E layer upward. These are approximately lower and upper limiting cases for what the electron density must have been.

Some definitions are in order at this point. Virtual or equivalent height is the height that results from multiplying the group delay time by the speed of light in free space. Virtual or equivalent path is the oblique path length defined in the same manner. It is shown below that for ionospheric propagation virtual height and path are geometrically related to a good approximation.

For the ordinary magnetoionic component the virtual height h' is approximately given by the integral of the non-magnetic phase index of refraction $\mu$, or

$$h' = \int_h \mu^{-1} \, dh \quad . \tag{11}$$

To find the equivalent range from the equivalent height, we shall apply an approximate method utilizing the Breit-Tuve equivalent path theorem and Martyn's equivalence theorem.

The equivalent path theorem states that the time taken by a wave traversing a horizontally stratified refracting medium is equal to the time taken by the wave at the same initial angle of incidence to propagate to the same horizontal distance in free space. Thus, for purposes of computing beginning and ending points or the path length of

a ray path through the ionosphere, one can replace the actual path through the ionosphere by the straight-line path formed by the ray propagating at the initial take-off angle to the horizontal distance of the midpoint or end point. The proof of this theorem and also of Snell's law are based on the fact that the component of wave velocity parallel to an interface is unchanged as a wave crosses the interface.

The equivalence theorem states that for propagation in a horizontally stratified refracting medium, waves at frequencies $f_1$ and $f_2$ will have identical incidence angles at some height if the wave frequencies are related by the secant law, or, equivalently,

$$f_1 \cos \theta_1 = f_2 \cos \theta_2 \tag{12}$$

where $\theta$ is the initial angle of incidence.

Combining these two theorems, then, it is possible to compute the equivalent path length to any point in the ionosphere by computing the equivalent height to the point in question and converting to oblique path length geometrically. The frequency is then transformed from vertical to oblique incidence by substituting the secant law [Eq. (11) reduces to the secant law for $\theta_1 = 0$] into the equivalent path equation. For long-distance propagation via the F layer, Smith [1939] has shown that a small correction depending upon distance must be applied; this corrected secant law is discussed by Davies [1965].

This is the technique that was employed for this study. For the ionosonde at College, plane-ionosphere geometry makes an excellent approximation.

The College ionograms in Figure 9 show that the E-layer critical frequency was approximately 2.1 MHz at 115 km. The virtual height h' for the constant-ionosphere case, found by integrating Eq. (11) for a constant-plasma-frequency profile, is given by the following relation:

$$h = 115 + 60f \left(f^2 - 4.41\right)^{-\frac{1}{2}} \tag{13}$$

where f is in MHz.

For the linear ionosphere, the plasma frequency at the release height (175 km) must be specified. Computations were made for values of 2.5, 2.6, and 2.7 MHz. For 2.6 MHz the equivalent height was found by integrating Eq. (11) to be

$$h = 115 + 51.06f\left(\sqrt{f^2 - 4.41} - \sqrt{f^2 - 6.76}\right) \quad . \quad (14)$$

Under the plane-earth approximation, the equivalent path for an obliquely propagating frequency $f_o$ is found from the following relations:

$$P'(f_o) = h'(f_o) \sec \theta \qquad (15)$$

$$f_o = f \sec \theta \qquad (16)$$

$$\sec \theta = \sqrt{1 + \left[\frac{D}{h'(f_o)}\right]^2} \qquad (17)$$

where D = 100 km, the approximate ground distance between College and the HEMLOCK release.

These equations are shown plotted in Figure 10 along with points obtained from the cloud echoes in the ionograms in Figure 9. Figure 10 indicates that the retardation in the cloud echoes in Figure 9 was caused by the local electron density at the cloud and not that at the penetration point in the E layer, or from an increase in geometrical path length. The reasons for this conclusion are outlined below.

Figure 10 shows that the constant model does not supply enough retardation at the low frequencies, and the rate of increase in virtual path near the low frequency end of the observed echo trace is much greater than that calculated from the constant-electron-density model. Thus, the observed retardation had to be produced above the E layer. It is concluded that the observed retardation was caused by the local electron density at the cloud.

Figure 10 shows that the experimental data fit the calculated curve for the linear density model quite well, particularly at the

low-frequency end. The excellent fit between observed and computed data shows that the plasma frequency at the height of the cloud was 2.5 to 2.7 MHz.

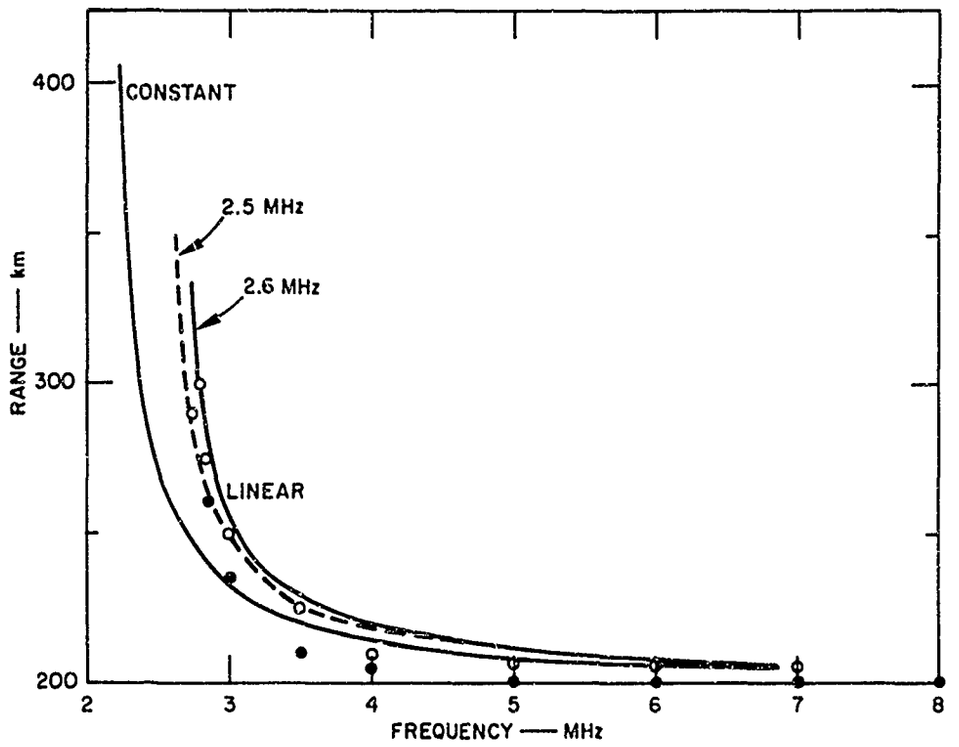


FIGURE 10 COMPARISON OF EXPERIMENTAL DATA WITH COMPUTED RETARDATION FROM THE LINEAR AND CONSTANT MODELS OF THE LOWER IONOSPHERE. The closed points were taken from the 0547 ionogram in Figure 9, and the open points from the 0549 ionogram.

Differential Doppler measurements made by the US Army Ballistic Research Laboratory indicate that the plasma frequency at 115 km was 2.1 MHz, reached a broad maximum of 2.6 MHz near 130 km, and decreased to 2.3 MHz at 175 km. The College ionosonde shows the maximum plasma frequency above 115 km to be less than 2.1 MHz, and the existence of a thick layer with a maximum of 2.1 MHz at 115 km (R. E. Prenatt, Personal Communication).

The differential Doppler technique relies upon the principle that the phase height $h_p$ of a radio wave is given by the integral of the phase index of refraction

$$h_p = \int_0^h \mu \, dh \tag{18}$$

Let us take a simple case for illustration; when the relationship between plasma frequency and electron density is substituted into Eq. (8), we have for propagation in a non-magnetic plasma,

$$\mu = \sqrt{1 - \frac{KN}{f^2}} \quad . \tag{19}$$

When the operating frequency is sufficiently high, the right side of Eq. (19) can be approximated by

$$\mu = 1 - \frac{KN}{2f^2} \quad . \tag{20}$$

Substituting Eq. (20) in Eq. (18) and integrating,

$$h_p = h - \frac{K}{2f^2} \int N dh \quad . \tag{21}$$

If two frequencies are used, the geometrical height can be eliminated:

$$h_{p1} - h_{p2} = \frac{K}{2} \left( \frac{1}{f_2^2} - \frac{1}{f_1^2} \right) \int N dh \quad . \tag{22}$$

If we now approximate the integral by a sum, we have

$$h_{p1} - h_{p2} \sim \sum_i N(h_i) \quad . \tag{23}$$

Finally, the difference in phase height, $\Delta h_p$, between adjacent heights is

$$\Delta h_p \sim N(h_i + 1) - N(h_i) \equiv \Delta N_i \quad . \tag{24}$$

Thus, the differential change in phase height is proportional to the differential increment in electron density.

A crucial assumption was made in going from Eq. (23) to Eq. (24)--if a change in phase height occurs in going from one height to another, the change is assumed to have been produced in the incremental height range. In general this is a good assumption; but not always.

A rocket fired obliquely traverses a curving path. No matter where the receivers are located, the part of the ionosphere below the rocket that is traversed by the radio rays used for the differential Doppler measurements is constantly changing. If horizontal gradients exist in the ionosphere below the rocket, changes in phase path can take place well below the rocket as well as in the incremental distance traversed by the rocket. Since there is no way of separating such changes, the differential Doppler data have to be used with care in the high latitudes where strong horizontal gradients are commonplace in the E region.

When all of the factors are considered, the 2.5-MHz value derived from the College ionosonde for the plasma frequency at the release height is well within the error limits of the differential Doppler technique. It is therefore concluded that the data are in substantial agreement and that the value of 2.5 MHz is realistic.

Returning to the experimental results, strong echoes were observed in most of the Homer and Kodiak records at about 13 and 18 MHz respectively. From Figure 8 we see that those frequencies correspond closely to the values expected for exact perpendicularity between RF wave and magnetic field at the cloud for a local ionospheric plasma frequency at the cloud of 2.7 MHz.

The analysis of the College ionogram presented above indicates that the plasma frequency at the release point was 2.5 to 2.6 MHz. From Figure 8 it can be seen that normality between ray and magnetic

field would occur at the observed frequency (18 MHz for Kodiak and 13 for Homer) for a plasma frequency of 2.5 MHz if the dip angle were approximately 77.3°. A plasma frequency of 2.3 MHz would require a dip angle of approximately 76.8°. The magnetic field expansion used [Cain et al. 1965] probably yields dip-angles in the ionosphere within one degree, so the various data are not consistent.

All of the evidence therefore suggests that the strong, fixed-frequency echo observed in the Homer and Kodiak records resulted from exact normality between radar wave and magnetic field. This echo, which is hereafter termed the 90° echo, was extremely aspect sensitive. The computed data in Figure 8 show that the amplitude of the 90° echo decreased of the order of 20 dB per degree of off-perpendicularity.

The GUM records were examined for the 90° echo, but the results are inconclusive. The corresponding College ionograms show that the E-layer plasma frequency was less than 1.5 MHz, considerably below that for HEMLOCK. (No ion cloud echo is visible on the College ionograms.)

The BRL data show that a ledge occurred in the E layer at a height near 110 km with a plasma frequency of 2.0 MHz, which decreased to 0.8 MHz at 160 km, 10 km below the release height of GUM. If we use this value and 77.3° for the magnetic field, the 90° echo should have been recorded at 4.6 MHz at Homer and 7.0 for Kodiak. No such echoes are obvious in the records, but those frequencies were deep in the strong interference band, where the echoes would be extremely difficult to recognize in any case. There is also the problem of how much confidence can be placed on the value of 0.8 MHz for the plasma frequency at the release height. The existence of such deep valleys in the ionosphere has not been confirmed by other techniques. Thus the GUM records do not confirm the HEMLOCK results, but neither do they contradict them. The records for the other releases are unusable for the purpose of confirming the existence of the 90° echo because the Homer echoes were conpletely confined to the strong interference band, and none of the other releases were observed by the College ionosonde in such a manner as to yield electron densities at the release height.

Once the plasma frequency at the release height is established, the aspect sensitivity can, in principle, be determined because the angle between RF ray and magnetic field is known. One unknown remains, however--the frequency dependence of the backscatter cross section--and this is difficult to determine. It is here that the failure of the bistatic part of the project hurts, since the bistatic echoes would have supplied an intermediate point.

Before striation little can be said about the aspect sensitivity of the echoes other than that of the 90° echo because the echo amplitudes were so variable with frequency. After pronounced striations appeared, the echo amplitudes were well enough behaved that some idea of the aspect sensitivity can be deduced. For GUM, at 710 s the amplitude was roughly 50 dB at 20 MHz, and 20 dB at 35 MHz; at 1060 s the amplitude at 20 MHz was 45 dB, and at 30 MHz was 15 dB. After striation of HEMLOCK, the amplitude at 230 and 270 s was about 45 dB at 25 MHz, and 15 dB at 45 MHz; at 350 s the amplitude was about 35 dB at 20 MHz and 20 dB at 30 MHz. For Homer at 190 to 280 s the amplitude was 35 dB at 15 MHz, and 10 dB at 30; at 340 to 460 s the amplitude was 30 dB at 15 MHz, and 10 dB at 20 MHz.

Neglecting, for the moment, the frequency dependence for the backscatter cross section, these data can be used with Figure 8 to obtain rough estimates of the aspect sensitivity. For HEMLOCK shortly after striation, the amplitude at Kodiak dropped 30 dB between 25 and 45 MHz, and at Homer 25 dB between 15 and 30 MHz. If the plasma frequency at the release height was 2.5 MHz, these values correspond to changes of 30 dB in approximately 0.8° for Kodiak and 25 dB in 2.1° for Homer.

At times well after the striation of HEMLOCK, the amplitude change [illegible] 15 dB in 1.0° at Kodiak, and 25 dB in 2.1° at Homer for a frequency [illegible] MHz.

[illegible]per limits for the aspect sensitivity at early times after [illegible] for HEMLOCK are roughly 40 dB per degree for Kodiak and [illegible] degree for Homer; at late times these values are respectively

15 dB per degree for both sites. In the next section it will be suggested that this discrepancy between the Homer and Kodiak data was due primarily to the frequency dependence of the backscatter cross section.

An upper limit of the aspect sensitivity can be made for the GUM release if we take a value of 1.0 MHz for the plasma frequency at the release height. The relationship between off-perpendicular angle and frequency can be found to a good approximation from Figure 8 by dividing the ordinate by the plasma frequency listed for each curve--i.e., 2.5 for the dashed curves. The observed amplitude decreases correspond to a change of 30 dB in approximately $0.2^{\circ}$. Had the plasma frequency at the height of the GUM release been 2.0 MHz, the amplitude decrease would have been 30 dB in $0.8^{\circ}$.

## VIII DISCUSSION

The Kodiak and Homer records indicate that all of the backscatter echoes recorded were strongly aspect-sensitive, even those at early times when the cloud appears to be an overdense ball. The echoes before striation had to be aspect-sensitive; otherwise, Homer and Kodiak should have shown the same results, excluding equipmental differences, because the propagation paths to the clouds were nearly identical, so that the same portion of the cloud would produce the echo for both sites. All of the data show, however, that the results are far from identical, and the differences are so great that they cannot be entirely equipmental. For HEMLOCK and GUM the sounders were synchronized to within a millisecond, so the observed differences cannot be attributed to temporal changes. Thus, we are forced to the conclusion that even when the cloud was overdense to the sounding frequency at early times, backscatter was produced by scatterers that were very strongly aspect-sensitive with respect to the geomagnetic field.

Since the echoes from near normal incidence to the magnetic field were strongly aspect-sensitive, it is intriguing to speculate about whether the echoes recorded by the College ionosonde in Figure 9 were also aspect-sensitive. If so, the aspect-sensitivity requirements must have been satisfied by refraction within the cloud, because there was not enough refraction in the ionosphere around the cloud to produce normality for a frequency of 8 MHz. The ion cloud acts as a diverging lens, so the analysis in this case is not at all easy. Ray-tracing techniques would have to be used, and it is hoped that this will be done sometime in the future.

Returning now to the Homer and Kodiak data, the amount of aspect sensitivity noted at the end of Section VII differs considerably between the two sites. This computation was made under the assumption

that the backscattering cross section did not depend upon frequency, an assumption that is undoubtedly incorrect. It is more likely that above 30 MHz the backscattering cross section of HEMLOCK decreased so rapidly that the frequency dependence dominated the aspect-angle dependence. The system sensitivity also decreased above about 40 MHz but not enough to account for the large changes observed. (It is unfortunate that the bistatic part of the experiment failed because those data would have been useful for computing the frequency dependence of the scattering cross section.)

Before striation the 90° echo was the strongest echo by many dB, and the drop in amplitude away from the center frequency was 5 to 10 dB/MHz, or roughly 25 dB per degree. This rapid drop-off in 90° echo amplitude must have been caused by the aspect-dependent part of the cross section, because it is highly improbable that the scattering cross section would have strong peaks located so fortuitously at 13 and 18 MHz.

As Figure 5 illustrates, the Kodiak 90°-echo amplitude was 10 to 15 dB greater than that at Homer. While the antenna pattern could have caused part of this difference, it does not seem likely that all of the difference was equipmental. Hence, it is probable that the scattering cross section increased with frequency between 13 and 18 MHz.

Above the frequency of the 90° echo, the Homer echo amplitude relative to that of the 90° echo exceeds the Kodiak amplitude considerably for a given aspect angle (Figure 8 illustrates the relationship between frequency and aspect angle for Homer and Kodiak.) These results are interpreted as indicating that the backscattering cross section increased with frequency between 10 and 30 MHz.

It is therefore concluded that before striation, backscatter from the HEMLOCK barium cloud had an exceedingly aspect-sensitive echo component and the scattering cross section increased with frequency between about 10 and 30 MHz.

With the onset of striation, echo amplitudes tended to increase toward that of the 90° echo. Relative to the 90° echo, the Homer echo is stronger than the Kodiak echo for a given aspect angle, suggesting that

although the antenna gains could have been a contributing factor, the difference is probably attributable to an increase in backscattering cross section with frequency below about 30 MHz.

At the high-frequency end of the backscatter echoes recorded at Kodiak, particularly right after pronounced striation, the drop-off in amplitude was abrupt. If it is assumed that the aspect sensitivity does not change markedly with frequency, the aspect sensitive drop-off should be the same for Homer and Kodiak; this is a good assumption for naturally occurring ionospheric irregularities [Bates and Albee 1969, 1970], but how good it is in this case is unknown. As noted in Section VII, however, the Homer echo between about 15 and 30 MHz decreased about 15 dB per degree of off-perpendicularity from the magnetic field, while the Kodiak echo decreased 40 dB per degree between 25 and 45 MHz. At late times after striation when the frequency ranges of the Homer and Kodiak echoes were comparable, the aspect sensitivities were about equal.

One way of explaining this apparent discrepancy is that below 30 MHz the backscatter cross section increased with frequency, whereas above 30 MHz it decreased. Here again, part of this drop-off above 40 MHz was equipmental; one characteristic of most Granger sounders is that the power output and the receiver sensitivity drop markedly above 40 MHz.

It is therefore concluded that the aspect-sensitive decrease in the backscattering cross section for HEMLOCK after striation was probably between 10 and 20 dB per degree of off-perpendicularity from the magnetic field and that the backscattering cross section had a maximum near 30 MHz.

The decrease in amplitude of the GUM echoes between 20 and 30 MHz at late times was too great to attribute to aspect angle alone if we take the plasma frequency at the release height to be 1.0 MHz, because the aspect angle apparently changed very little. If, however, the plasma frequency at the release height had been as high as 2.0 MHz, the aspect sensitivity would agree with that for HEMLOCK. It seems most likely that some intermediate value occurred, indicating that the backscatter cross section for GUM was dropping rapidly with frequency in the 20-to-30-MHz region.

The amplitude of the Kodiak GUM echoes after striation dropped rapidly above 20 MHz. The maximum echo amplitude occurred near 17 MHz (Figure 6 and Appendix A), this maximum may have been partly equipmental because the system sensitivity at Kodiak was considerably depressed between about 10 and 16 MHz. The Homer echoes were confined to the low frequencies, suggesting that the backscatter cross section for GUM had a maximum well below 20 MHz. It is therefore concluded that the aspect dependence for GUM was probably about the same as that for HEMLOCK but that the maximum in the backscattering cross section occurred well below 20 MHz, so that transverse irregularity sizes were greater for GUM than for HEMLOCK by roughly a factor of 2.

There are two ways of visualizing the cause of aspect sensitivity. One is, to think of the scattering structure as a group of irregularities whose characteristics can be represented by an average irregularity. In this case diffraction theory can be used to deduce the length of the average irregularity. For example let us consider the Kodiak 30-s record in Appendix A. The peak of the 90° echo is at about 18 MHz, and nulls appear to be near 16 and 20 MHz. Figure 8 shows that such a frequency range corresponds to approximately 1.3° change in incidence angle. If we therefore assume that the average irregularity can be approximated by a long conductor in the plane of incidence of the electric vector, the length can be found from the first zeros in the diffraction pattern for a conductor of length L:

$$\frac{\sin (k\ L \sin \alpha)}{k\ L \sin \alpha} = 0 \qquad (25)$$

The first zero of Eq. (25) occurs for the first zero of the numerator, or when the argument of sine is $\pi$. For small off-perpendicular angles, $\alpha$,

$$L = \frac{\alpha\lambda}{2} \quad . \qquad (26)$$

The length of the average irregularity producing the 90° echo in the 30-s Kodiak record is therefore approximately 750 m.

A decrease in aspect sensitivity implies a decrease in length of the average irregularity. The increase in echo amplitude at frequencies well above that of the 90° echo at the onset of pronounced striation therefore implies that the length of the average irregularity decreased abruptly at the onset of pronounced striation.

This behavior seems to be considerably different from that of natural F-layer irregularities such as auroral and spread-F irregularities. Bates and Albee [1970] found that the aspect sensitivity of natural echoes was of the order of 5 dB per degree and the backscattering cross section was strong well below 10 MHz. Thus, how the barium cloud echoes compare with natural echoes is unknown.

One problem in attempting to relate the echo behavior of barium clouds with natural irregularities is that the barium clouds present a discrete target, while natural events are extended targets. Thus, for the natural events one obtains an integrated result, and this integration could cause the measured aspect and frequency dependencies to be weaker than they are. Much work needs to be done to understand how the natural and barium cloud echoes are related.

The behavior of the echoes can be used to deduce what sort of irregularities inhabit barium clouds. Booker's [1956] scattering theory, outlined in Section II, is quite useful for this endeavor, because it provides a physical basis for relating the backscatter results to the irregularities in the clouds. Backscatter echo amplitude at a given radar frequency is linearly proportional to the amplitude of that Fourier component of the irregularities whose wavelength is precisely one-half the radar wavelength. For example, the existence of a strong backscatter echo at 30 MHz, 10-m radar wavelength, indicates that the scattering medium has a substantial component in irregularity spectrum transverse to the magnetic field at 5-m wavelengths.

The HEMLOCK backscattering cross section apparently increased with frequency in the 10-to-30-MHz region during the entire event. After striation the backscattering cross section had a maximum near 30 MHz and decreased rapidly above that frequency: the behavior of the

cross section above 30 MHz before striation is unknown because the echoes did not extend high enough in frequency. The maximum in the backscatter cross section near 30 MHz is therefore interpreted as evidence that the irregularity spectrum was peaked for transverse sizes near 5 m.

The sudden increase in echo strength near the time of striation at frequencies away from that for exact normal incidence to the magnetic field suggests that the aspect sensitivity decreased with the onset of striation. Had the backscatter cross section increased markedly, the amplitude of the 90° echo should also have increased appreciably, but it did not. In fact, the other echoes appeared to increase to equal the amplitude of the 90° echo. This change implies a rather drastic change in the cloud at the onset of striation.

The alternative way of visualizing what happened is to view the results in light of the Booker scattering theory. In this instance, the irregularities are assumed to be decomposed by Fourier transformation into infinite plane waves having strict aspect sensitivity--i.e., exact normality is required for backscatter. (These "waves" are not necessarily propagating waves; they are called waves because they result from Fourier transformation and behave mathematically as though they were waves. In some cases, such as for plasma instabilities, the irregularities are set up by propagating waves, and the analogy is exact.) A finite aspect sensitivity is therefore produced from such a system by an angular spectrum of plane waves in which the wave amplitude varies with angle in precisely the same manner as the signal amplitude varies with off-perpendicular angle.

Applying this notion to the barium clouds, the higher aspect sensitivity before striation is interpreted as showing that the angular spectrum of the wave components in the irregularities was strongly peaked in the direction normal to the magnetic field. The decrease in aspect sensitivity at the onset of striation is then interpreted as a widening of the angular spectrum away from the perpendicular to the magnetic field.

In either case, there was a sudden change in the backscattering structure in the cloud at the onset of pronounced striation. What caused this change would be a nice problem in plasma physics.

At early times, well before striation, the echoes observed at Homer and Kodiak were very aspect-sensitive. The 90° echo, which was strongly aspect-sensitive, appeared immediately after the HEMLOCK release and exceeded the remainder of the echoes by 20 to 30 dB. This observation indicates the presence of field-aligned structure immediately after the release; on the basis of simple diffraction theory the strong aspect sensitivity of the 90° echo requires structure of the order of 50 wavelengths long. Since the frequency of the 90° echo was about 13 MHz at Homer, and 18 at Kodiak, this implies the existence of field-aligned structure with lengths of the order of a kilometer.

A well-developed 90° echo was observed at Kodiak 30 seconds after the release, indicating that immediately after the release, field-aligned irregularities roughly a kilometer long appeared in the cloud. This notion does not seem unreasonable because the HEMLOCK cloud expanded to a diameter of about 10 km within several tens of seconds; for example, in the 45-s photo shown in Appendix B, the cloud covers the second graticule ring, which is 3° or 10 km in diameter.

At sites from which the radar waves met the barium clouds near normal incidence to the magnetic field, backscatter was strongly aspect-sensitive; however, at a site near College, where the radar waves were well off-perpendicular, the backscatter echoes observed by Thome [1969] apparently were not. Considering the strength of the aspect-sensitive echoes, the question arises as to how the two different results fit together. Two possibilities exist: (1) The backscatter echoes observed at all sites were strongly aspect-sensitive, or (2) the echoes observed at the two classes of sites were produced by fundamentally different mechanisms.

The method used by Thome [1969] to analyze the radar echoes obtained from well off-perpendicular to the magnetic field is based upon the assumption that the ion cloud is a smooth, overdense ball at

all frequencies below the cloud maximum plasma frequency. Backscatter is then the result of critical reflection from the surface within the cloud where the plasma and radar frequencies are equal. For this model the backscatter cross section decreases with increasing radar frequency for a given ion distribution, or, conversely, with decreasing maximum plasma frequency for a given radar frequency. The disappearance of the echo on any given frequency is interpreted as evidence that the size of the volume with a plasma frequency in excess of the radar frequency is less than some critical value set by the radar parameters. Therefore, for a very sensitive radar, the frequency at which the echo disappears is interpreted directly as the maximum plasma frequency of the cloud.

For possibility (1) above to hold, refraction within the ion cloud would be required to produce normality between RF wave and magnetic field line. Unfortunately, this problem cannot be approximated by some simple model but can only be modeled with the aid of a ray-tracing technique. We can, however, examine the problem qualitatively to see what sort of behavior would be expected. For a radar near College the deviation required to produce normality between ray and magnetic field is approximately $63^{\circ}$. Refraction within the cloud could satisfy this condition over a surface within the cloud, the size and shape of the surface depending upon the ion distribution within the cloud. The size of this surface of normality would decrease with increasing radar frequency for a given ion distribution, or, alternatively, would decrease with decreasing maximum plasma frequency for a given radar frequency. The maximum frequency of such an echo would be greater than, and would probably be linearly related to, the maximum plasma frequency within the cloud, so that the cloud ion density could be found from the radar measurements, although the maximum plasma frequency would be substantially less than the frequency at which the echo disappears. The computation of the constant of proportionality between maximum plasma frequency and radar frequency would require ray-tracing techniques and some knowledge of the ion profile within the cloud.

The two mechanisms described above yield results that are proportional but not equal. The application of the analysis technique for scatter from a smooth ball to the case of aspect-sensitive scatter utilizing refraction within the cloud would lead to a computed maximum plasma frequency greater than that occurring. An effort should be made to determine which mechanism is operative.

If the smooth-ball mechanism is found to hold, then possibility (2) above must be true--i.e., the echoes observed at Homer and Kodiak are fundamentally different from those observed near College. A possible cloud model for producing the echoes in this instance is that of an overdense ball inside a weak-scattering cloud containing field-aligned structure--in other words, a smooth ball embedded in a shimmering cloud. In this case the shimmering cloud would provide the aspect-sensitive echoes observed near normal incidence to the magnetic field while the smooth ball would produce the echoes observed elsewhere. This model is physically reasonable in that it explains why no echoes were observed at Homer or Kodiak for which the frequency fell with time as did the maximum plasma frequency of the ion cloud. In the case of a smooth spherical ball the backscatter cross section is equal to the projected area of the sphere. The area of the cloud of irregularities, however, is larger than the entire area of the smooth ball, and scatter would be equally possible from all parts of the cloud. It is therefore possible that the scattering area of the cloud of irregularities is many orders of magnitude greater than that of the ball; thus, the backscattered echo amplitude from the shimmering cloud could exceed that from the ball by several orders of magnitude, in which case the ball echo would have been completely obscured at Homer and Kodiak by the aspect-sensitive echoes.

The aspect-sensitive-ball-of-irregularities model has a major difficulty when considered in the light of all the evidence from the tests. Thome [1969] showed that interference between the ordinary and extraordinary components of the echo from the ball produced a distinctive fading pattern (Faraday fading) in the echoes. G. N. Oetzel of

SRI subsequently showed that this Faraday fading had to be produced entirely within the cloud and could therefore be used to find the electron density of the cloud [Oetzel and Chang, 1969]. The basis of the technique is the fact that most of the observed Faraday rotation must occur from that part of the cloud where the plasma frequency is nearly equal to the radar frequency. For the case where refraction is utilized to produce exact normality to the magnetic field, normality occurs at frequencies somewhat above the plasma frequency--possibly one-third higher for a radar near College.

It is therefore questionable whether the aspect-sensitive-ball model will produce enough Faraday rotation to agree with that observed.

While this study has not solved the problem of backscatter from barium clouds, or even explained how the various echoes are related to one another, it is hoped that enough questions have been raised and data presented to stimulate further definitive work on the problem.

Whether the Booker scattering theory can be applied at early times when electron densities were high depends critically upon which cloud model is correct. If the model of the ball embedded in a shimmering cloud is correct, all of the echoes observed at Homer and Kodiak were produced by Booker scatter from underdense irregularities. If the cloud itself was composed of overdense, aspect-sensitive irregularities, Booker scatter is not applicable, although the basic concept can be used as an aid in visualizing the irregularities.

Before striation the backscatter cross section appears to have increased between 15 and 30 MHz. This conclusion, if it is true, indicates that the scattering structure had substantial Fourier components in the 5-to-10-m size range. This is rather small structure, but it may be a significant fact that such a size range is of the order of the gyro radius for barium ions in the geomagnetic field.

The echoes for GUM and HEMLOCK were different in that the frequency extent of the HEMLOCK echoes exceeded that of most of the GUM echoes. The amplitudes of the echoes were roughly comparable after

striation, but beforehand the GUM amplitudes were apparently somewhat lower. It is suggested below that this difference was primarily due to differing ionospheric conditions, in particular to the occurrence of strong spread-F during the HEMLOCK event.

For HEMLOCK, 96 kg of barium was released at a height of 175 km at 1939 AST (150° WMT), March 20, 1969, for GUM, 48 kg of barium was released at 168 km at 1919 AST, March 19, 1969. Except for the factor of two in barium mass, the two releases were almost identical. The behavior of the ion clouds, however, was far from identical. The HEMLOCK ion cloud drifted clear of the neutral cloud within a minute, whereas the GUM ion and neutral clouds took many minutes to drift apart. The basic difference between the clouds, therefore, must have been ionospheric in origin. Since the east-west separation of the ion cloud from the neutral cloud is caused by a north-south electric field, there must have been a considerable difference in horizontal electric fields present in the lower F layer on the two evenings.

Another marked difference between the two releases was in the occurrence of spread-F. Figure 9 shows that for GUM there was almost no spread-F, whereas for HEMLOCK spread-F was strong. The ELM and JUNIPER releases were also observed by the Homer and Kodiak radars, but their echoes were at low frequencies and very weak. These releases were smaller than GUM and HEMLOCK, and only weak to moderate spread-F existed.

It is therefore suggested that the strong spread-F markedly enhanced the HEMLOCK barium-cloud echoes at the higher frequencies. One problem with the explanation, however, is that the enhancement was rather selective as to irregularity size. The indicated peak in backscattering cross section around 30 MHz for HEMLOCK implies that 5-m irregularities predominated in the barium cloud, whereas natural spread-F does not show any such preference for small irregularities. On the contrary, as the ionograms in Figure 9 show, spread-F irregularities may have a strong size component in the range of 100 m, and

the existence of the oblique spread-F echo* with little apparent change in amplitude between roughly 5 and 20 MHz indicates that the size spectrum for spread-F irregularities is flat. The transverse irregularity size for GUM was apparently 10 m or greater. If spread-F was involved, it somehow decreased the irregularity size.

Thus, if the spread-F irregularities somehow interact with the electrons in the ion cloud to produce enhanced irregularities, they do it in a rather selective way. Possibly the observation that the gyro radius of the barium ions is of the order of 5 m is of importance.

Other important factors are: (1) the electron density at the release height was appreciably greater for HEMLOCK than for GUM, and (2) the ion and neutral clouds drifted apart ten times sooner for HEMLOCK than for GUM. The latter observation indicates that the north-south transverse electric field was much greater for HEMLOCK than for GUM.

---

* The IF echo [Bates 1959, 1960] and subsequently termed the slant-F echo [Bates et al, 1966, Bates and Albee 1970].

# IX CONCLUSIONS

The basic conclusions of this study are as follows.

1. The backscatter cross section calculated for isotropic scatter from barium clouds near normal incidence to the magnetic field is orders of magnitude greater than the geometric area as measured from photographs.

2. The great difference between the results of the Homer and Kodiak radars and the large cross sections are interpreted as evidence that the echoes are strongly aspect-sensitive.

3. Very strong echoes were observed that remained fixed in frequency throughout the HEMLOCK event. These echoes are interpreted as being produced when the radar wave was at the proper frequency to propagate exactly at normal incidence to the magnetic field. This echo is termed the 90° echo.

4. The 90° echo was extremely aspect-sensitive--of the order of 20 dB per degree of off-perpendicularity, even at early times after the release. Such a great decrease in amplitude with angle indicates that the length of the field-aligned irregularities was of the order of a kilometer.

5. The 90° echo could not be positively identified in the GUM records. Strong interference at Homer tended to obscure echoes in the most likely frequency range for the GUM 90° echo.

6. The simultaneous behavior of the HEMLOCK echoes observed at Homer and Kodiak is interpreted as evidence that the backscatter cross section had a maximum near 30 MHz. Such a maximum indicates that the scattering structure had a dominant size near 5 m, the order of the radius of gyration of the barium ions in the geomagnetic field.

7. The backscatter cross section for GUM apparently had a maximum below 20 MHz, implying a dominant transverse irregularity size of about 10 m, or twice as great as for HEMLOCK.

8. The aspect-dependent part of the backscattering cross section decreased approximately 10 to 20 dB per degree of off-perpendicularity from the magnetic field.

9. Strong, aspect-sensitive echoes were observed throughout the GUM and HEMLOCK events. This result indicates that even immediately after the release the ion cloud contains strong field-aligned structure. This finding raises the question of the correctness of the smooth, overdense-ball model of the cloud at early times after the release.

10. Two possible models that explain most of the observation are suggested: (1) the cloud is a ball of dense, field-aligned irregularities, and (2) the cloud is composed of a smooth, overdense ball embedded within a larger field-aligned cloud of weak, field-aligned irregularities.

(a) Model 1 explains most of the observed features of HF echoes from barium clouds. One apparent discrepancy, however, is that it does not seem to be able to explain the observed Faraday rotation. If this model is correct, electron densities computed under the assumption of a smooth-ball model will be somewhat too high.

(b) Model 2 explains the observed features.

11. The onset of pronounced optical striations in the ion cloud was accompanied by a strong increase in echo amplitude at high frequencies. Considering all of the data obtained indicates that the aspect sensitivity of the irregularities decreased abruptly at the onset of pronounced striation.

12. Echo amplitudes were quite variable, particularly at early times after the release and at near the onset of striation. With the exception of the increase at the onset of pronounced striation, these echo changes could not be correlated with optical changes in the clouds.

13. At times well after striation the echoes slowly died away, and no large, abrupt changes occurred. Echo amplitudes continued to be somewhat variable.

14. Amplitudes for GUM and HEMLOCK echoes were generally comparable at both sites, except that the frequency of the echoes was generally higher for HEMLOCK.

15. Strong spread-F was present during HEMLOCK, whereas almost none occurred during GUM, and little during JUNIPER and ELM. It is suggested that spread-F irregularities were somehow enhanced by presence of the barium ions; this enhancement appeared to be selective, however, because under the assumption of weak scatter, irregularity sizes near 5 m were apparently preferentially enhanced when spread-F was strong. Larger irregularities apparently predominated in the ion clouds when little or no spread-F was present than when spread-F was strong.

## REFERENCES


Bates, H. F., "The Height of F Layer Irregularities in the Arctic Ionosphere," J. Geophys. Res., Vol. 64, pp. 1257-1265 (1959).

Bates, H. F., "Direct HF Backscatter from the F Region," J. Geophys. Res., Vol. 65, pp. 1993-2002 (1960).

Bates, H. F. and P. R. Albee, "Aspect Sensitivity of F-Layer HF Backscatter Echoes," J. Geophys. Res. (in press).

Bates, H. F. and P. R. Albee, "Aspect Sensitivity of HF Auroral Echoes," J. Geophys. Res., Vol. 74, p. 1164 (1969).

Bates, H. F., A. E. Belon, G. J. Romick, W. J. Stringer, "On the Correlation of Optical and Radio Auroras," J. Atmosph. Terr. Phys., Vol. 28, pp. 439-446 (1966).

Booker, H. G., "A Theory of Scattering by Non-Isotropic Irregularities with Application to Radar Reflections from Aurora," J. Atmosph. Terr. Phys., Vol. 8, pp. 204-221 (1956).

Cain, J. C., W. E. McDaniels, and S. J. Hendricks, "An Evaluation of the Main Geomagnetic Field, 1940-1962," J. Geophys. Res., Vol. 70, p. 3647 (1965).

Davies, K., Ionospheric Radio Propagation, U. S. Dept. of Commerce, NBS (1965).

Oetzel, G. N. and N. J. F. Chang, "Analysis of SECEDE III HF Data," Technical Report 3, Project SECEDE RADC-TR-69-412, Stanford Research Institute, Menlo Park, Calif. (November 1969).

Smith, N., "The Relation of Radio Sky-wave Transmission to Ionospheric Measurements," Proc. IRE, Vol. 27, pp. 332-347 (1939).

Thome, G. D., "Raytheon SECEDE III Radar Observations During SECEDE III," in "Preliminary Results of Test Series SECEDE III," Technical Report 2, Project SECEDE, R. S. Leonard, Ed., RADC-TR-69-239, Stanford Research Institute, Menlo Park, Calif. (May 1969).

# APPENDIX A

## POWER-VS.-FREQUENCY PLOTS

## APPENDIX A

## POWER-VS.-FREQUENCY PLOTS

This appendix presents the computer plots from the analog magnetic tapes recorded at Homer and Kodiak. The ordinate is power in decibels and was derived by fitting a quadratic to three of the six 10-dB calibration points put onto the tapes at each site. The receiver output was roughly logarithmic, so the output was nearly linear in decibels; the quadratic was used to allow for the small deviation present.

The reference level 0 dB was arbitrarily taken as 1 μV at the antenna output terminals. The threshold sensitivity varied from 1 to 5 μV, 0 to 17 dB. Power levels under 20 dB--10 μV--are unreliable because system noise added to signal levels, making the calibration inaccurate.

The plots were made by selecting the maximum signal recorded in a 20-km window centered on the barium-cloud echo for each sounder sweep (a sweep is defined as one 4-to-64-MHz sounding). The average and zero-level noise were read from the noise sample taken from each frequency scan of each sounder sweep. Echo signal maxima were then converted to decibels and plotted if (1) the average noise level was less than approximately 20 dB, (2) the signal maximum exceeded the average noise by about 3 dB, and (3) the signal maximum exceeded approximately 5 dB for Homer and 15 dB for Kodiak. (Signals below 5 dB are shown for Homer, but, as noted above, the calibration was not accurate at such low levels.) Thus, most of the echoes in the interference band below 15 MHz were discarded either because they were weak or because the interference was strong. To have preserved such echoes would have required considerably more time and a sophisticated computer analysis program; such a procedure was beyond the scope of the project.

The HEMLOCK records are shown on pages A-5 through A-21 and the GUM records from A-22 through A-28.

The time marked for each plot is approximately the ending time of each sweep relative to the release. Thus, the 10-s record for Kodiak actually began at the release and ended approximately 8 seconds afterward. Records are missing because of some problem. The first 500 seconds of GUM are unusable because the carrier frequency--i.e., the zero signal level--of the tape recorder varied widely and erratically for some unexplained reason.

The records do not go to the end of the events because the echoes just continue to fade away gradually and do not exhibit any different behavior than shown. All of the records were digitized, however, and preliminary plots were made to guide the subsequent analysis.

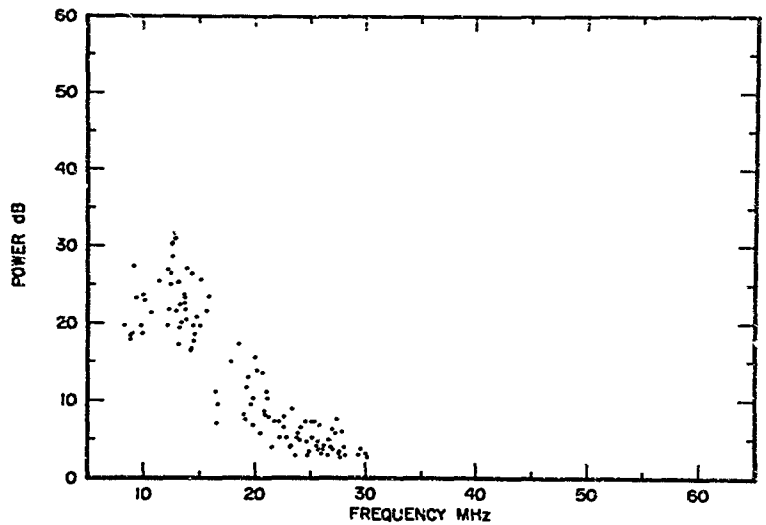


HOMER 30 s

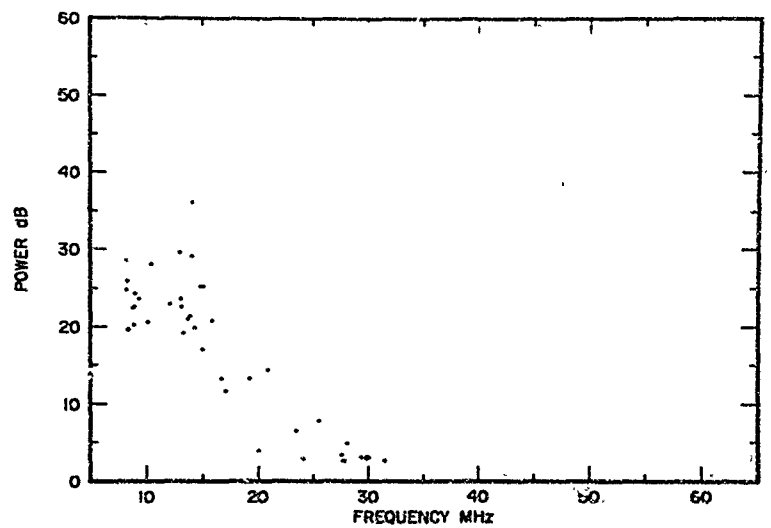


HOMER 40 s

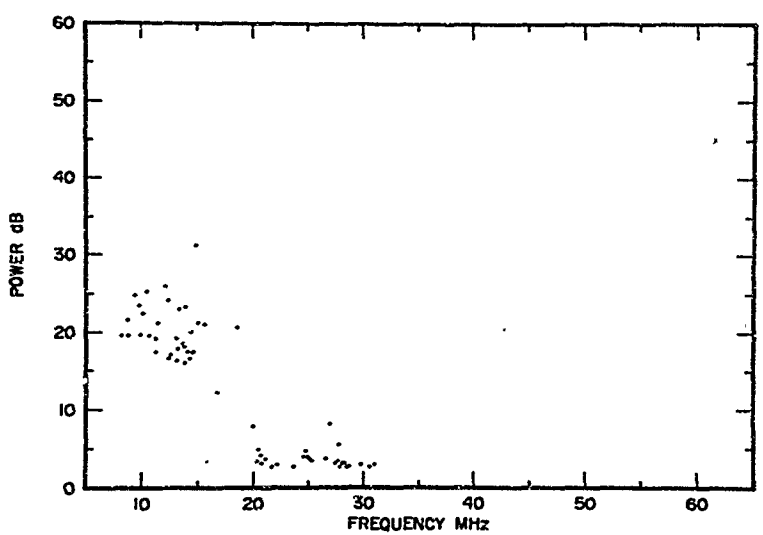


HOMER 50 s

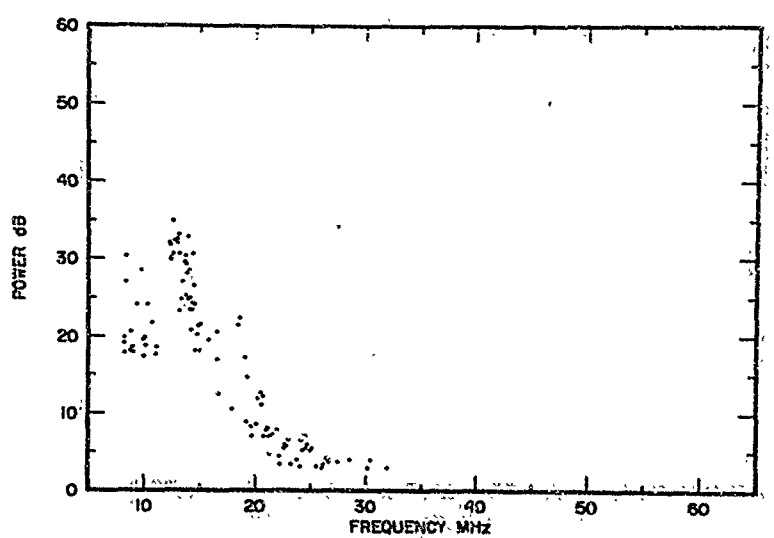


HOMER 60 s

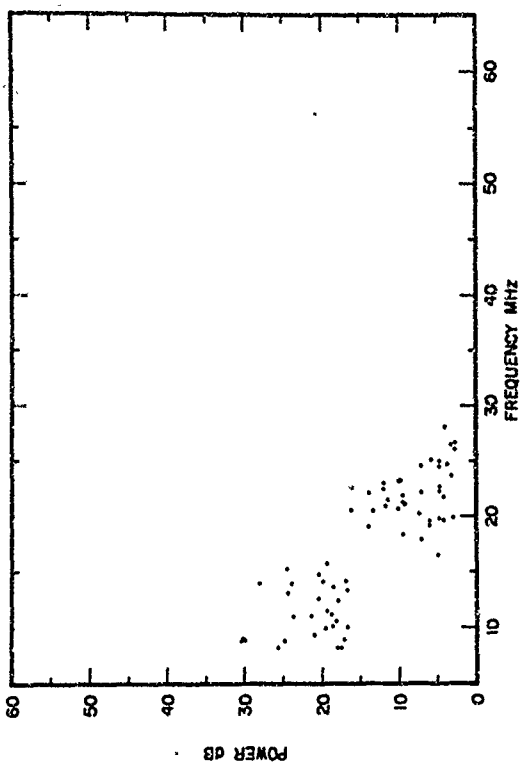
POWER dB
FREQUENCY MHz
HOMER 80 s

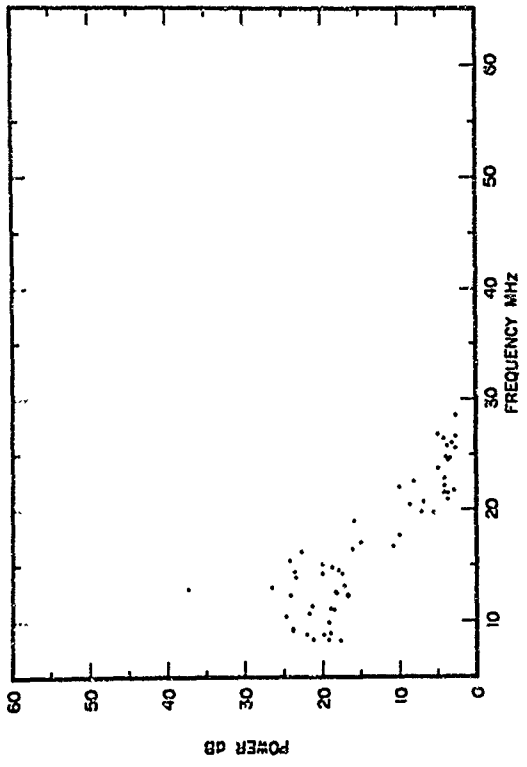
POWER dB
FREQUENCY MHz
HOMER 100 s

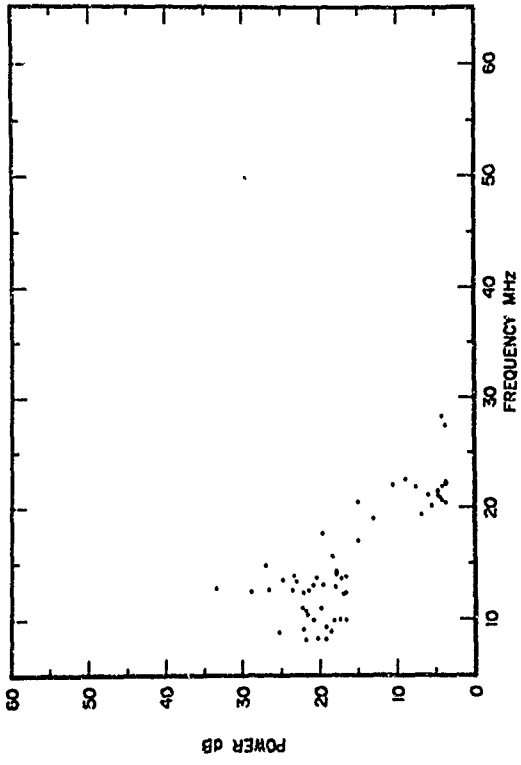
POWER dB
FREQUENCY MHz
HOMER 70 s

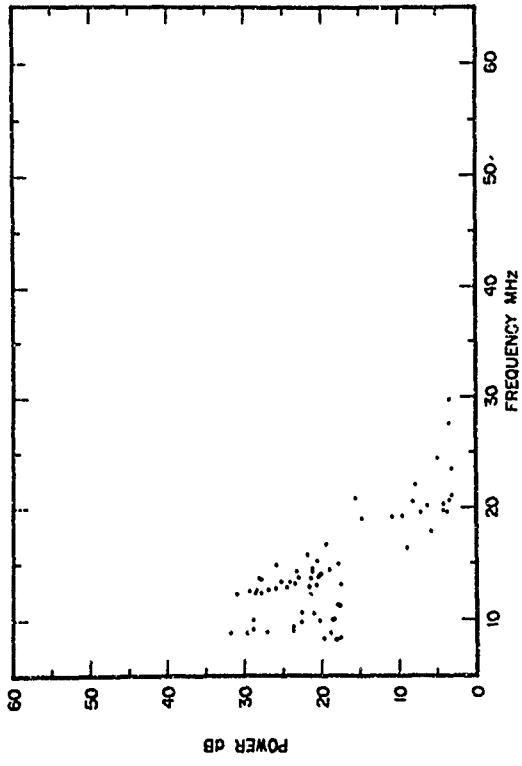
POWER dB
FREQUENCY MHz
HOMER 90 s

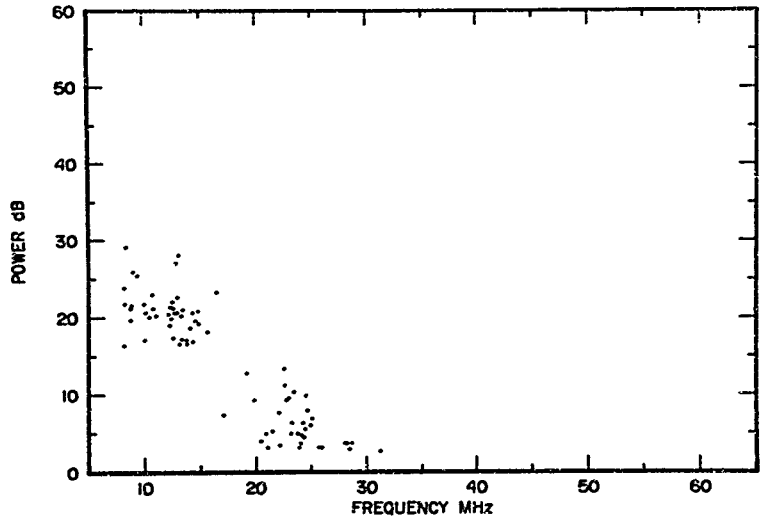


HOMER 110 s

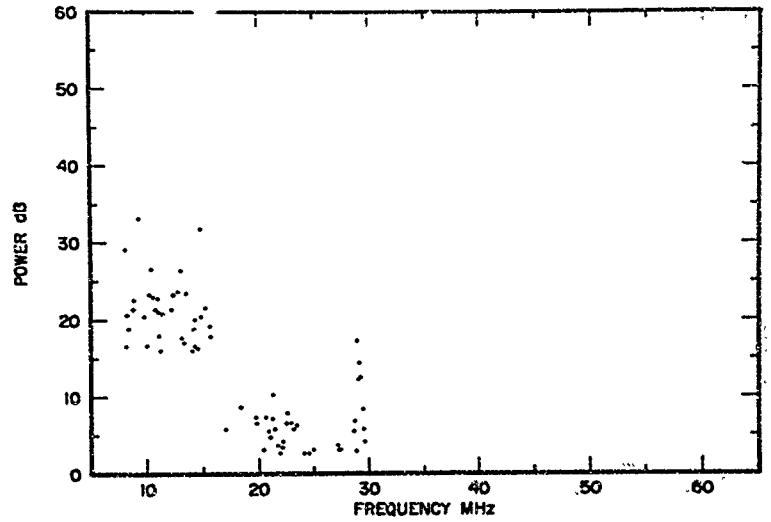


HOMER 120 s

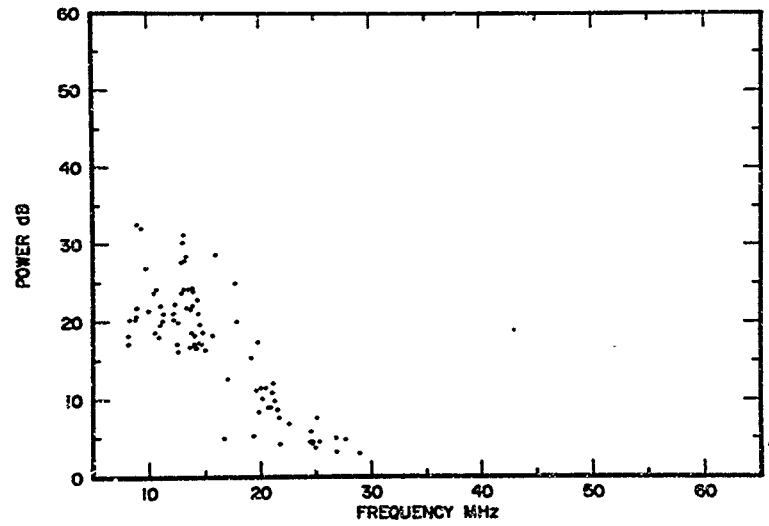


HOMER 130 s

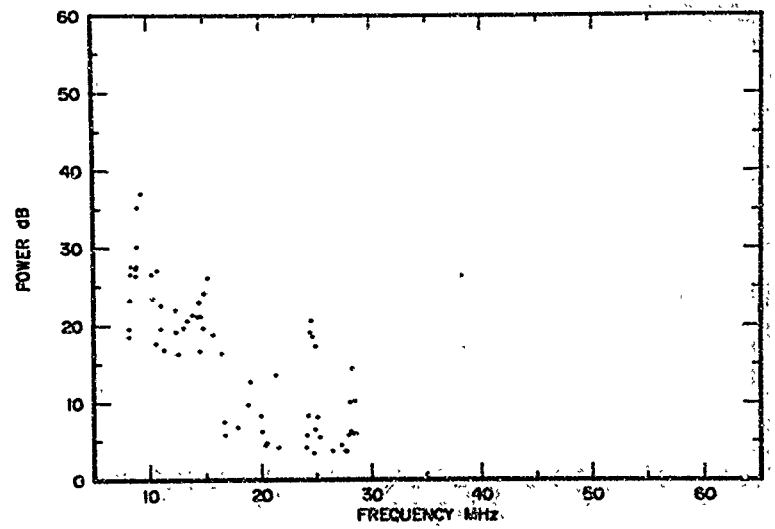


HOMER 140 s

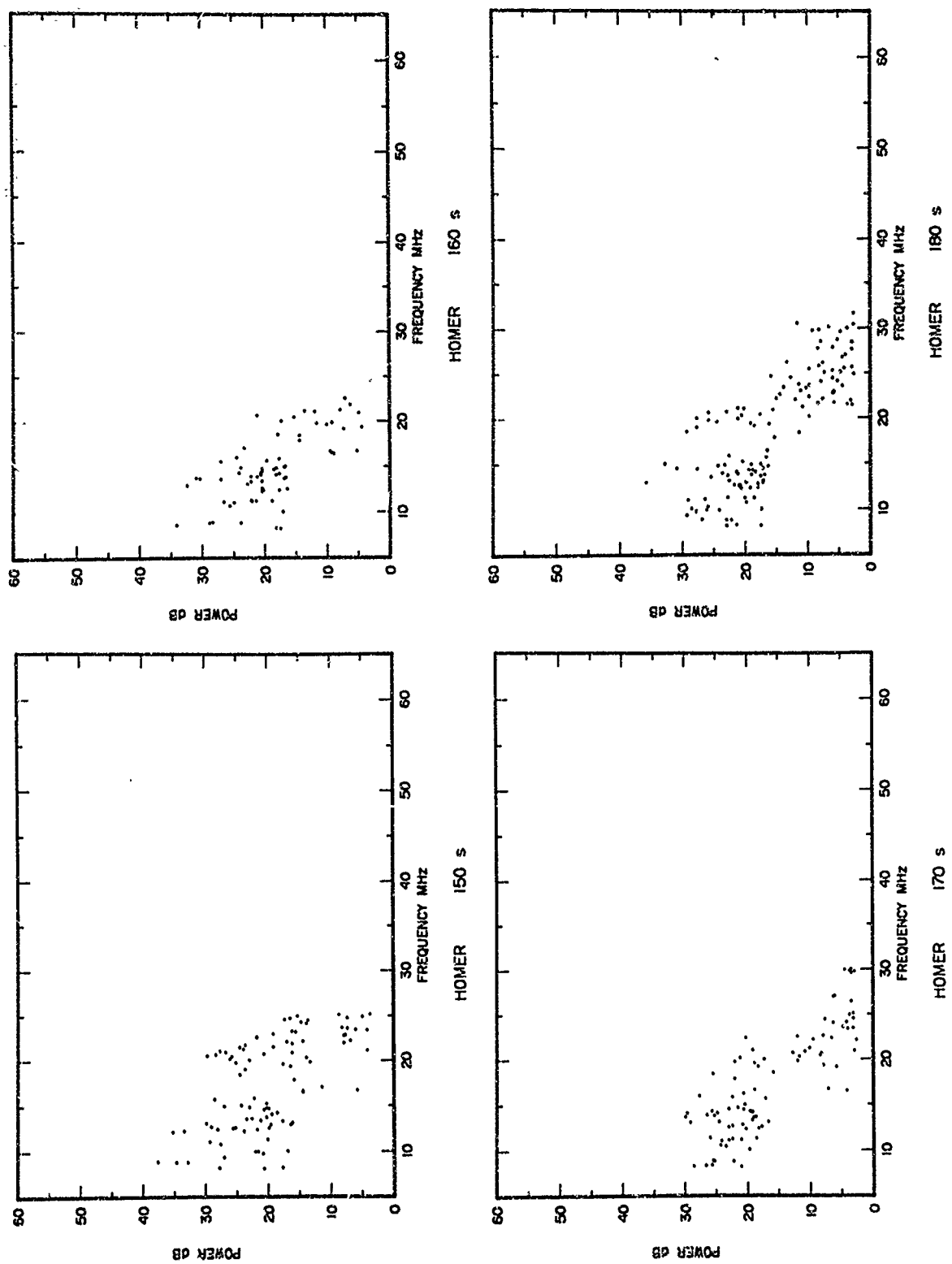
HOMER 150 s
HOMER 160 s
HOMER 170 s
HOMER 180 s
FREQUENCY MHz
POWER dB
0
10
20
30
40
50
60

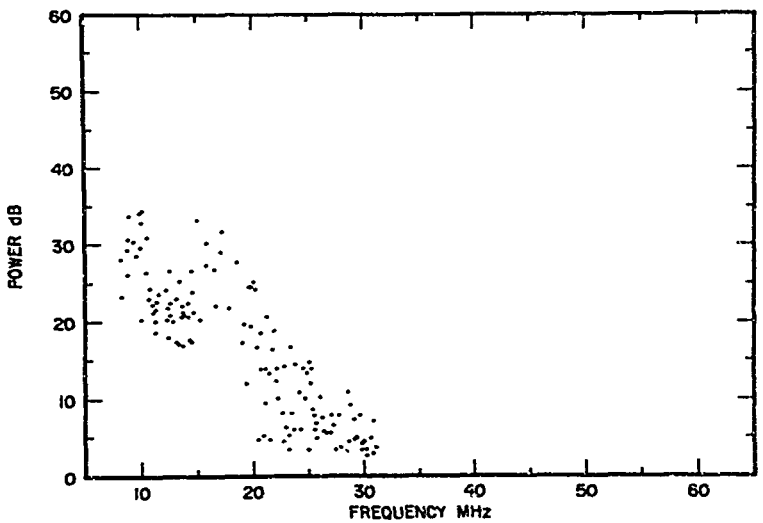


HOMER 190 s

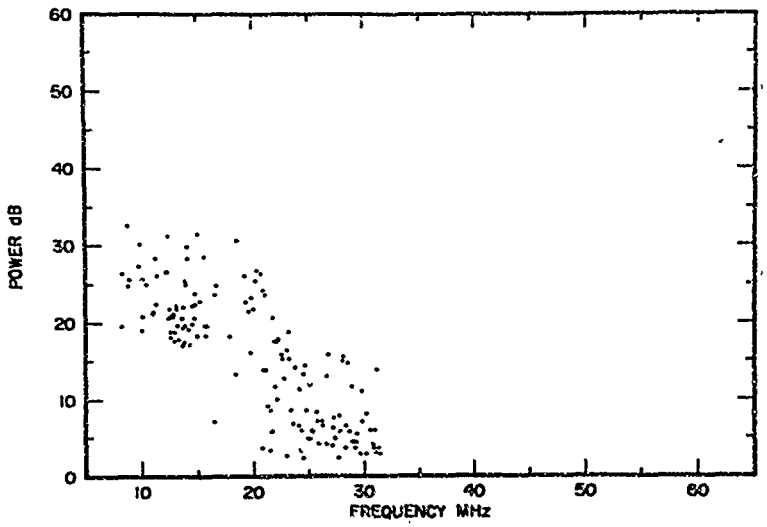


HOMER 200 s

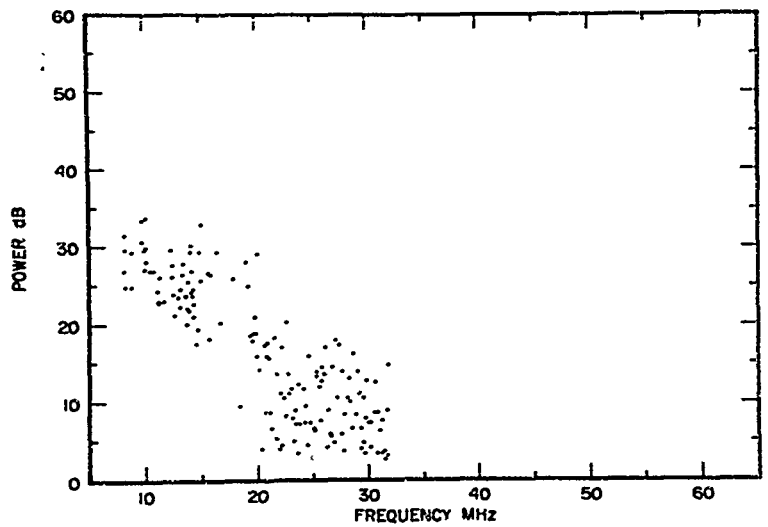


HOMER 210 s

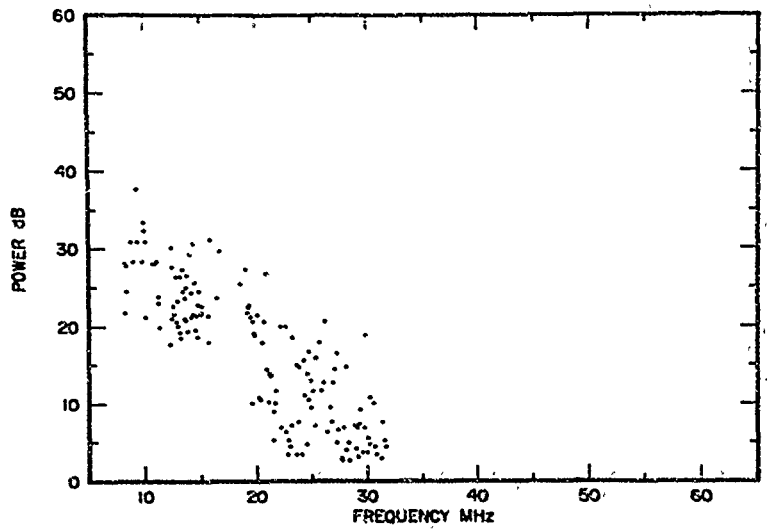


HOMER 220 s

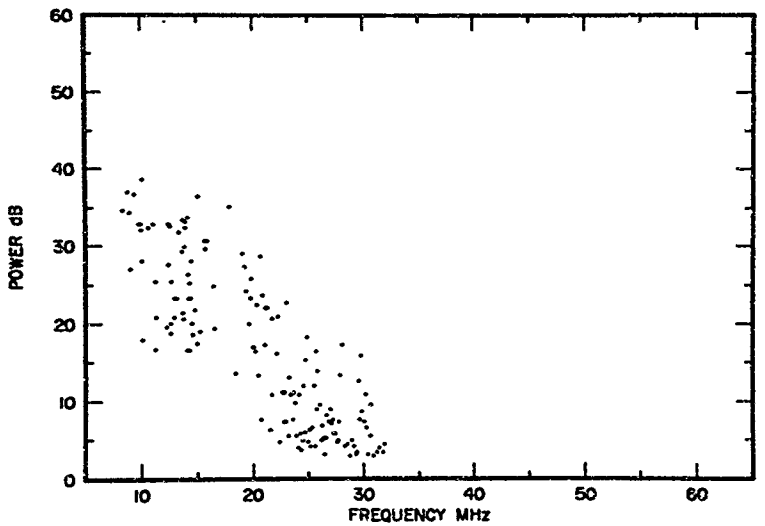


HOMER 230 s

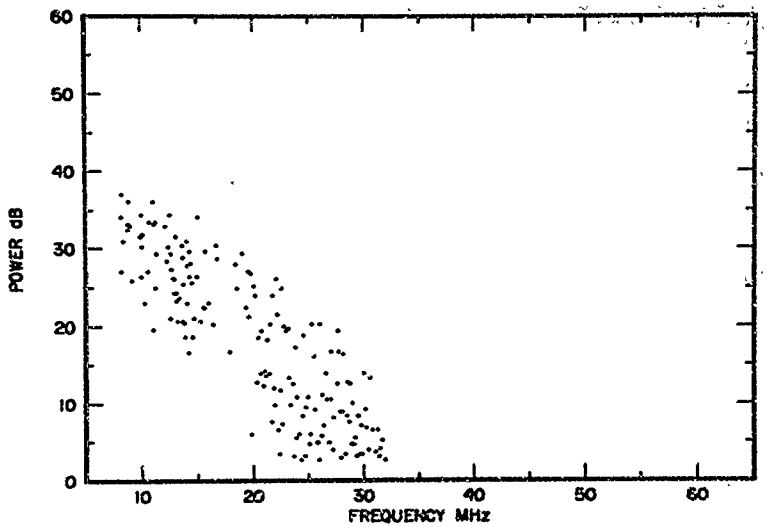


HOMER 240 s

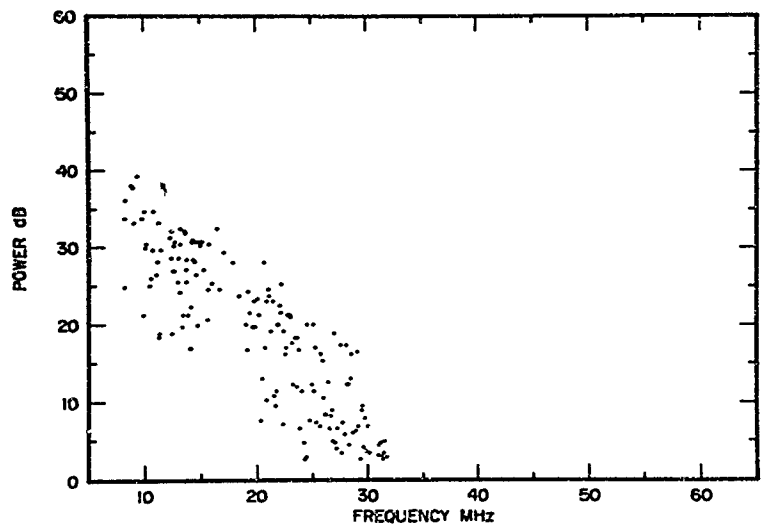


HOMER 250 s

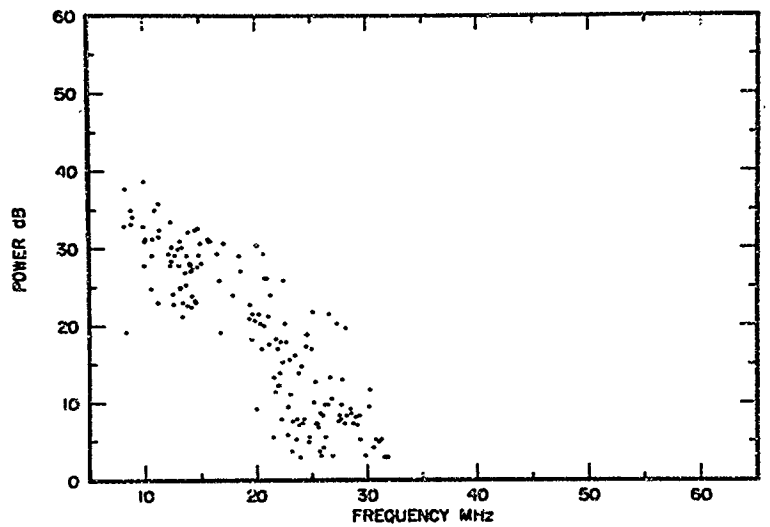


HOMER 260 s

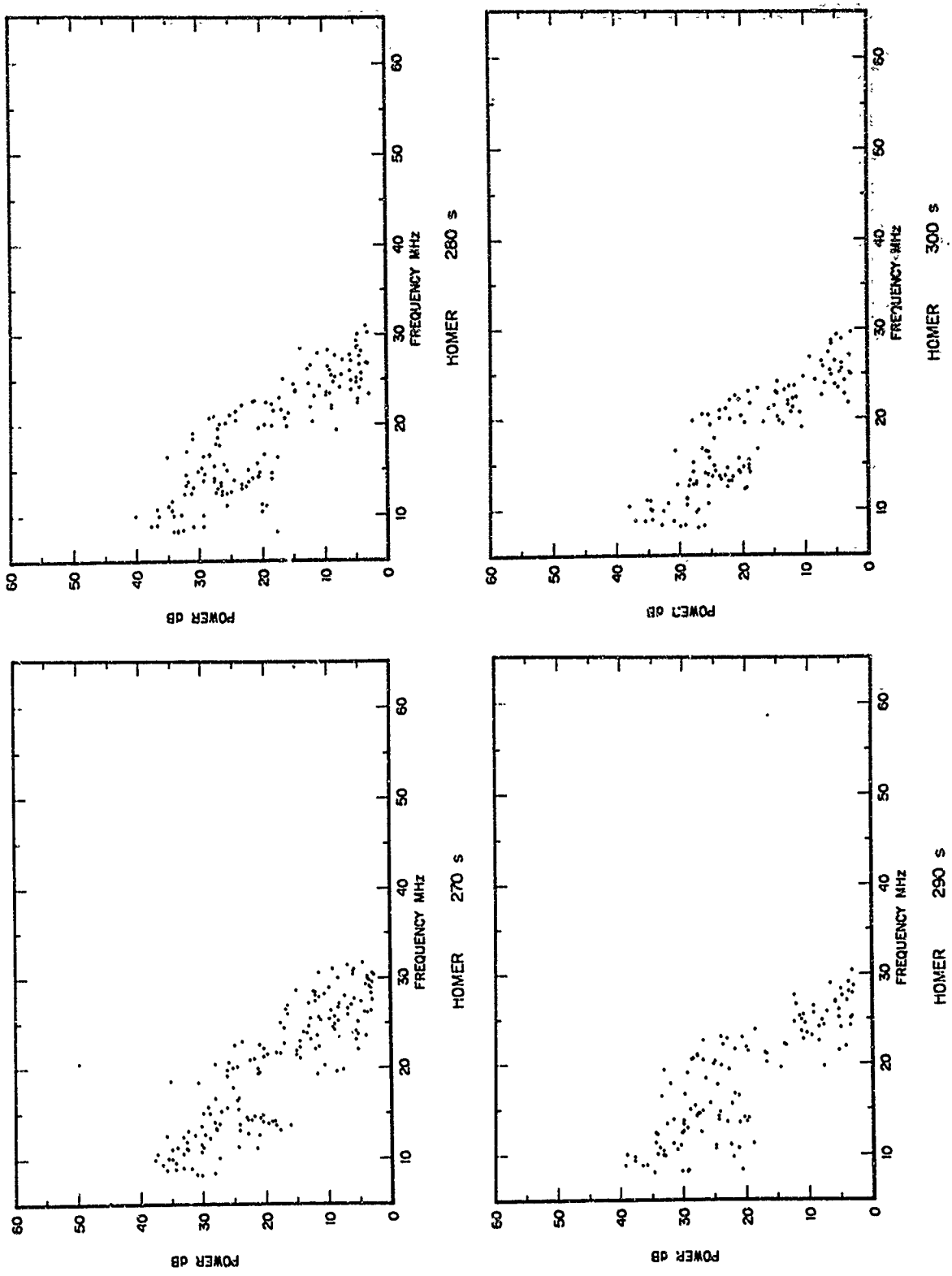
HOMER 270 s
HOMER 280 s
HOMER 290 s
HOMER 300 s
POWER dB
FREQUENCY MHz
0
10
20
30
40
50
60

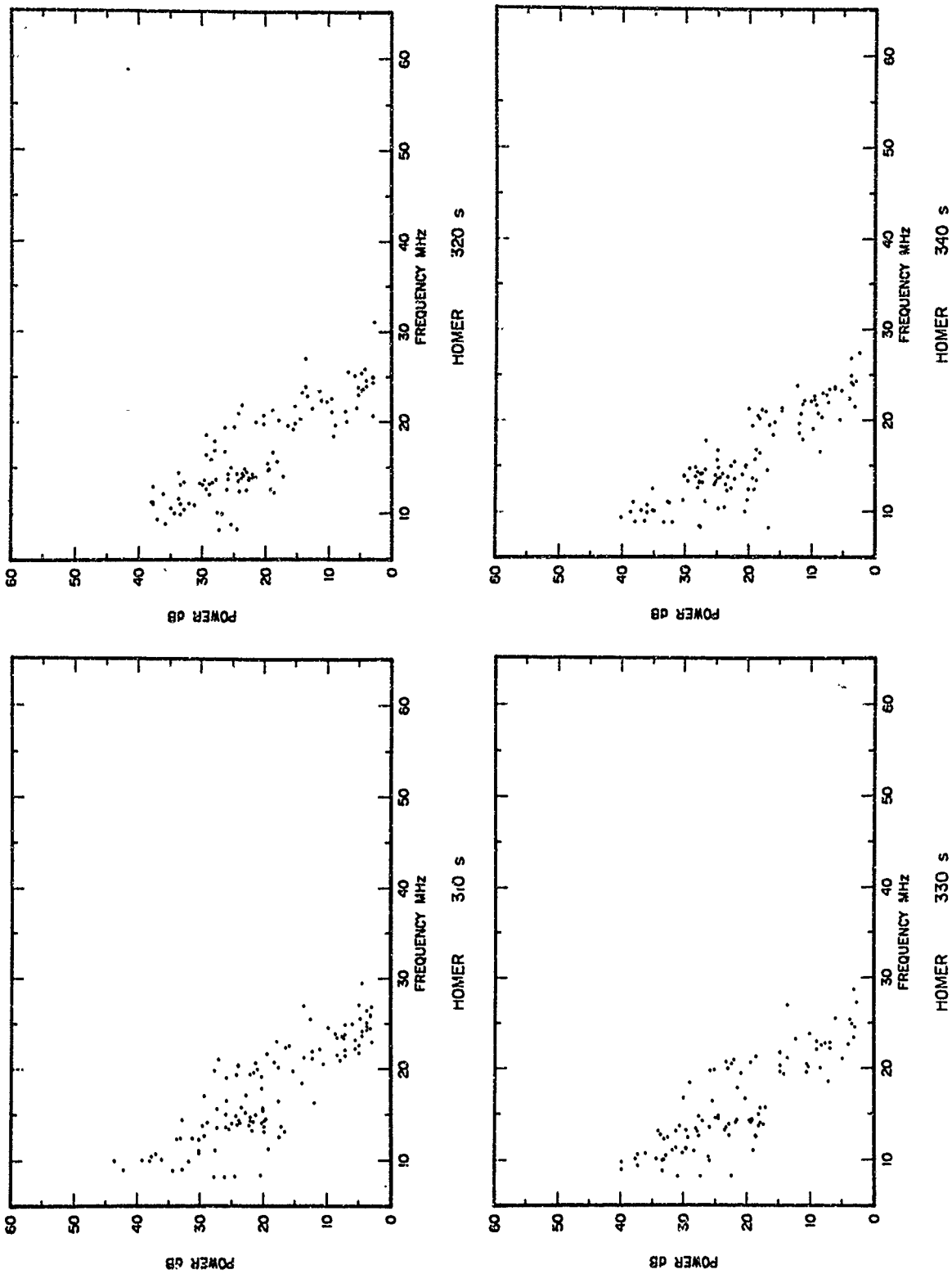
HOMER 310 s
HOMER 320 s
HOMER 330 s
HOMER 340 s
POWER dB
FREQUENCY MHz
0
10
20
30
40
50
60

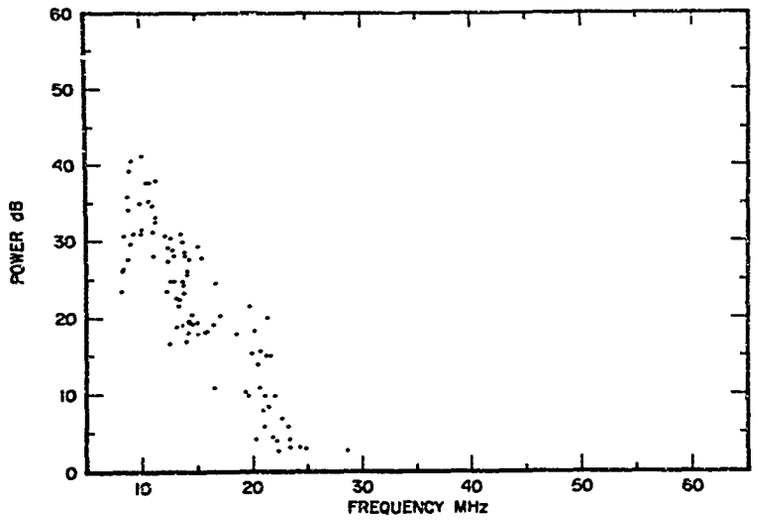


HOMER 350 s

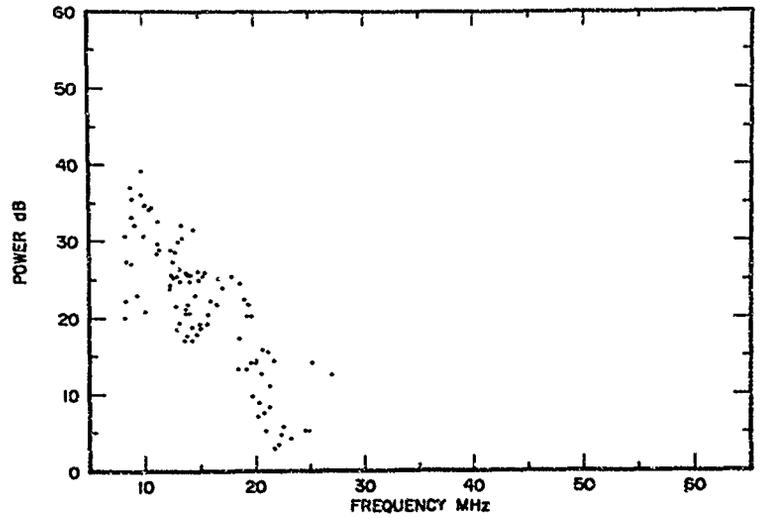


HOMER 360 s

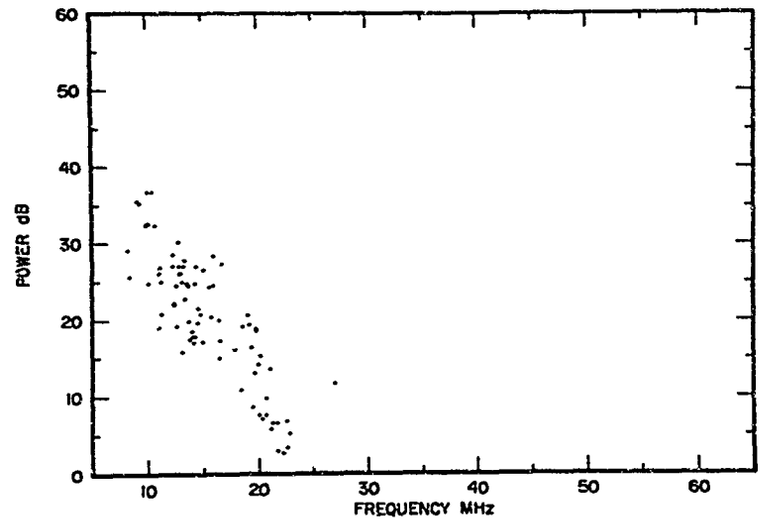


HOMER 370 s

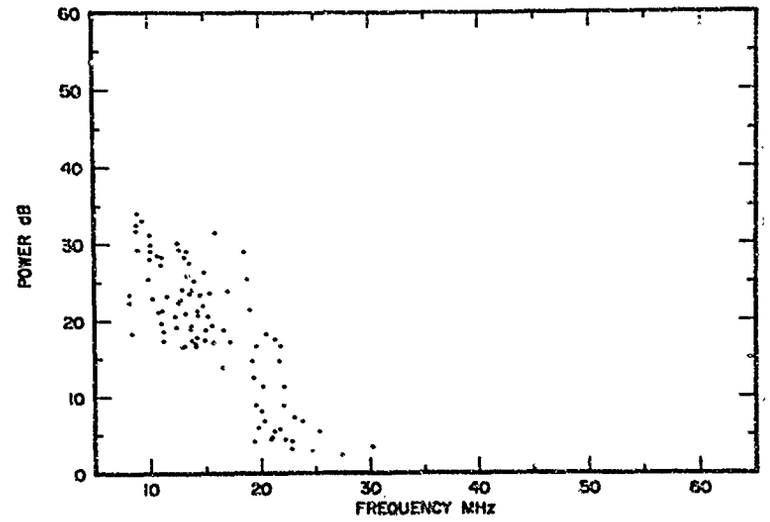


HOMER 380 s

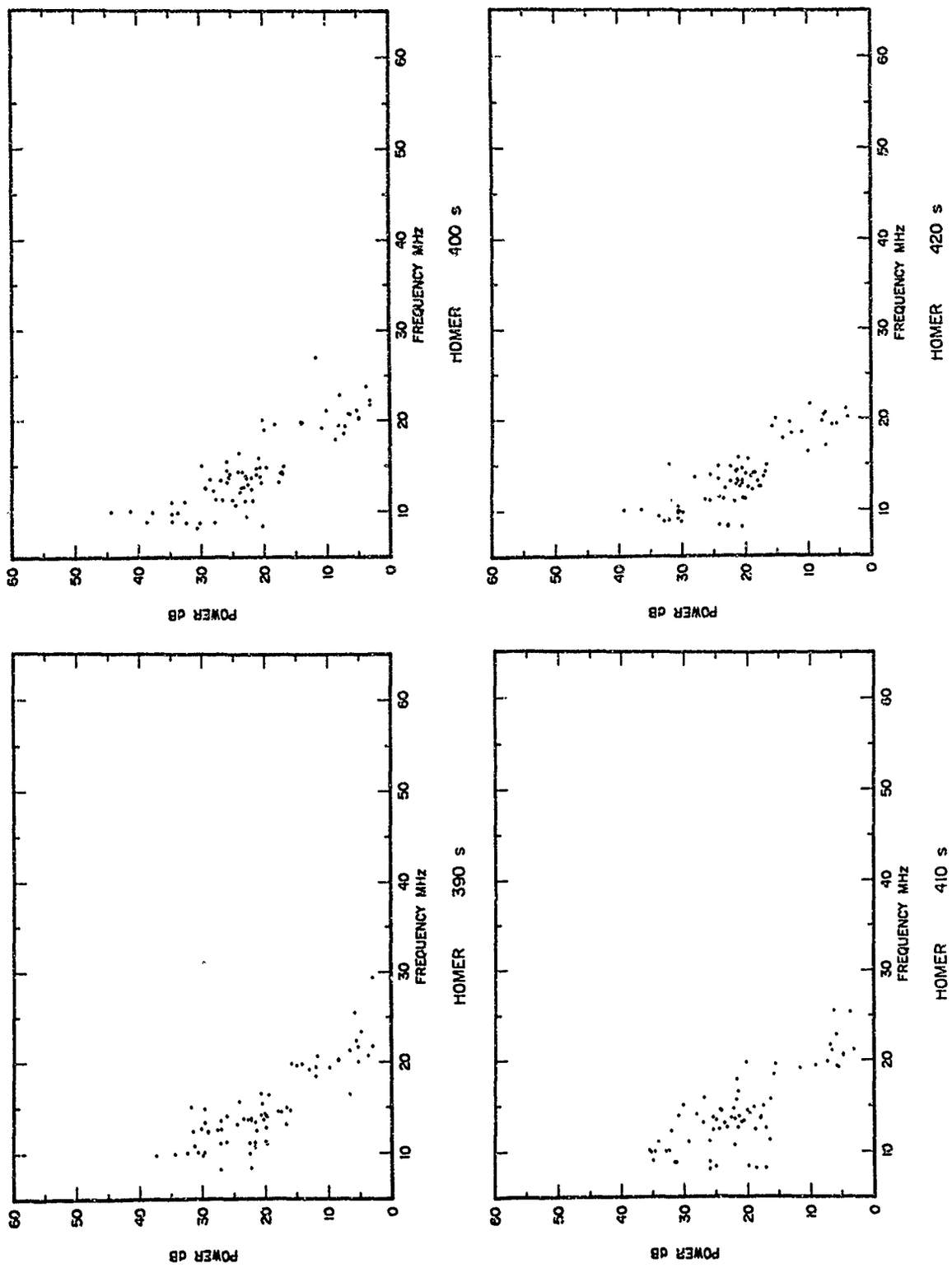
HOMER 390 s
HOMER 400 s
HOMER 410 s
HOMER 420 s
FREQUENCY MHz
POWER dB
0
10
20
30
40
50
60

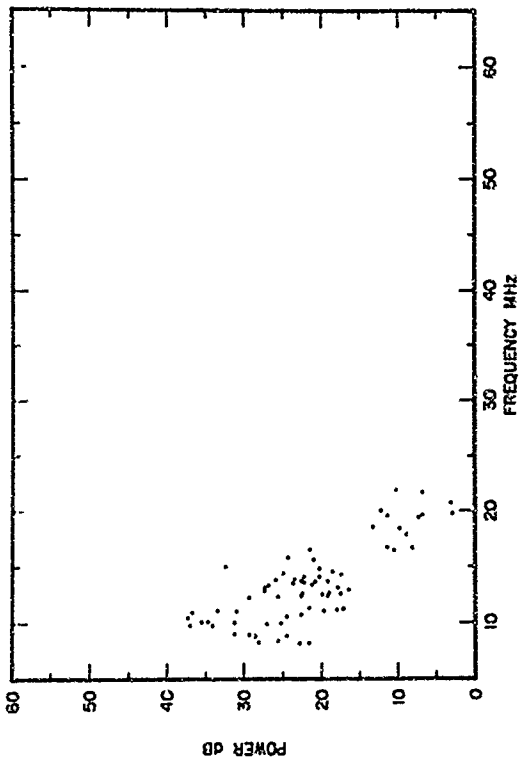
POWER dB
FREQUENCY MHz
HOMER 440 s

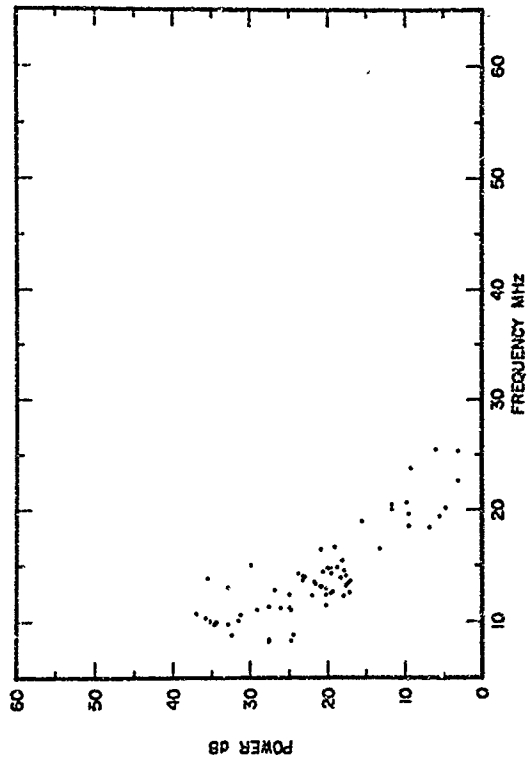
POWER dB
FREQUENCY MHz
HOMER 460 s

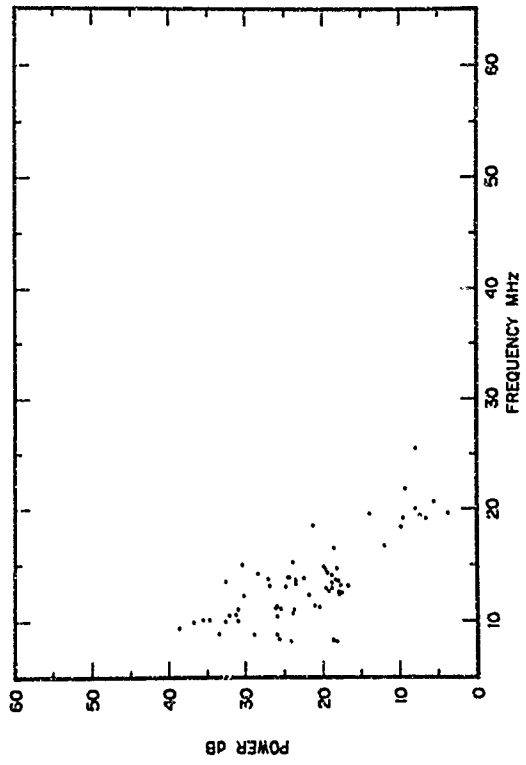
POWER dB
FREQUENCY MHz
HOMER 430 s

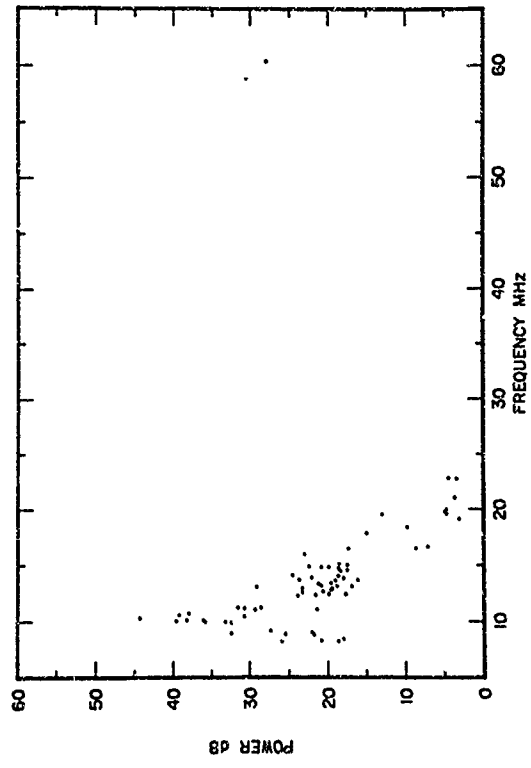
POWER dB
FREQUENCY MHz
HOMER 450 s

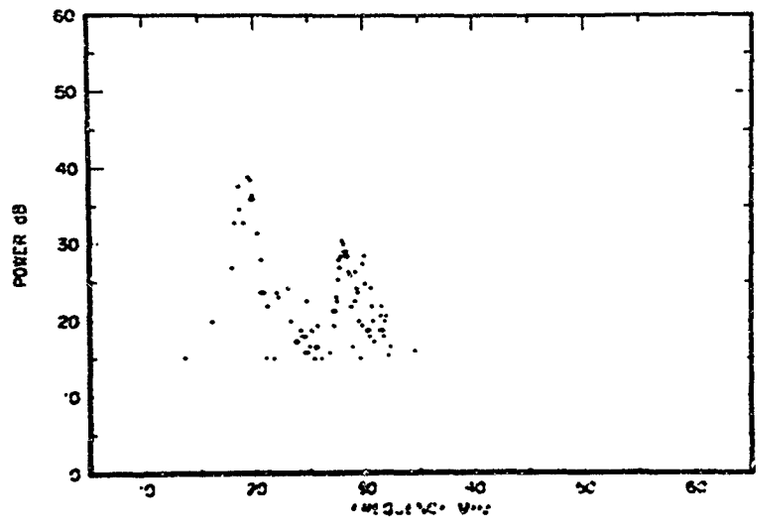


90 s

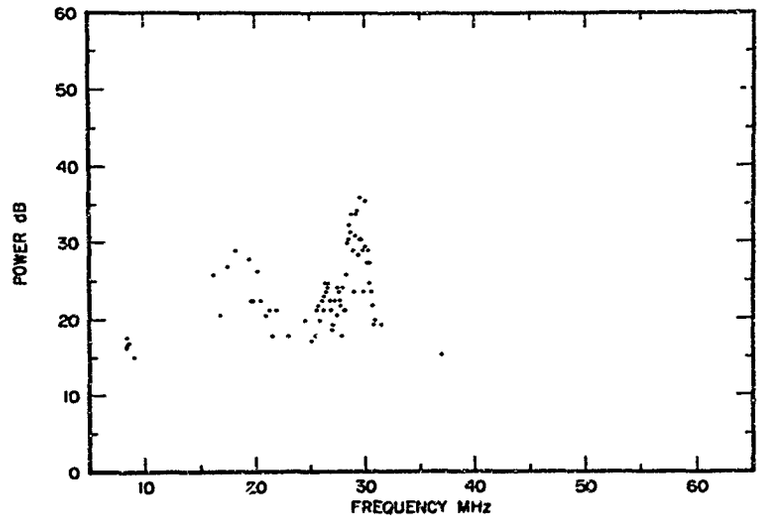


KODIAK 110 s

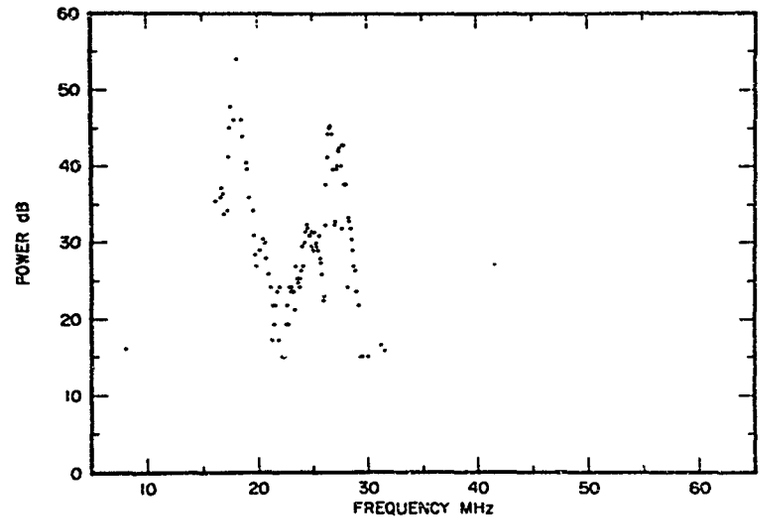


KODIAK 130 s

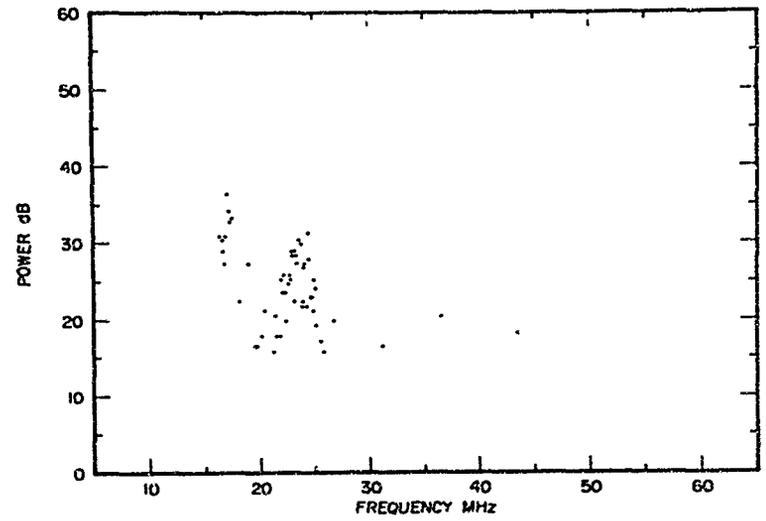


KODIAK 150 s

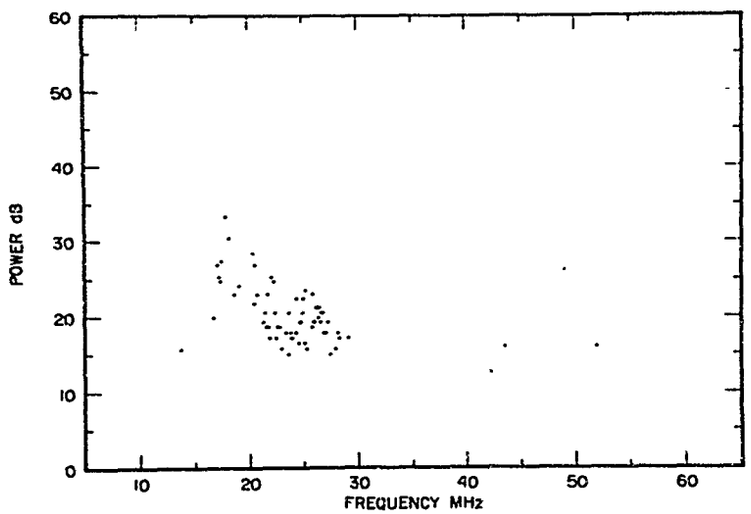


KODIAK 10 s

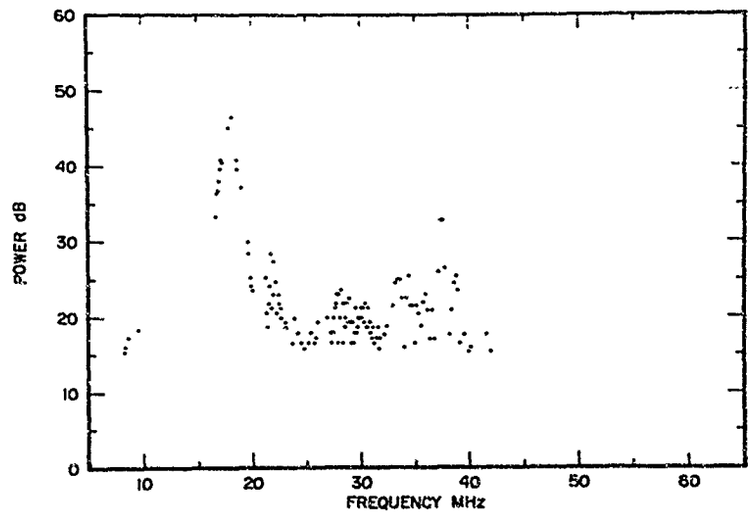


KODIAK 30 s

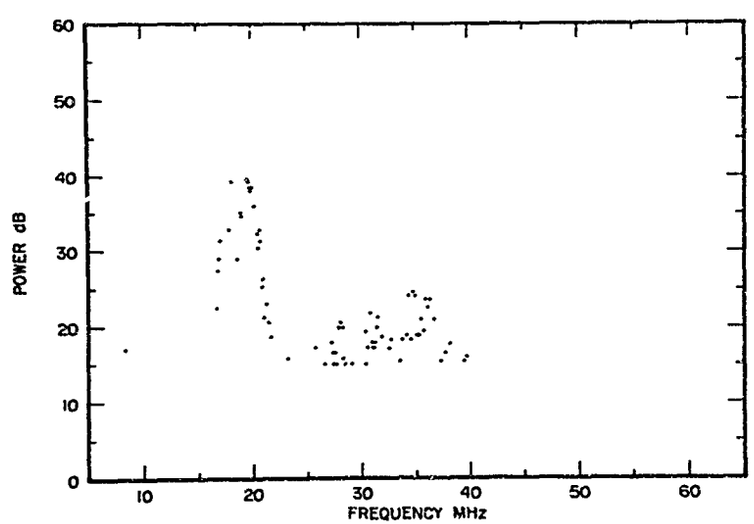


KODIAK 50 s

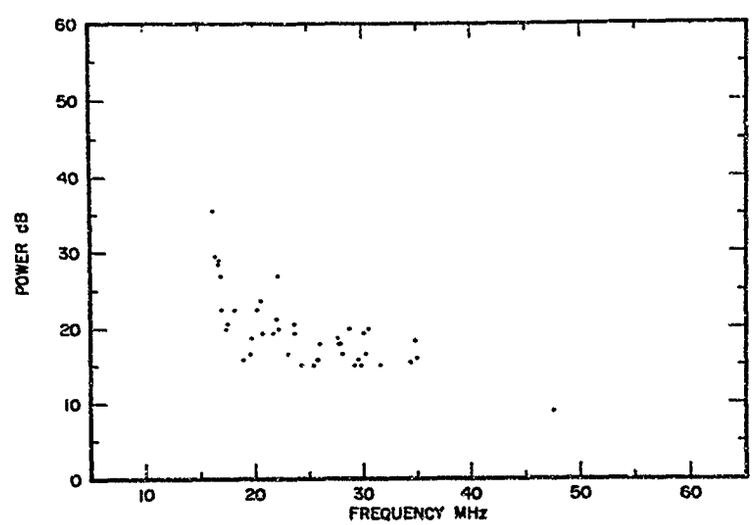


KODIAK 70 s

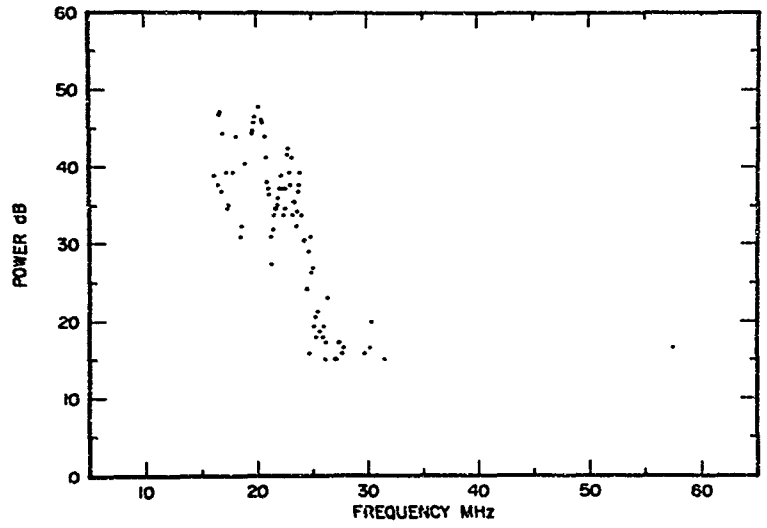


KODIAK 170 s

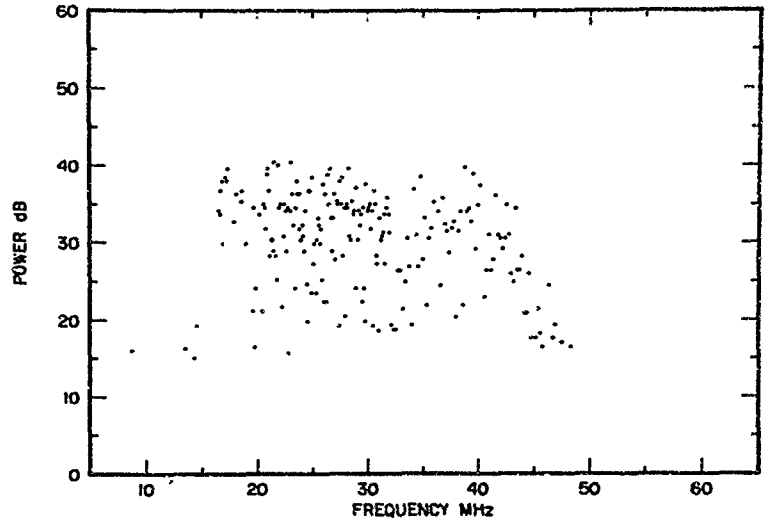


KODIAK 190 s

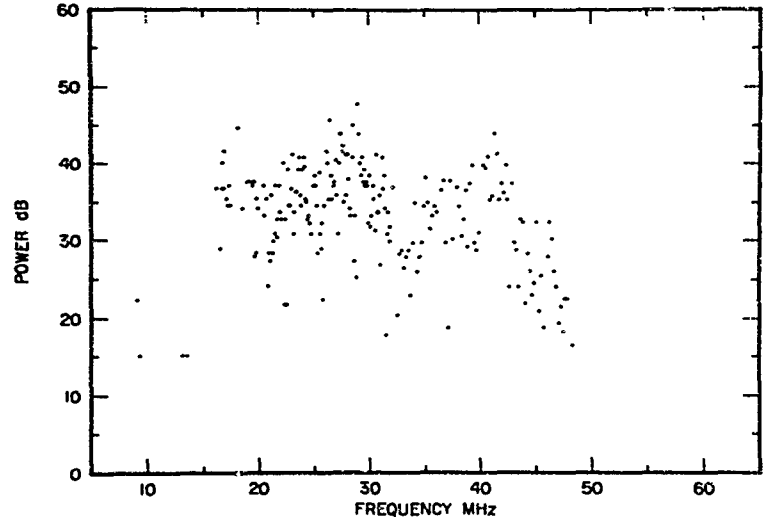


KODIAK 210 s

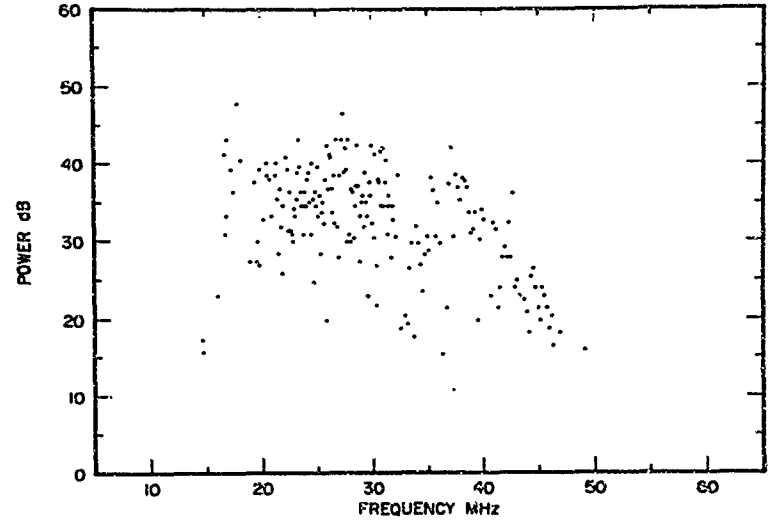


KODIAK 230 s

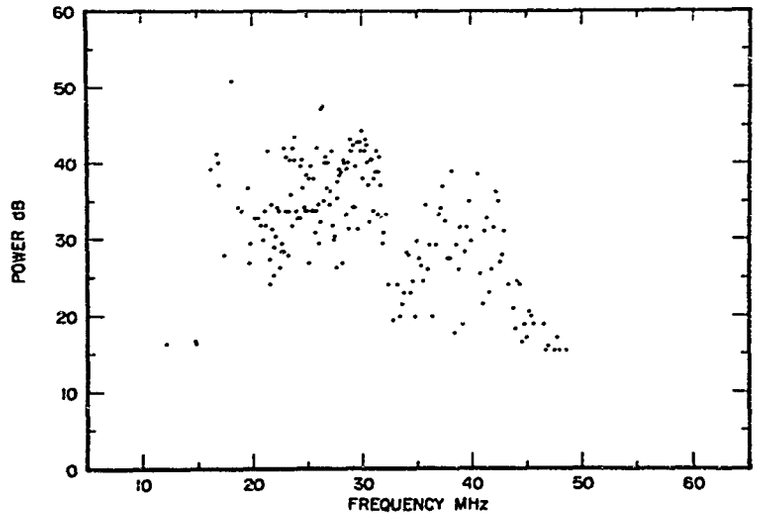


KODIAK 250 s

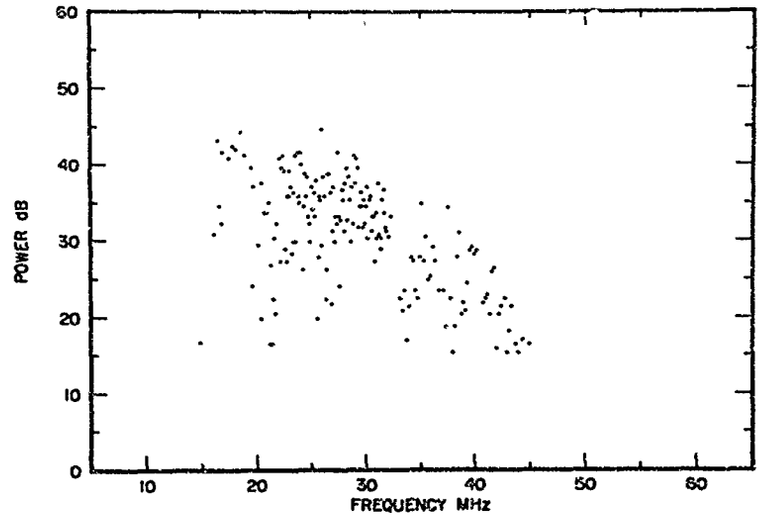


KODIAK 270 s

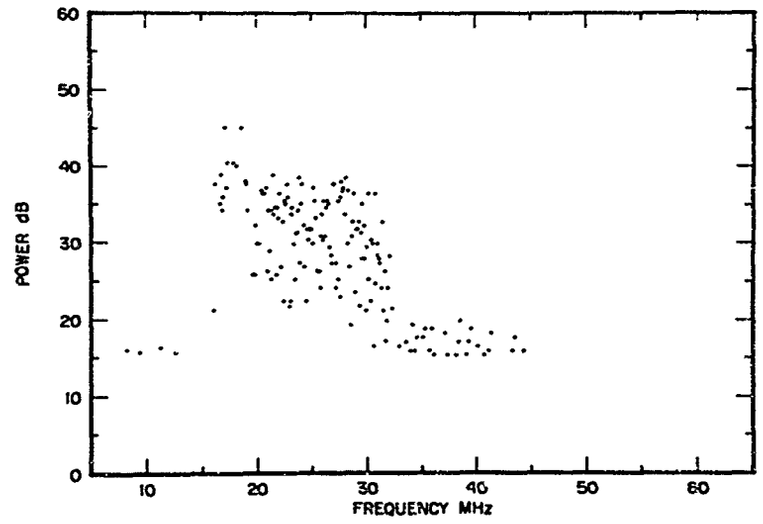


KODIAK 290 s

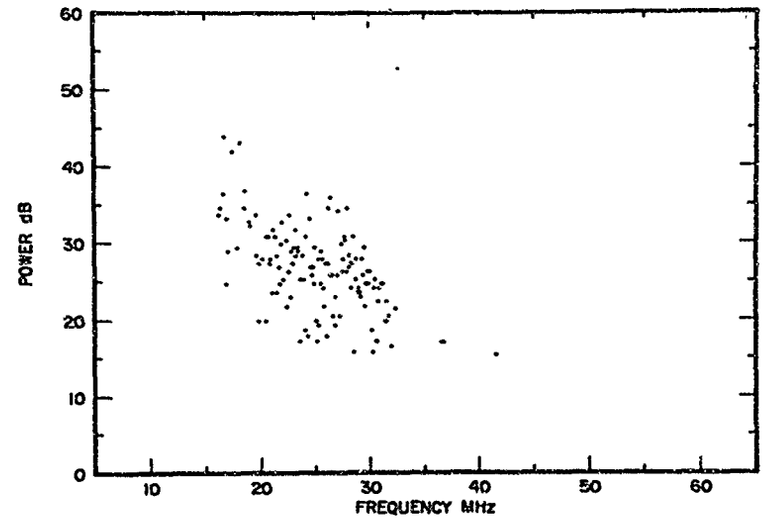


KODIAK 310 s

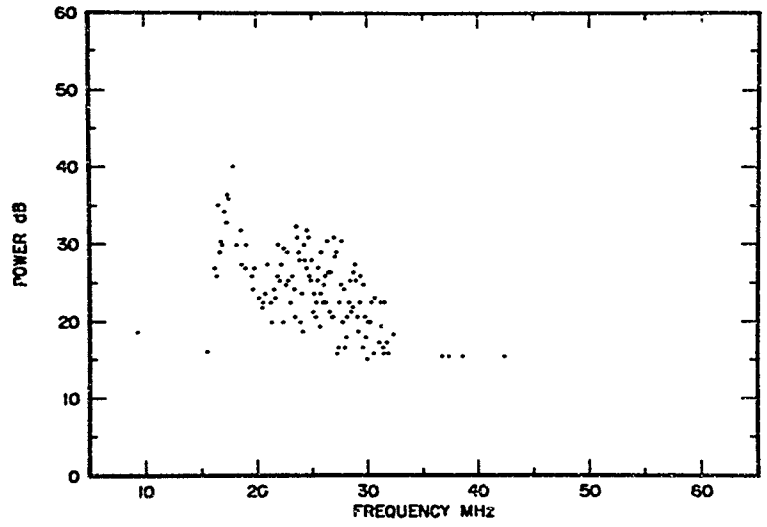


KODIAK 330 s

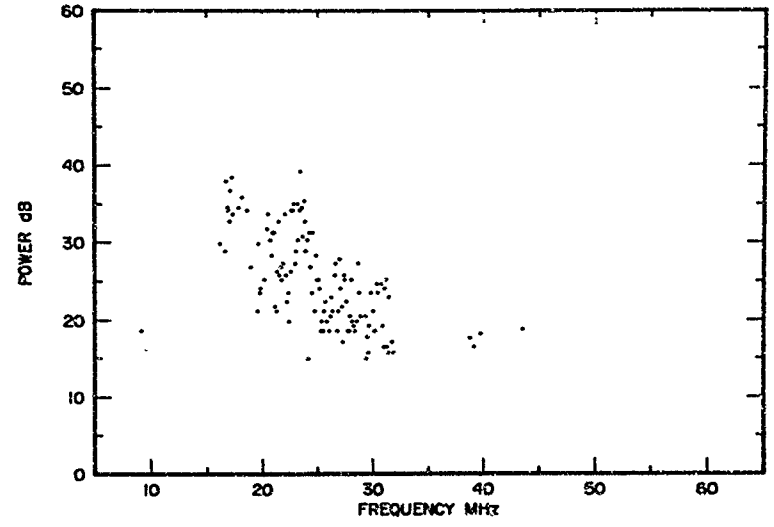


KODIAK 350 s

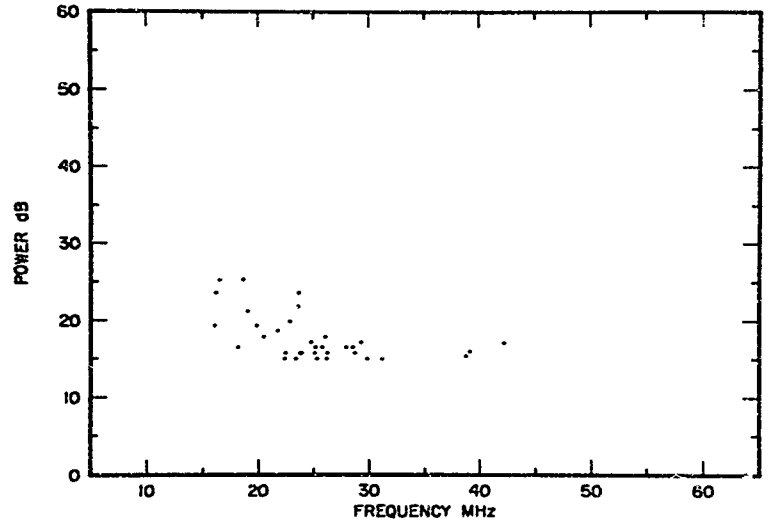


KODIAK 370 s

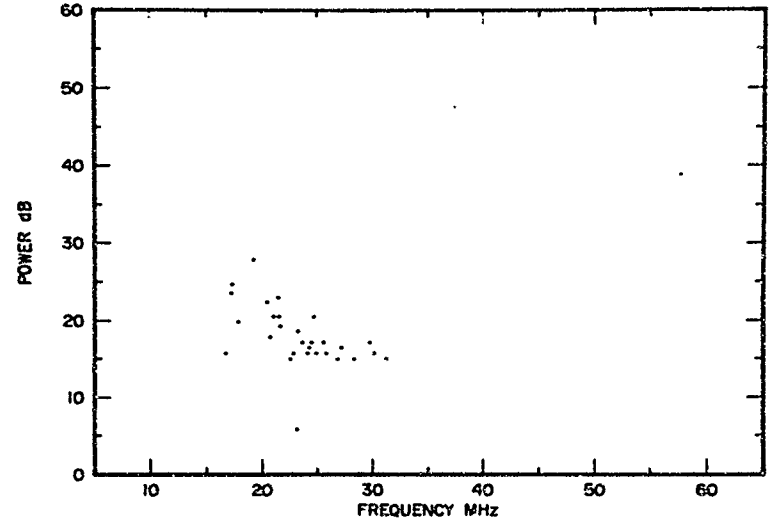


KODIAK 390 s

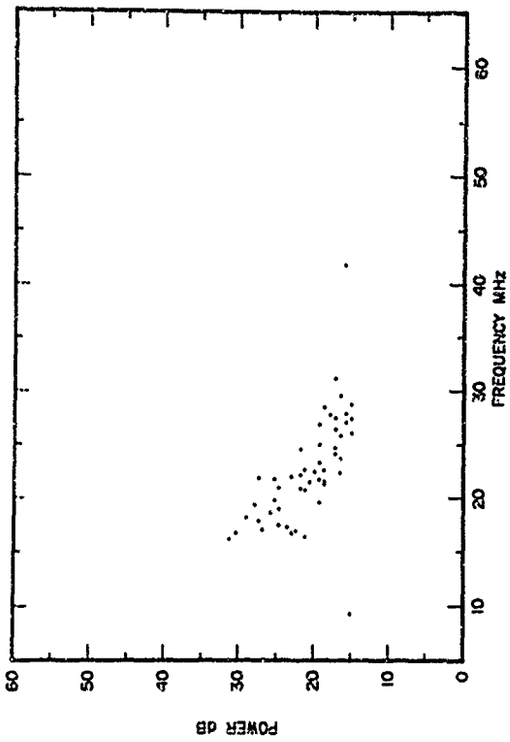


KODIAK 430 s

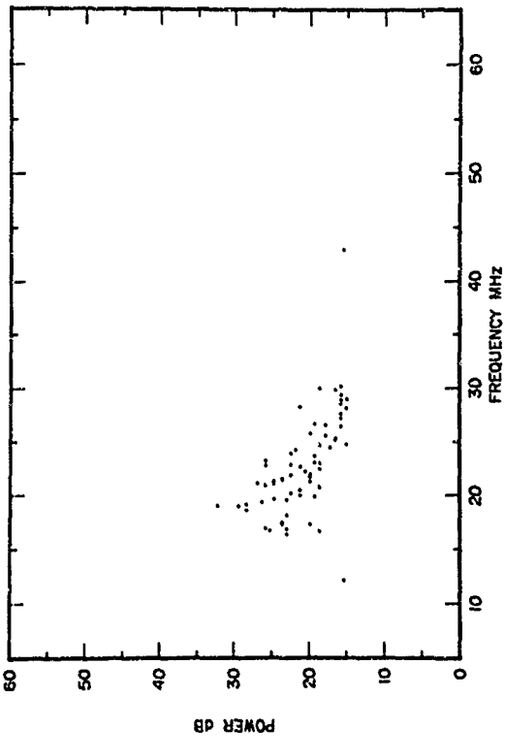


KODIAK 410 s

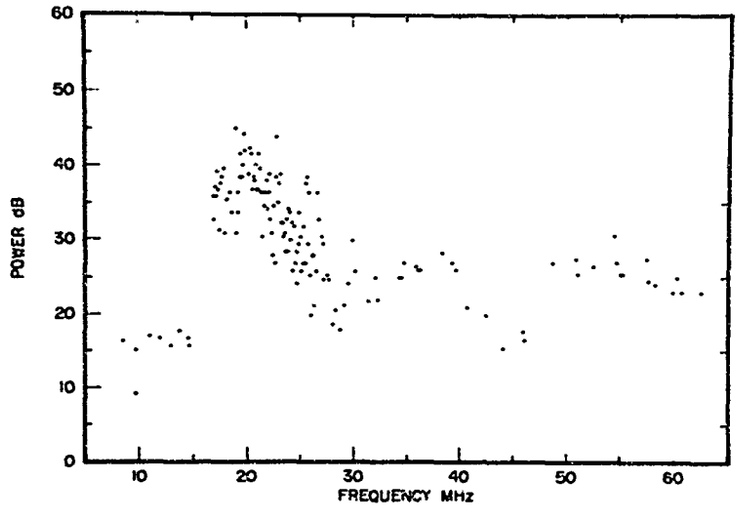


KODIAK GUM 500 s

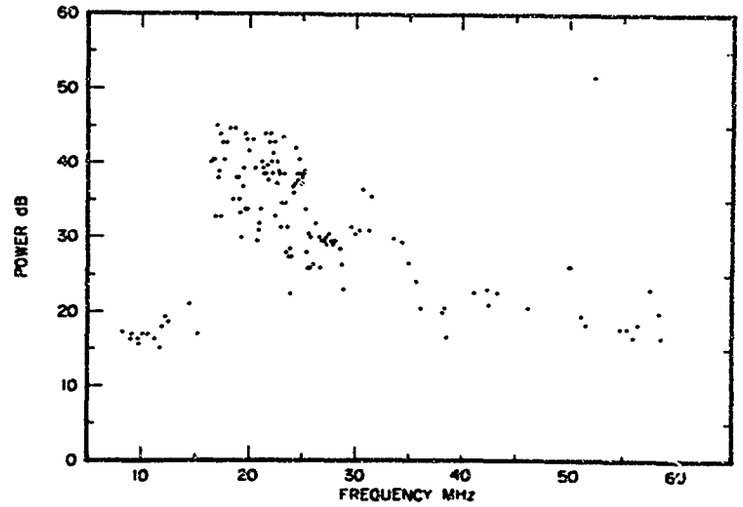


KODIAK GUM 520 s

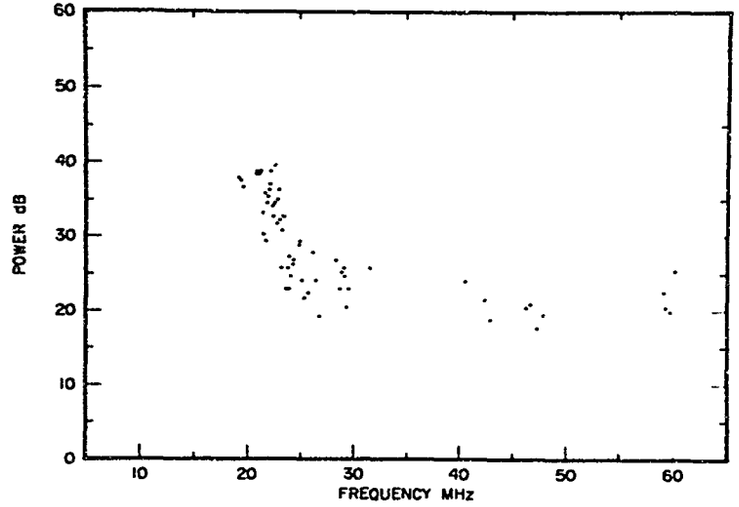


KODIAK GUM 540 s

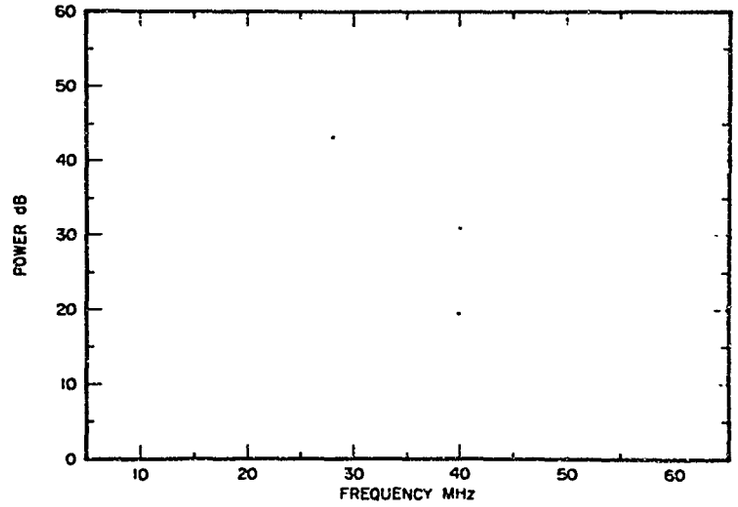


KODIAK GUM 560 s

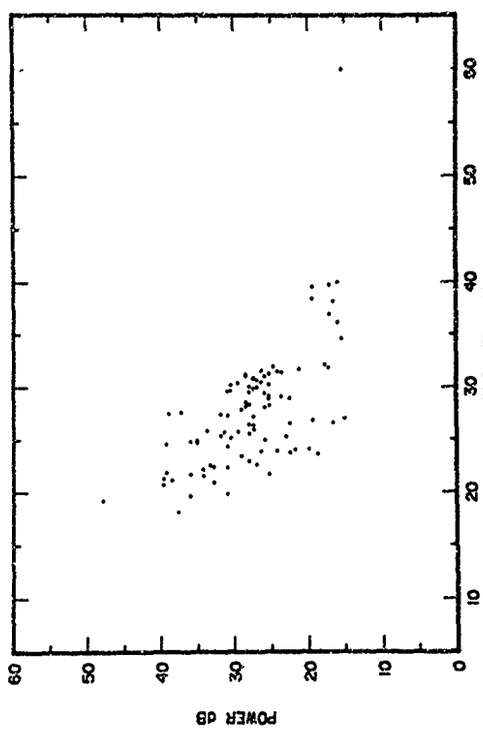


KODIAK GUM 660 s

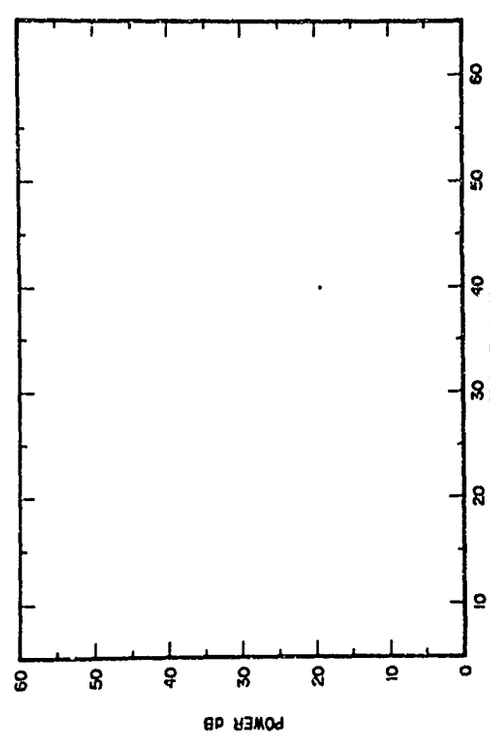


KODIAK GUM 680 s

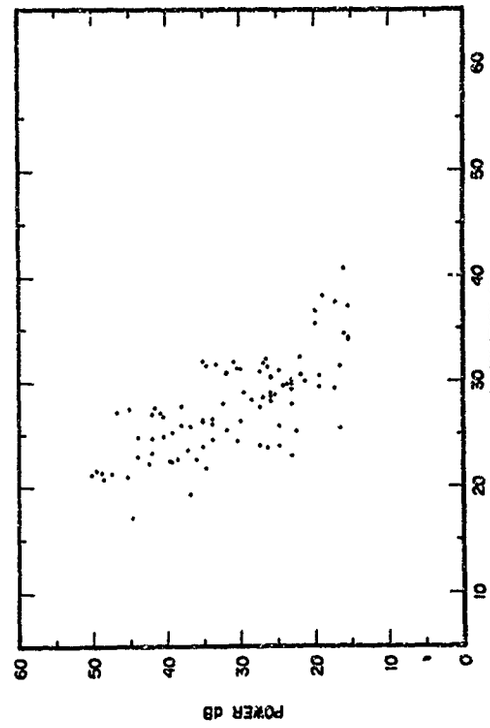


KODIAK GUM 700 s

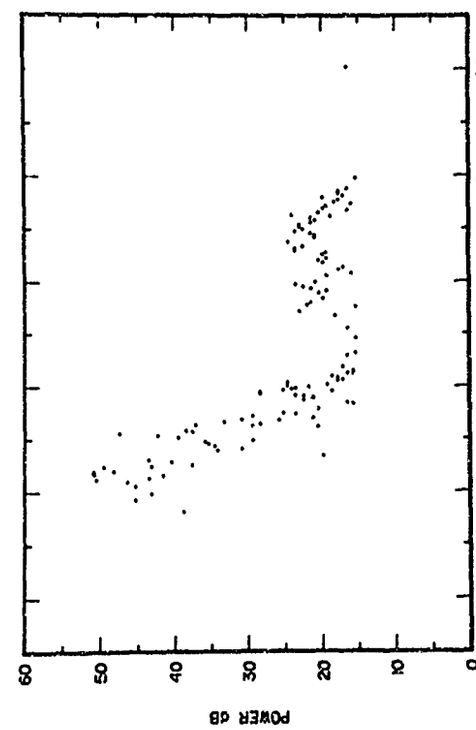


KODIAK GUM 710 s

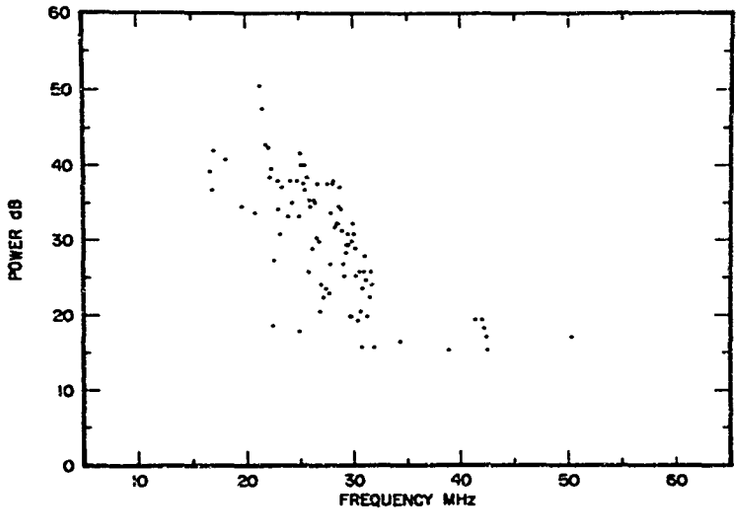


KODIAK GUM 720 s

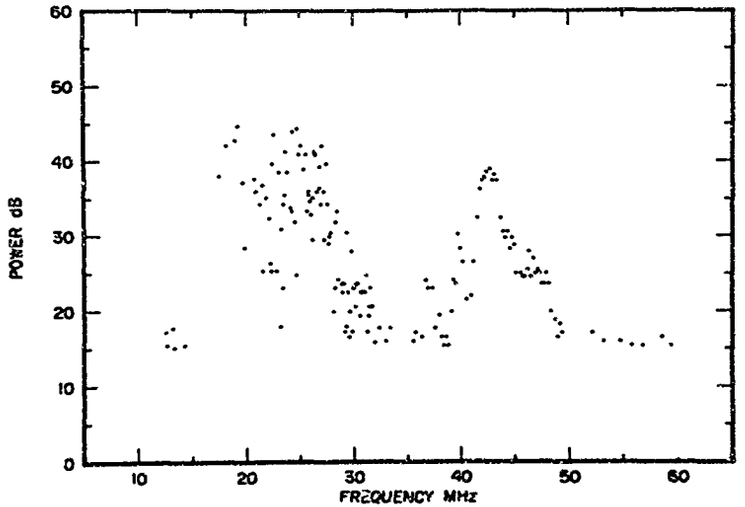


KODIAK GUM 740 s

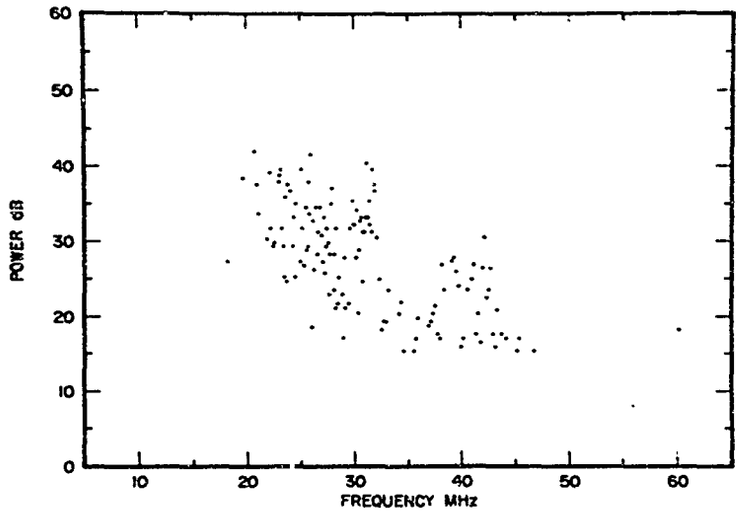


KODIAK GUM 760 s

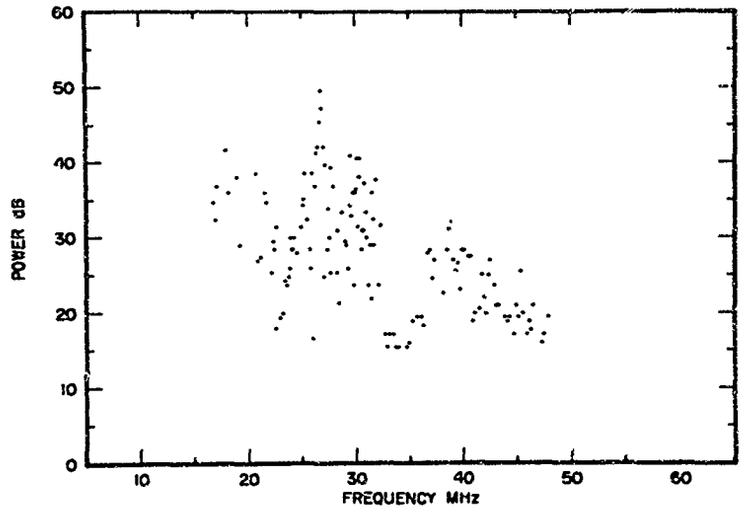


KODIAK GUM 770 s

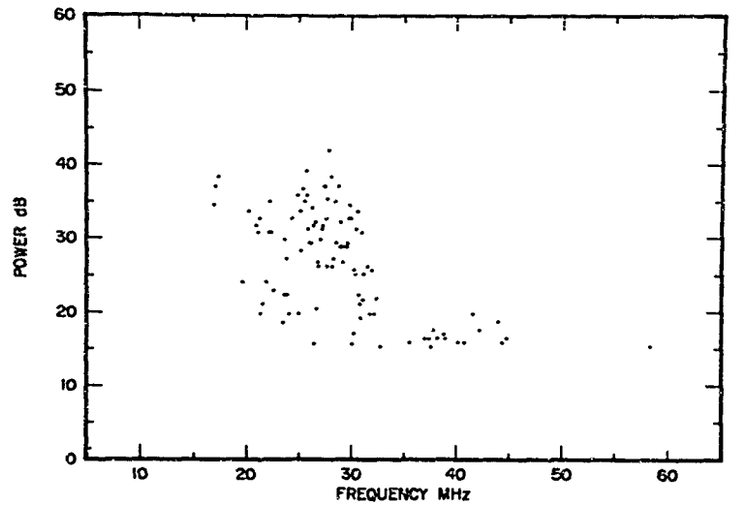


KODIAK GUM 780 s

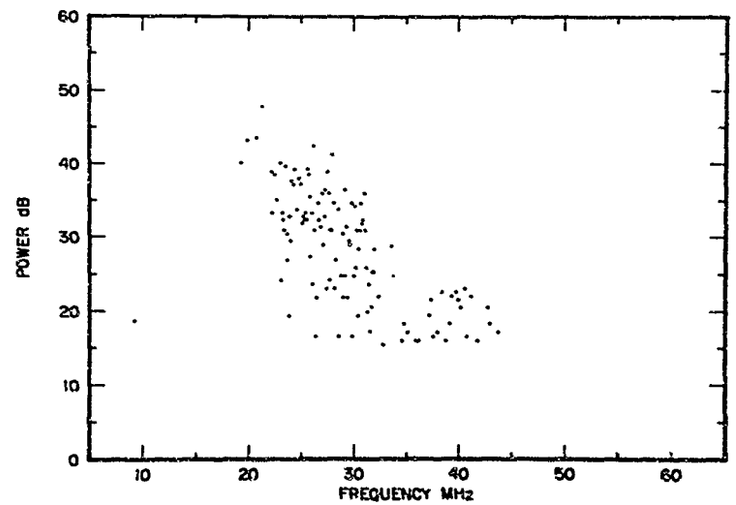


KODIAK GUM 800 s

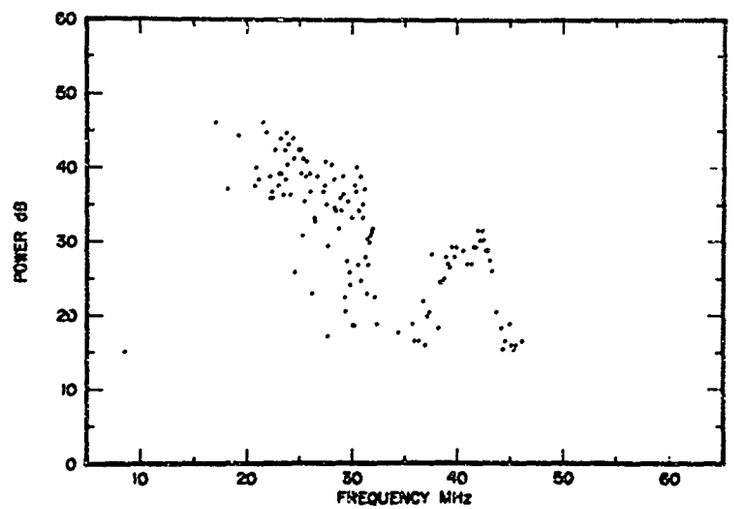


KODIAK GUM 840 s

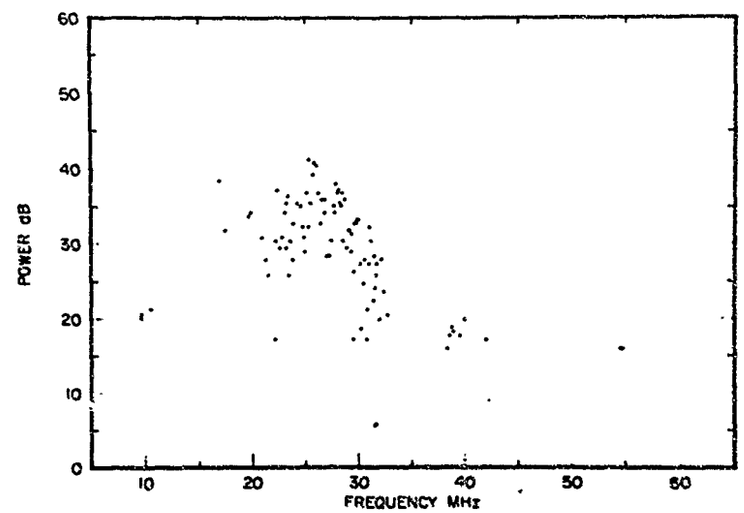


KODIAK GUM 860 s

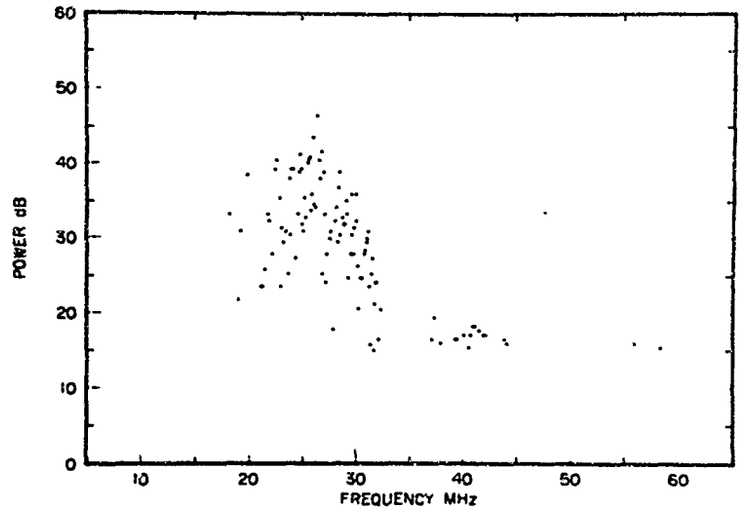


KODIAK GUM 880 s

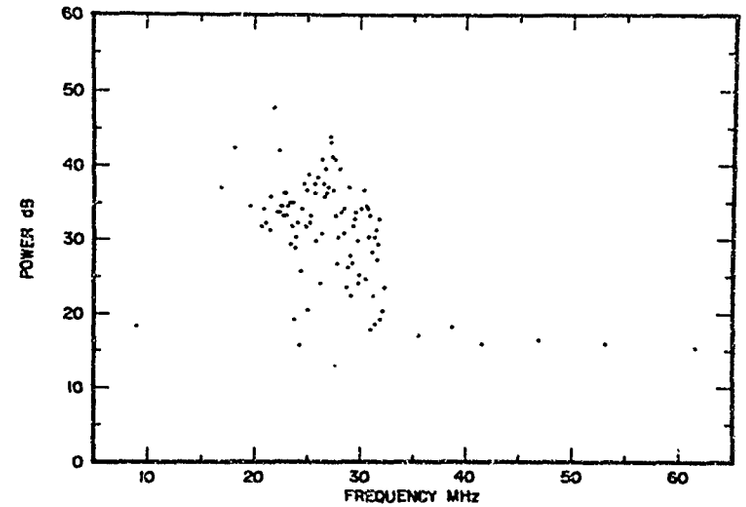


KODIAK GUM 900 s

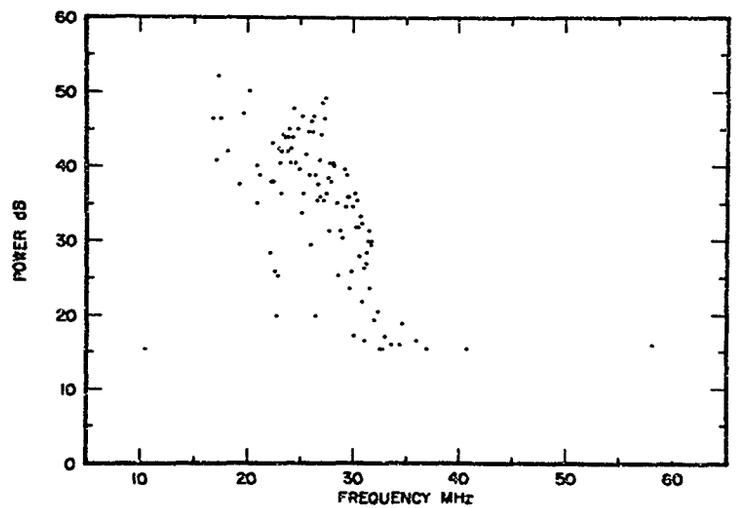


KODIAK GUM 920 s

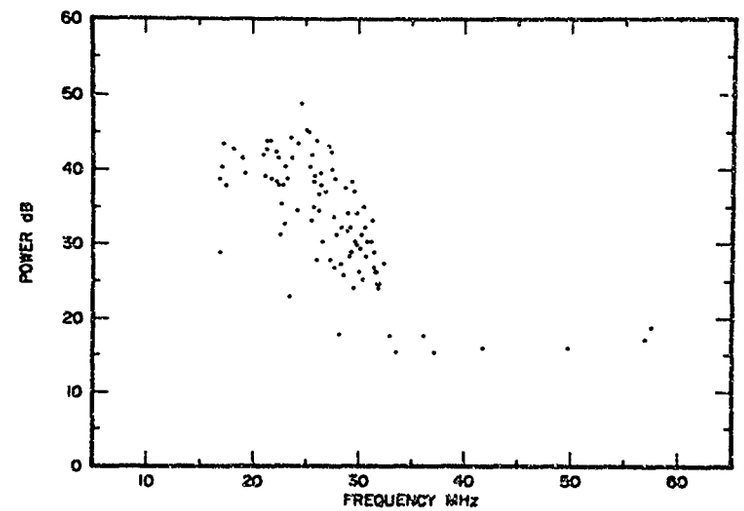


KODIAK GUM 940 s

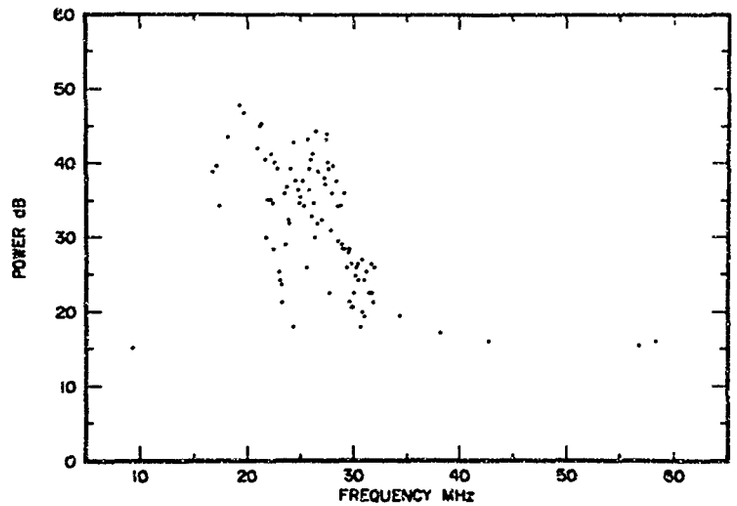


KODIAK GUM 960 s

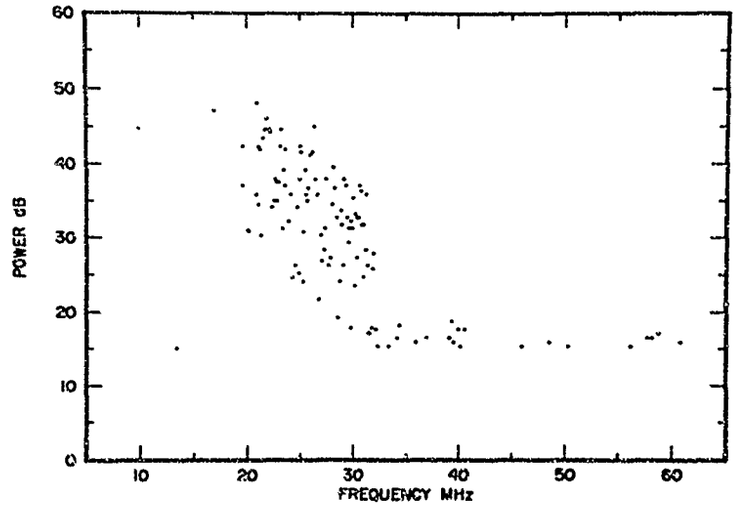


KODIAK GUM 980 s

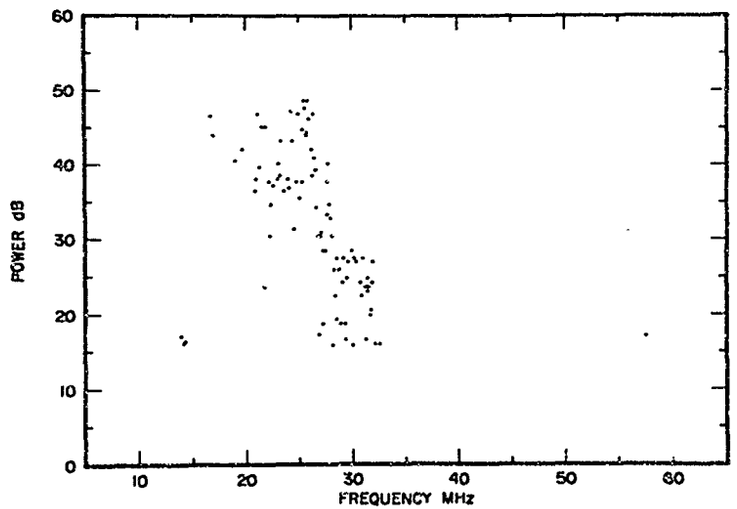


KODIAK GUM 1000 s

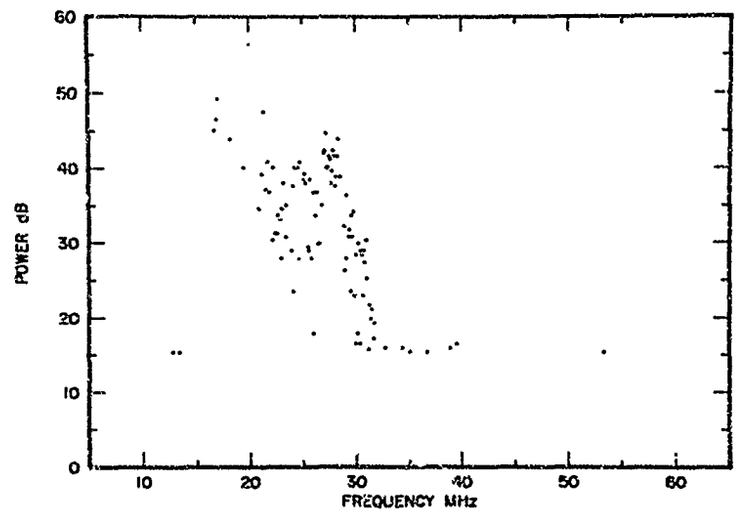


KODIAK GUM 1020 s

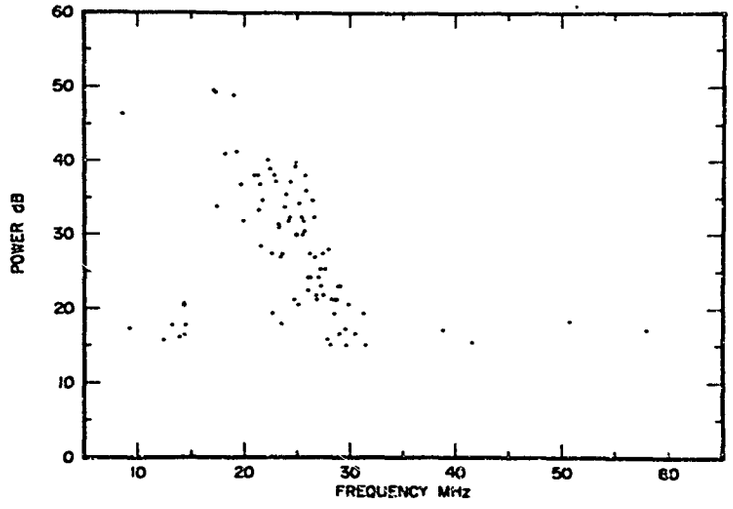


KODIAK GUM 1040 s

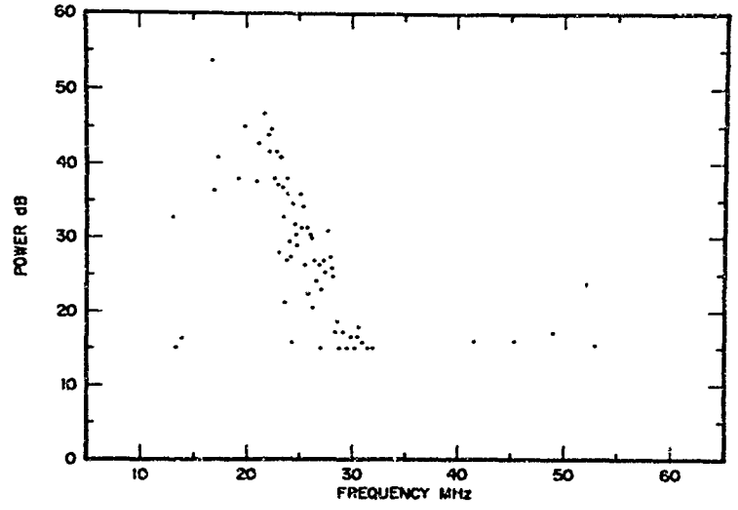


KODIAK GUM 1060 s

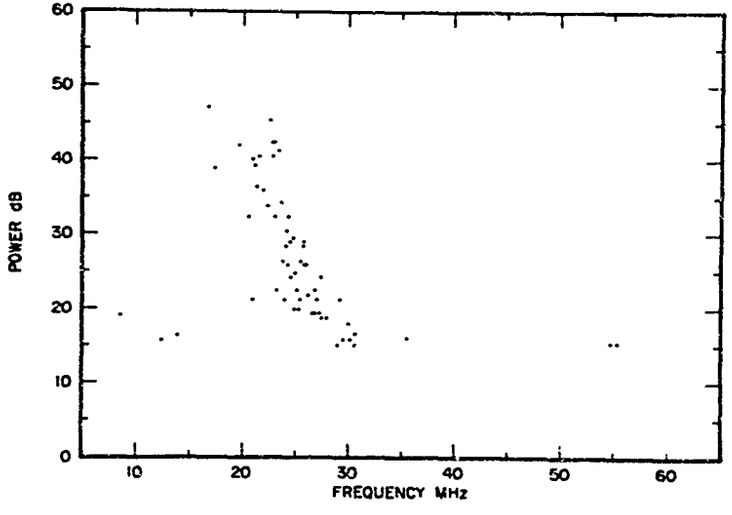


KODIAK GUM 1080 s

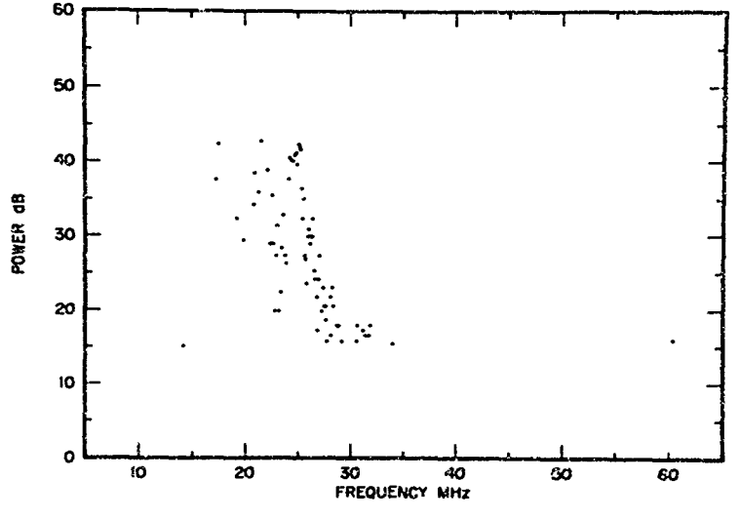


KODIAK GUM 1100 s

# APPENDIX B

## AVERAGE-POWER-VS.-TIME PLOTS

## APPENDIX B

## AVERAGE-POWER-VS.-TIME PLOTS

The records in this appendix were derived by averaging the maximum echo signal obtained from each frequency scan over a 2-MHz band and plotting the result as a function of time after release. The procedure was to convert the log-power data used for the plots in Appendix A to power, then average, and then convert back to log-power. All of the comments in Appendix A apply to the data in Appendix B.

The HEMLOCK records are shown on pages B-4 through B-10, and the GUM records from B-10 through B-14.

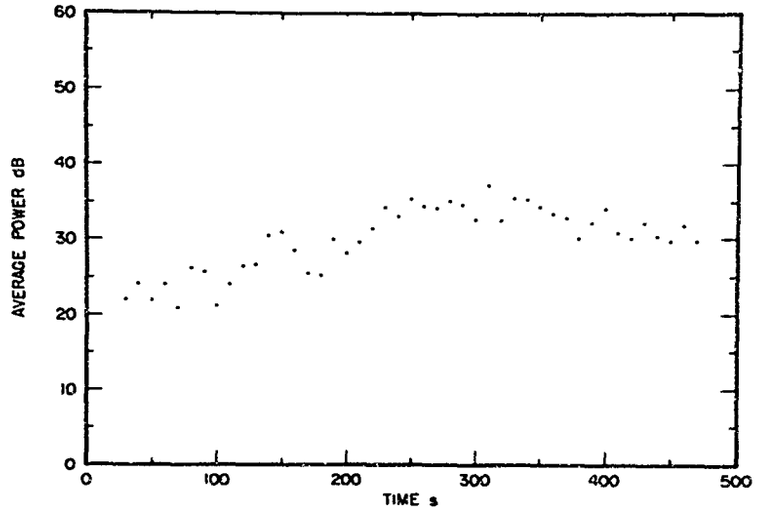


HOMER FREQUENCY= 9 MHz

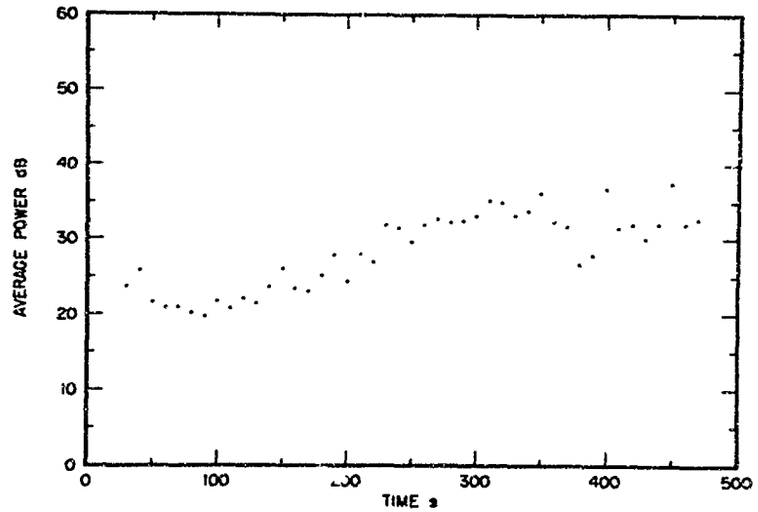


HOMER FREQUENCY= 11 MHz

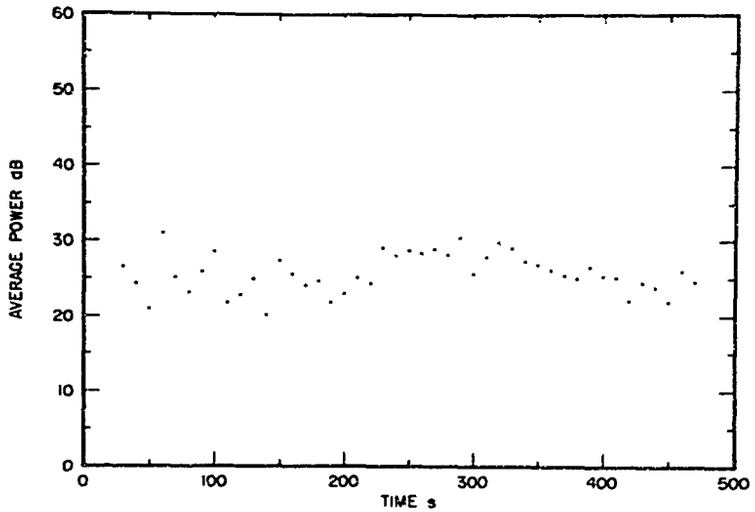


HOMER FREQUENCY= 13 MHz

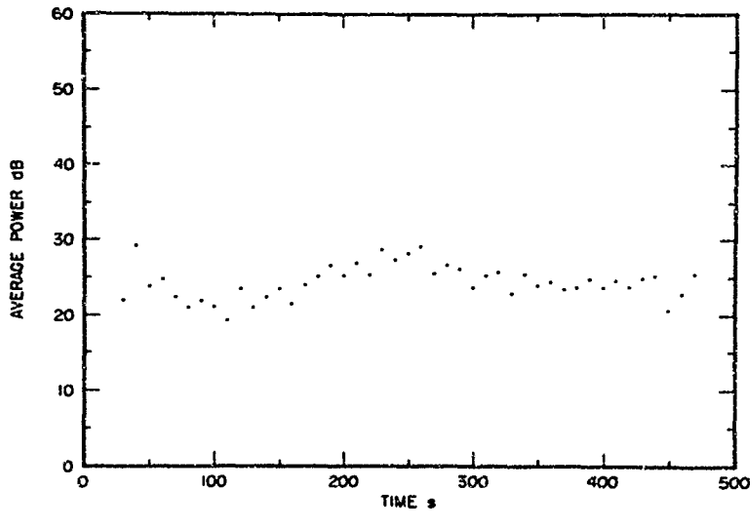


HOMER FREQUENCY= 15 MHz

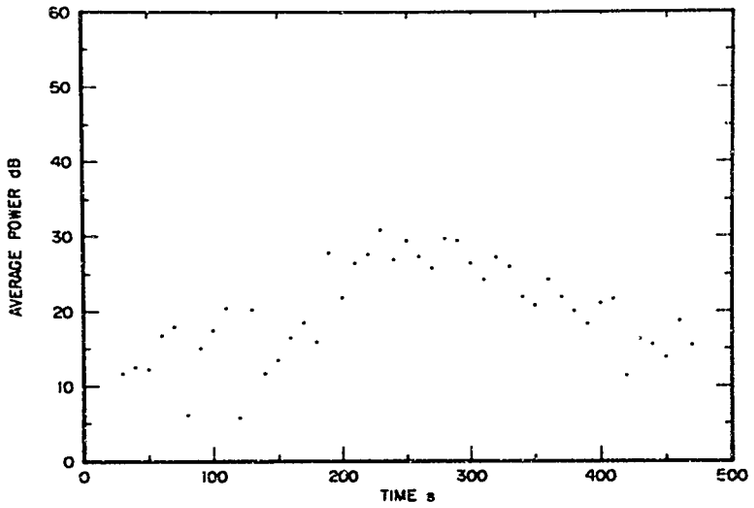


HOMER FREQUENCY= 17 MHz

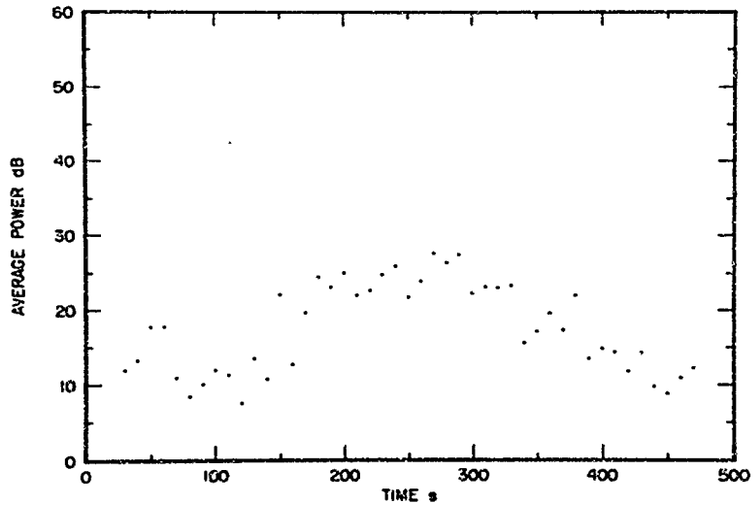


HOMER FREQUENCY= 19 MHz

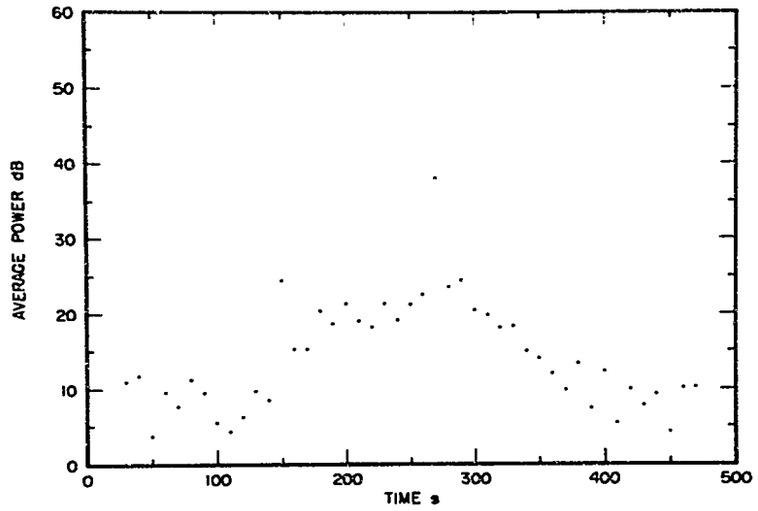


HOMER FREQUENCY= 21 MHz

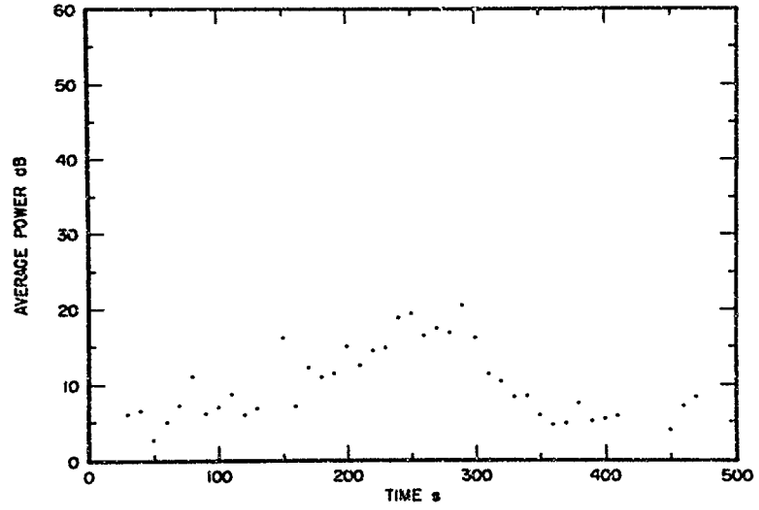


HOMER FREQUENCY= 23 MHz

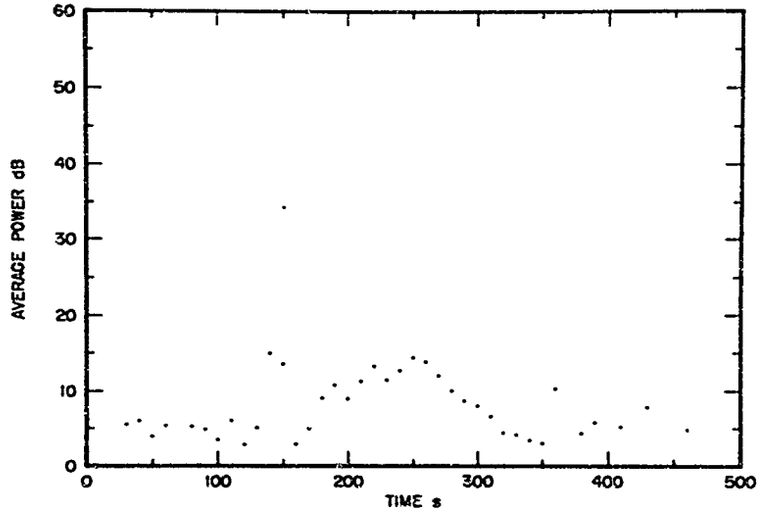


HOMER FREQUENCY= 25 MHz

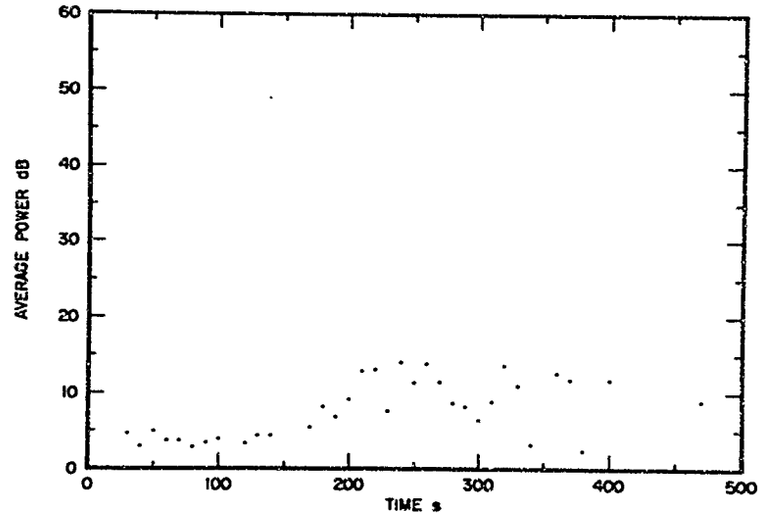


HOMER FREQUENCY= 27 MHz

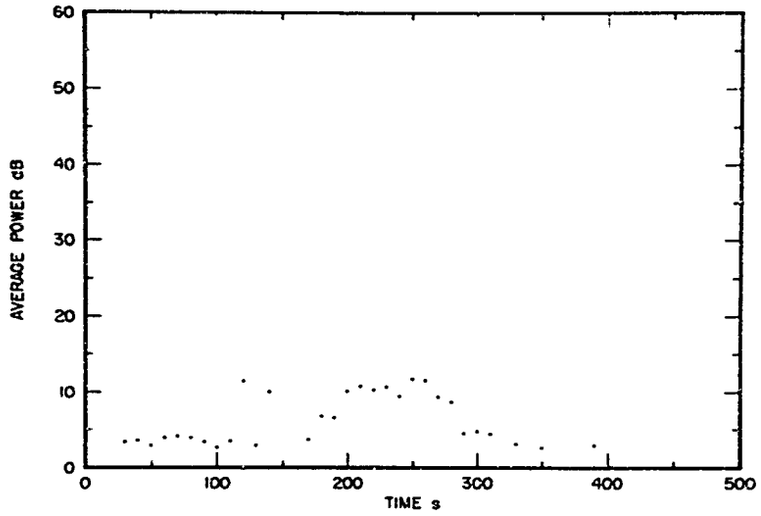


HOMER FREQUENCY= 29 MHz

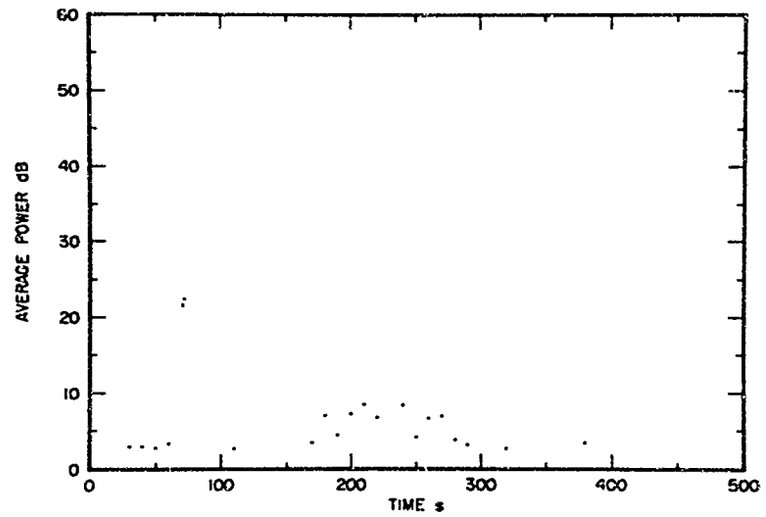


HOMER FREQUENCY= 31 MHz

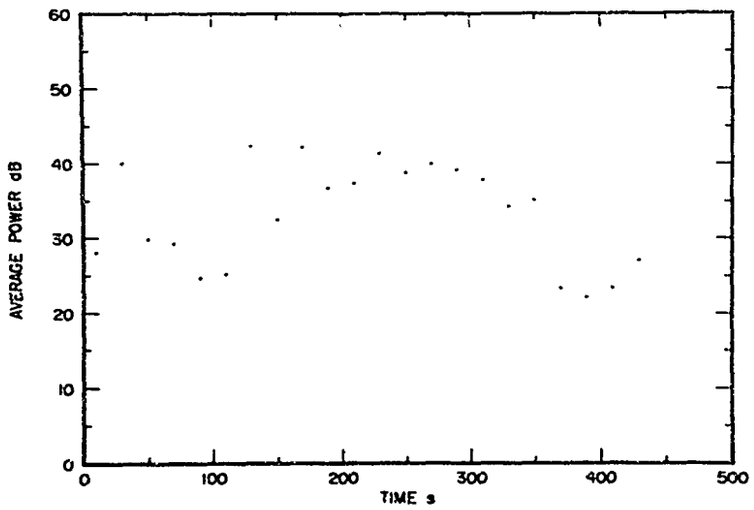


KODIAK FREQUENCY= 17 MHz

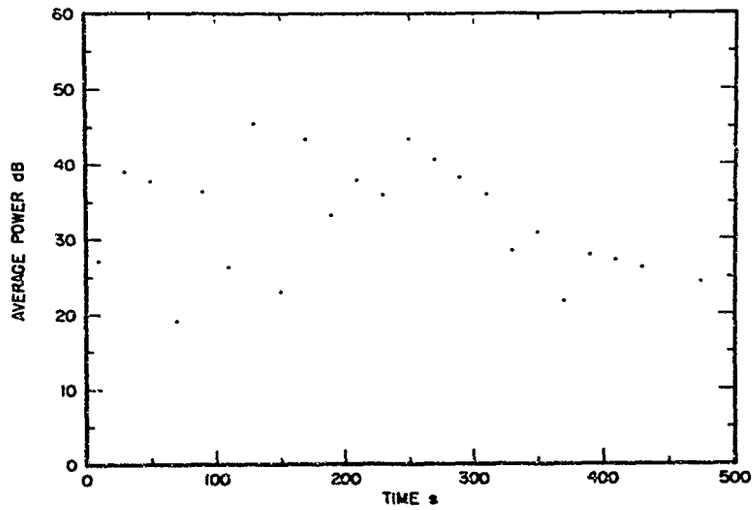


KODIAK FREQUENCY= 19 MHz

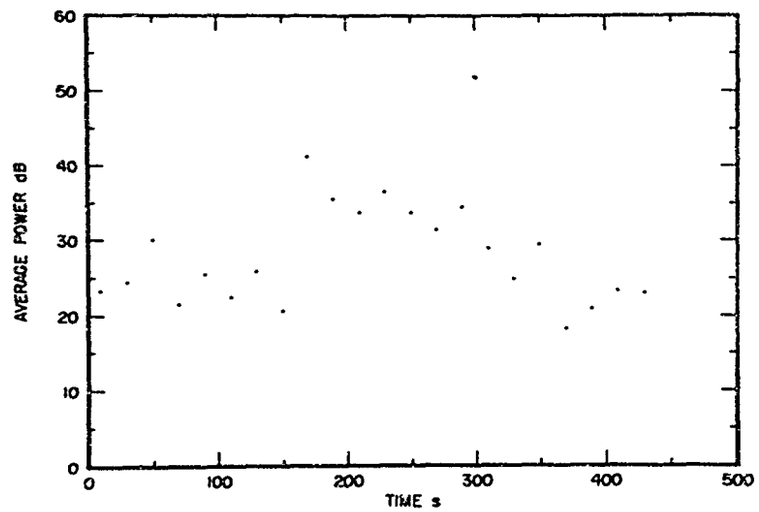


KODIAK FREQUENCY= 21 MHz

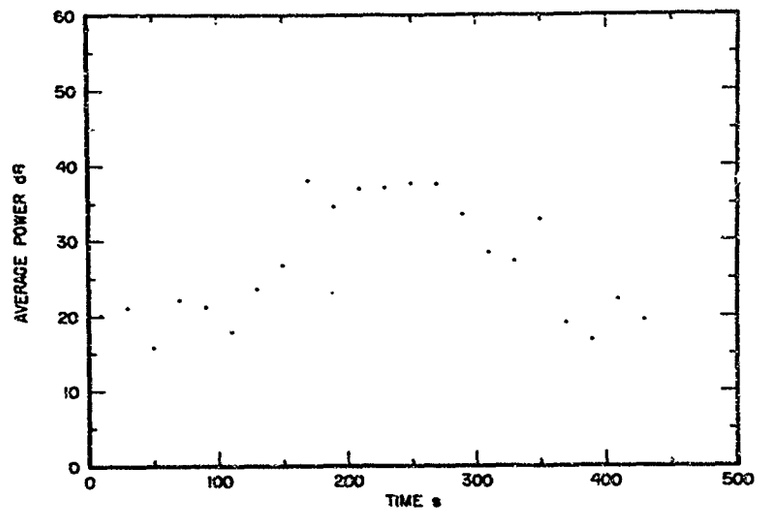


KODIAK FREQUENCY= 23 MHz

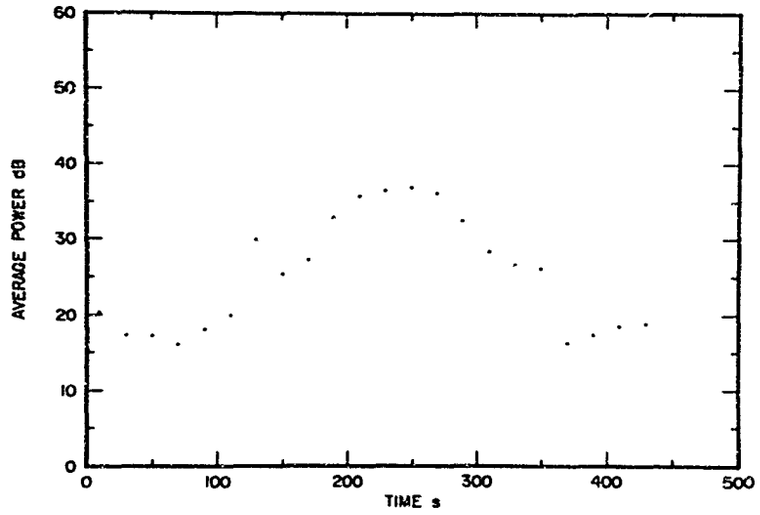


KODIAK FREQUENCY= 25 MHz

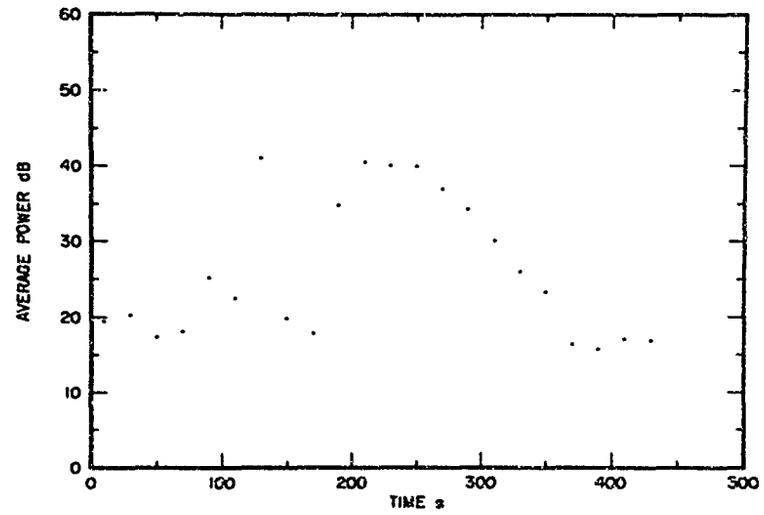


KODIAK FREQUENCY= 27 MHz

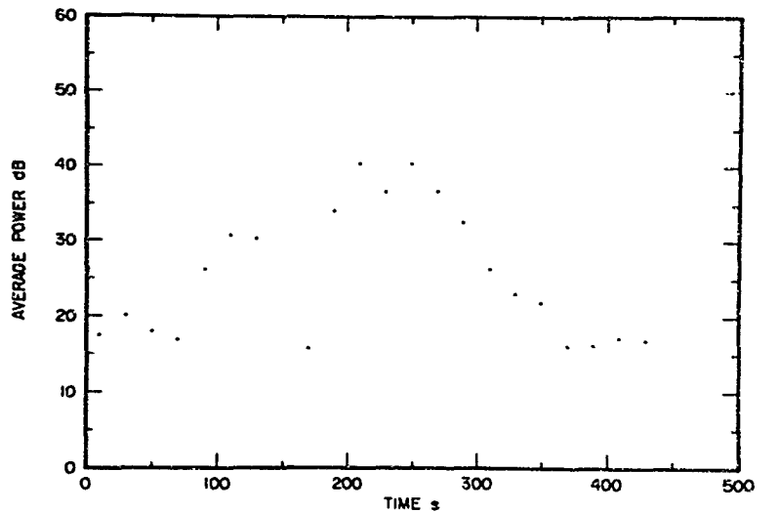


KODIAK FREQUENCY= 29 MHz

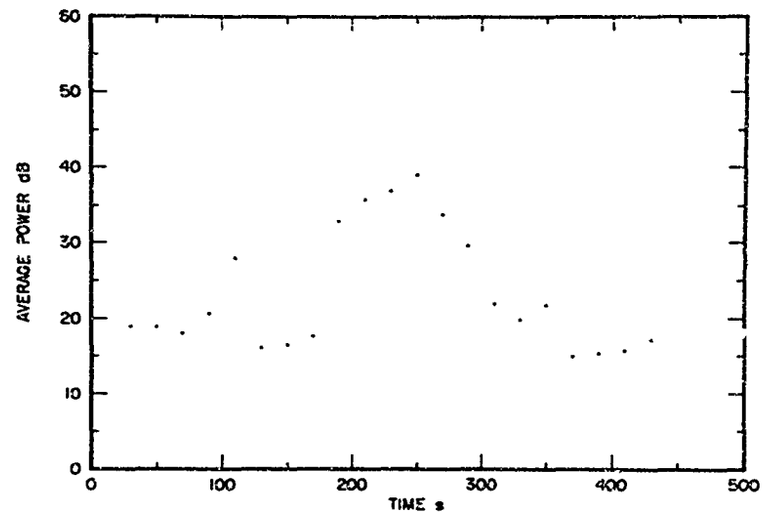


KODIAK FREQUENCY= 31 MHz

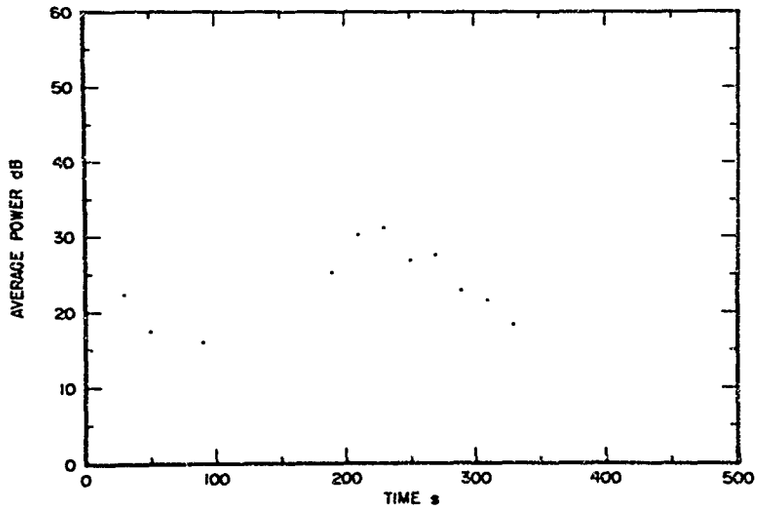


KODIAK FREQUENCY= 33 MHz

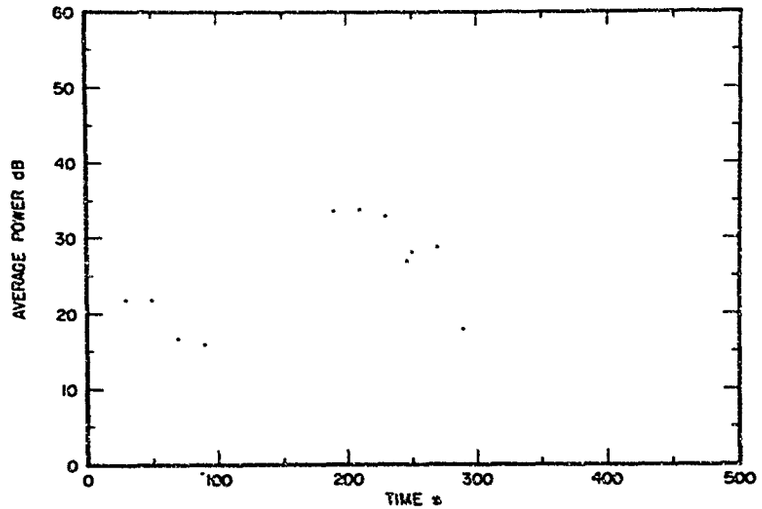


KODIAK FREQUENCY= 35 MHz

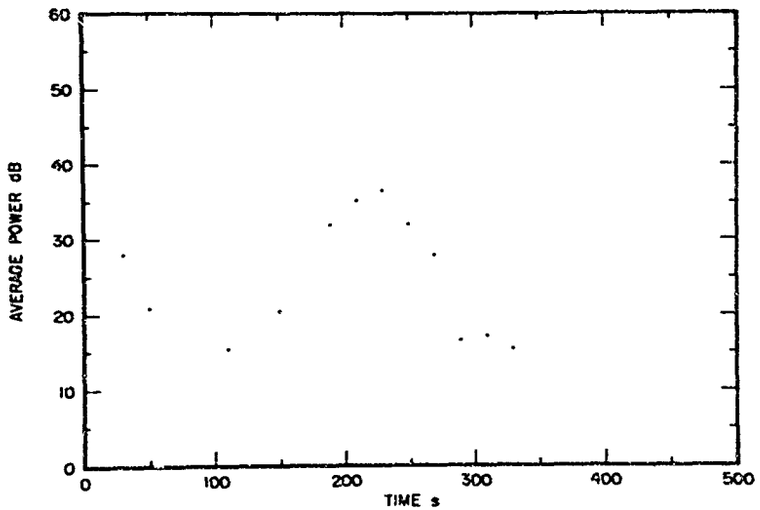


KODIAK FREQUENCY= 37 MHz

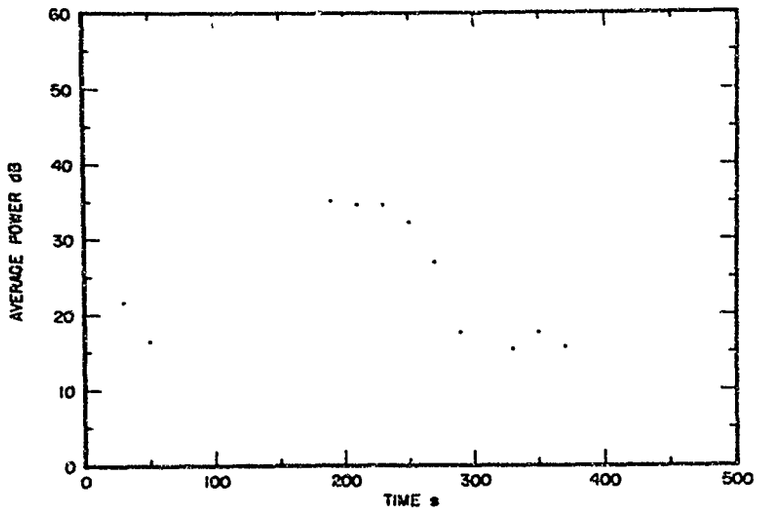


KODIAK FREQUENCY= 39 MHz

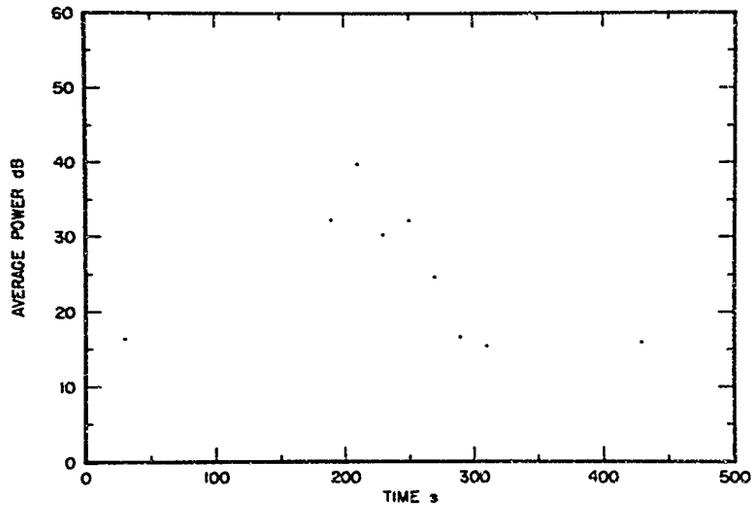


KODIAK FREQUENCY= 41 MHz

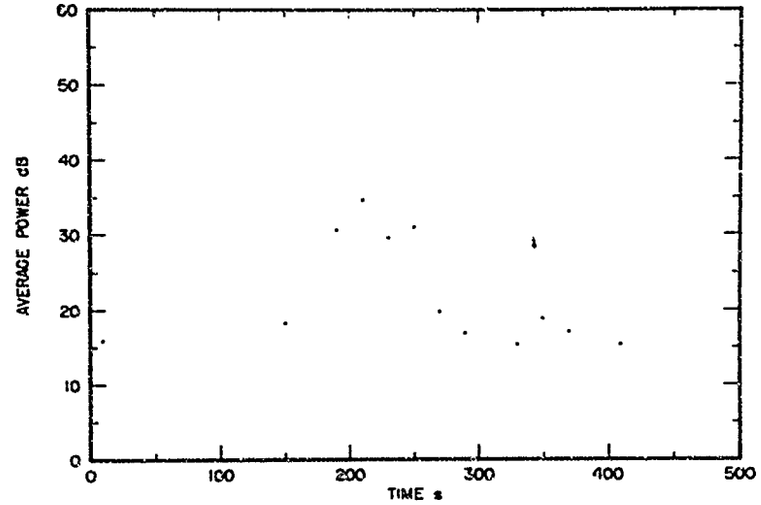


KODIAK FREQUENCY= 43 MHz

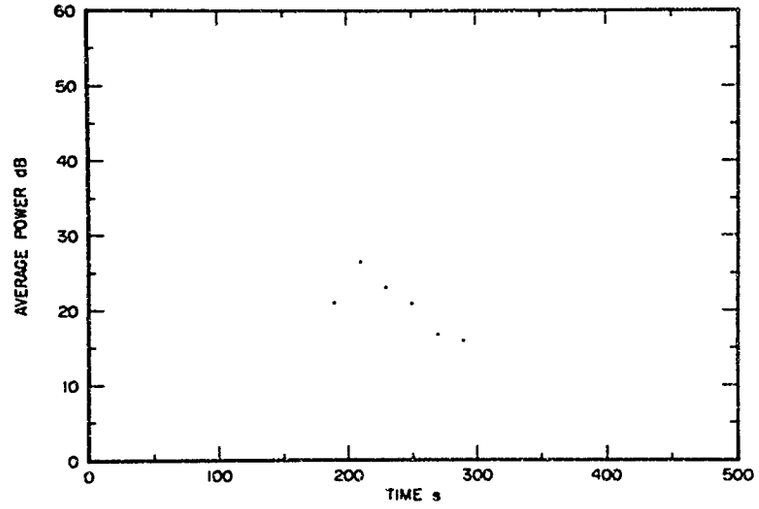


KODIAK FREQUENCY= 45 MHz

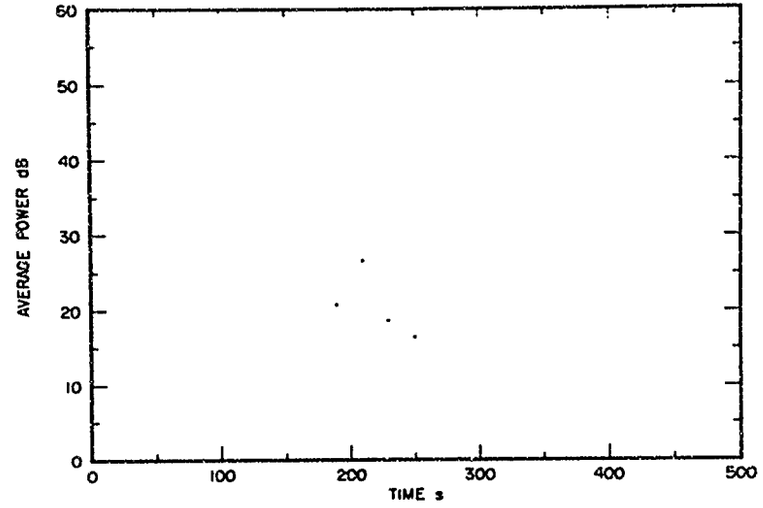


KODIAK FREQUENCY= 47 MHz

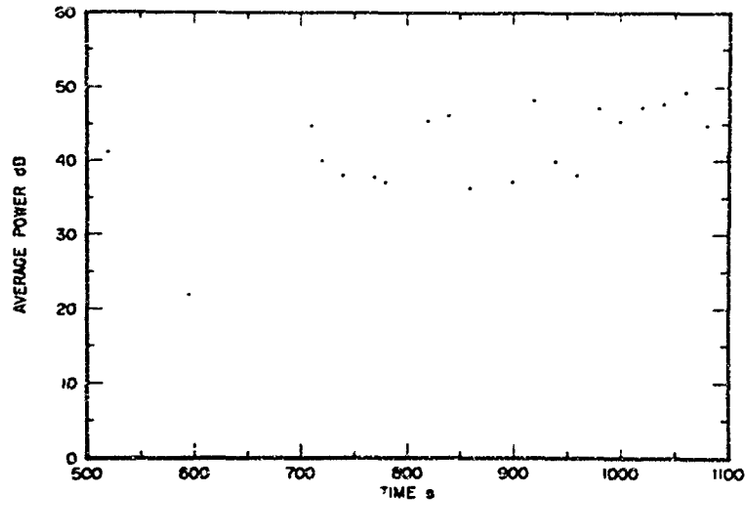


KODIAK GUM FREQUENCY= 17 MHz

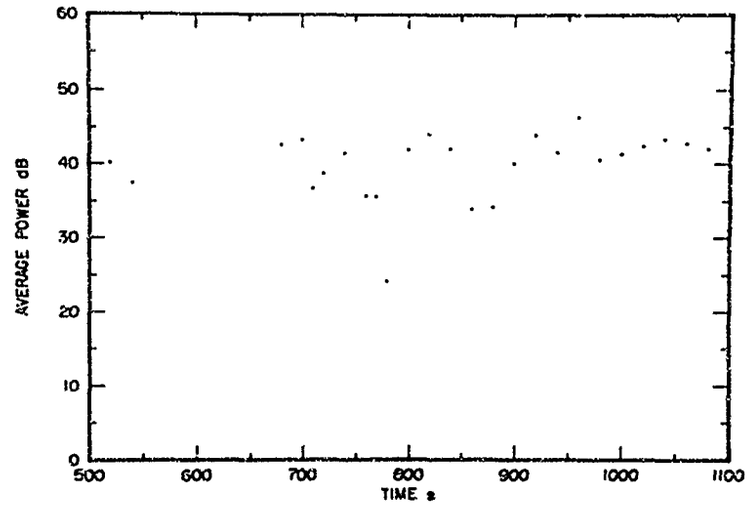


KODIAK GUM FREQUENCY= 19 MHz

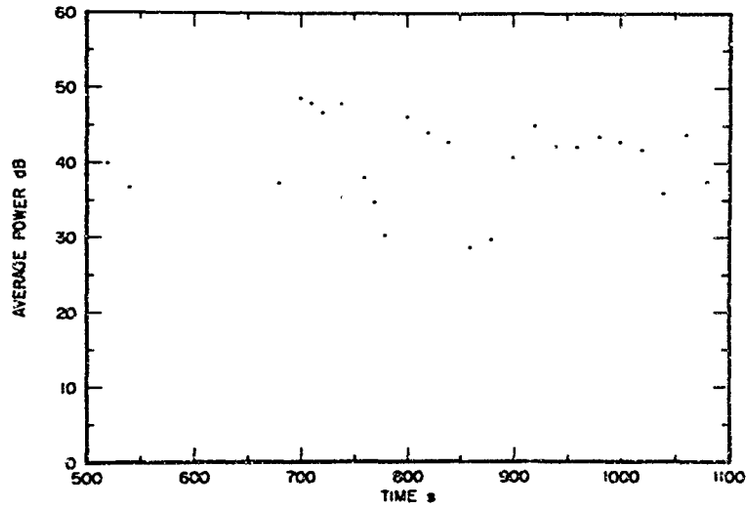


KODIAK GUM FREQUENCY= 21 MHz

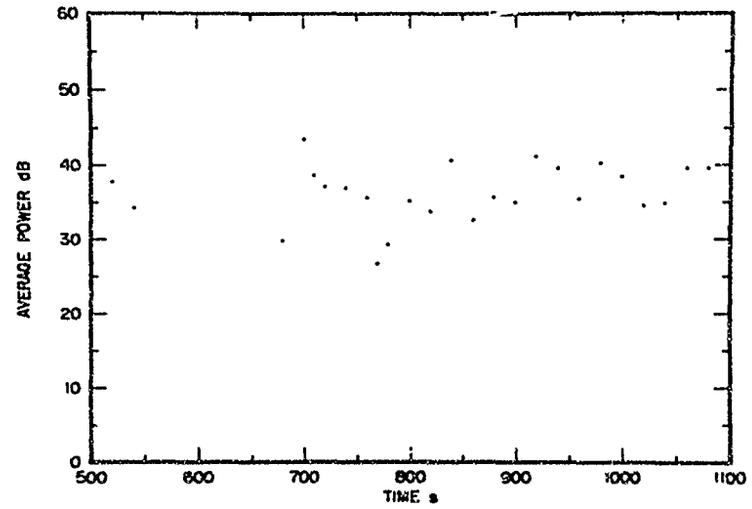


KODIAK GUM FREQUENCY= 23 MHz

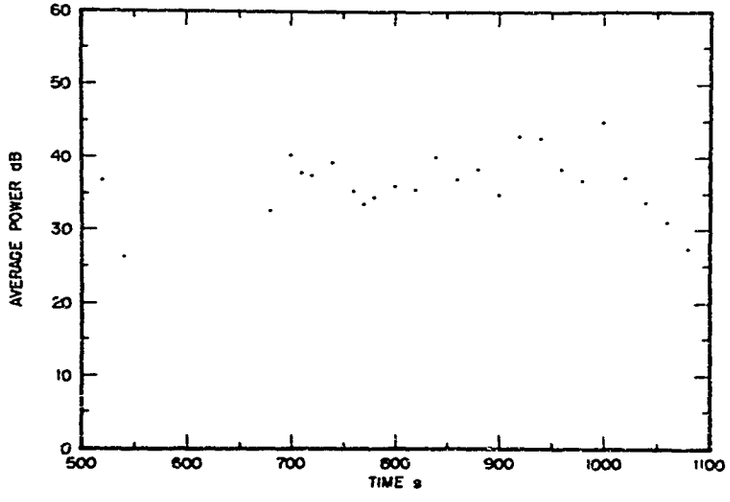


KODIAK GUM FREQUENCY= 25 MHz

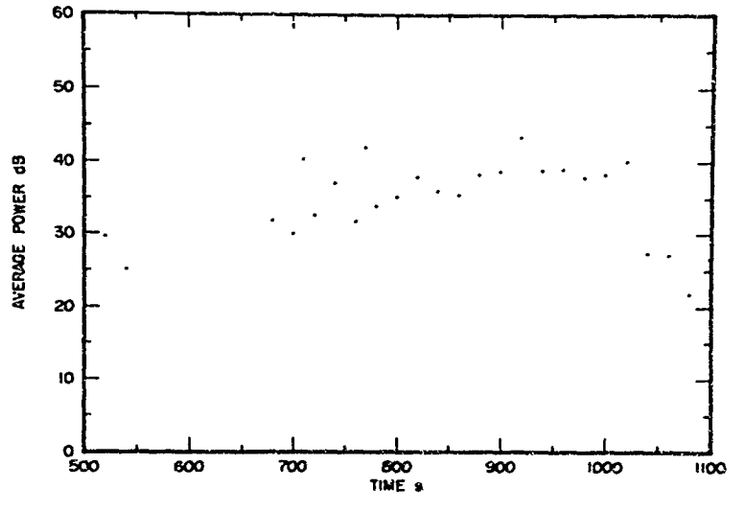


KODIAK GUM FREQUENCY= 27 MHz

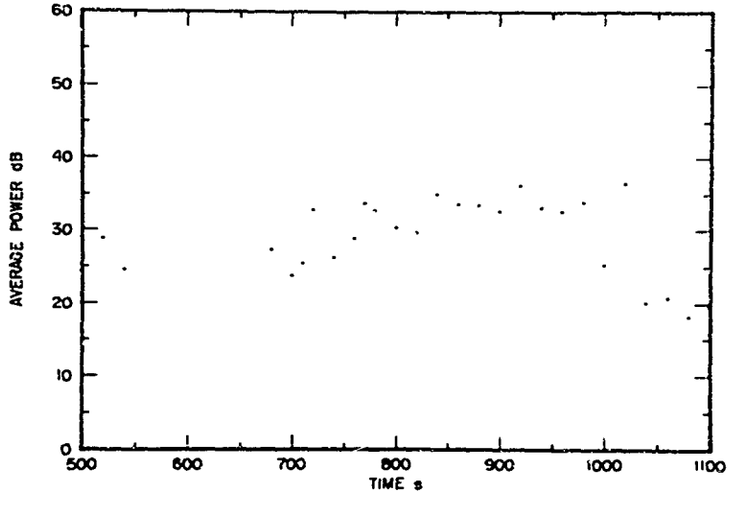


KODIAK GUM FREQUENCY= 29 MHz

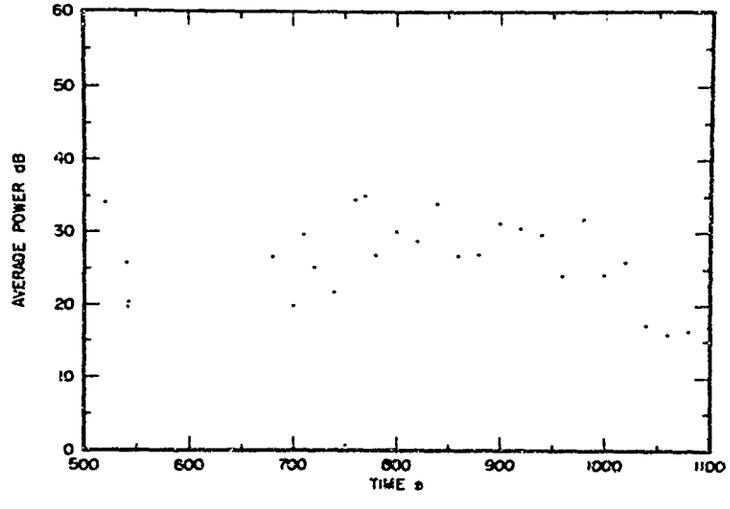


KODIAK GUM FREQUENCY= 31 MHz

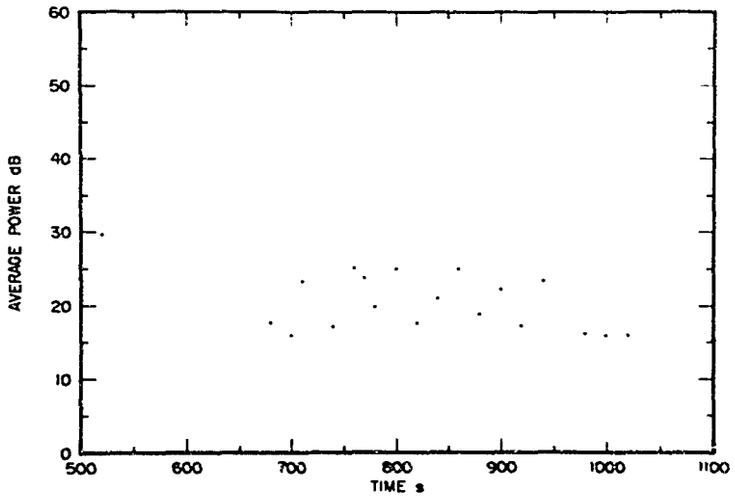


KODIAK GUM FREQUENCY= 33 MHz

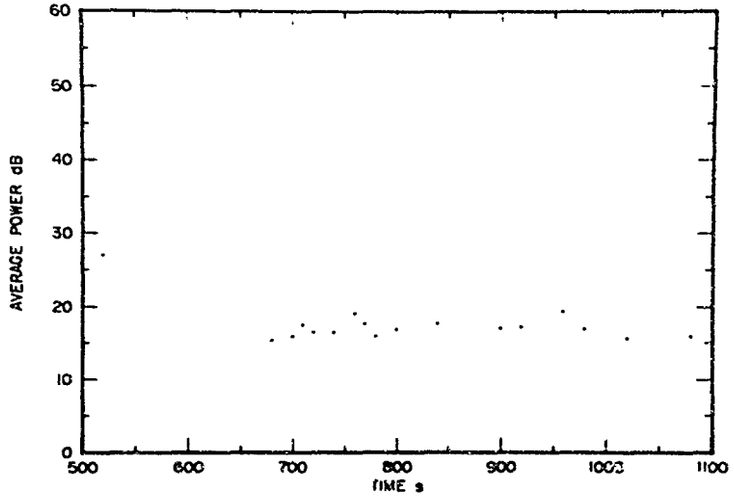


KODIAK GUM FREQUENCY= 35 MHz

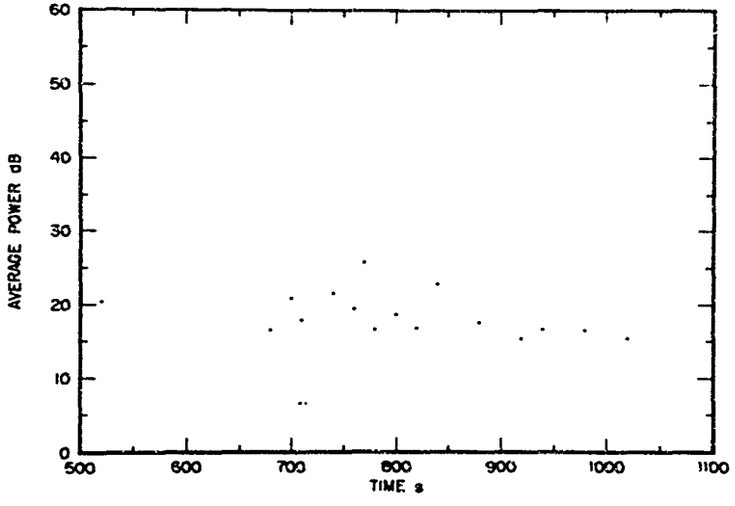


KODIAK GUM FREQUENCY= 37 MHz

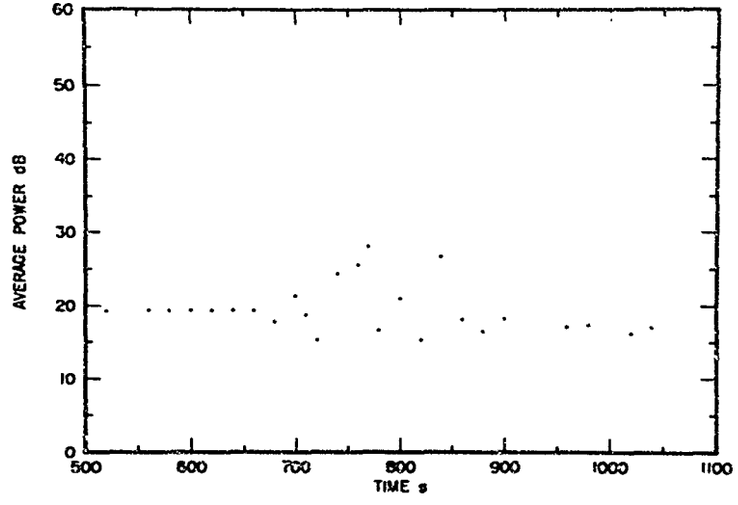


KODIAK GUM FREQUENCY= 39 MHz

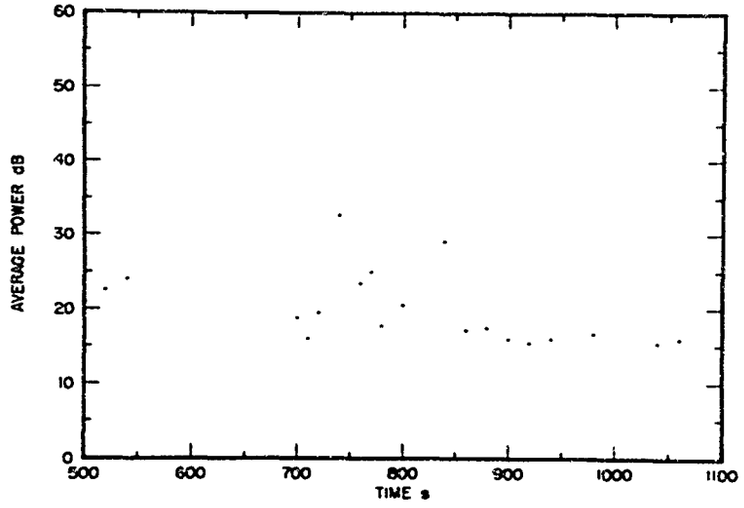


KODIAK GUM FREQUENCY= 41 MHz

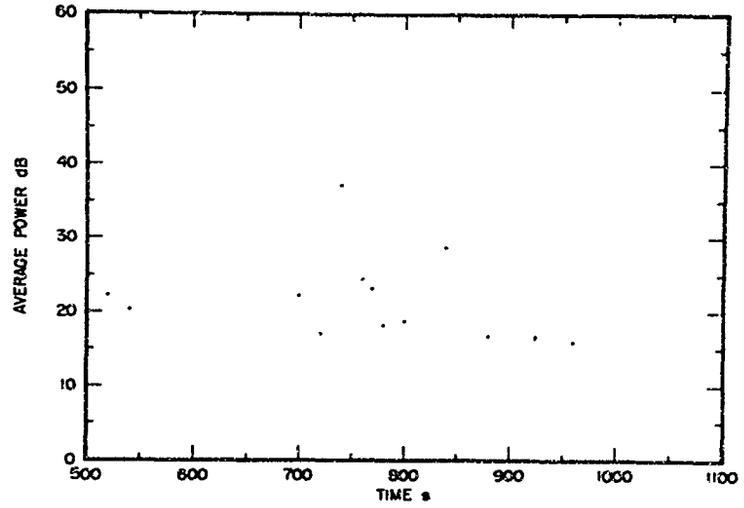


KODIAK GUM FREQUENCY= 43 MHz

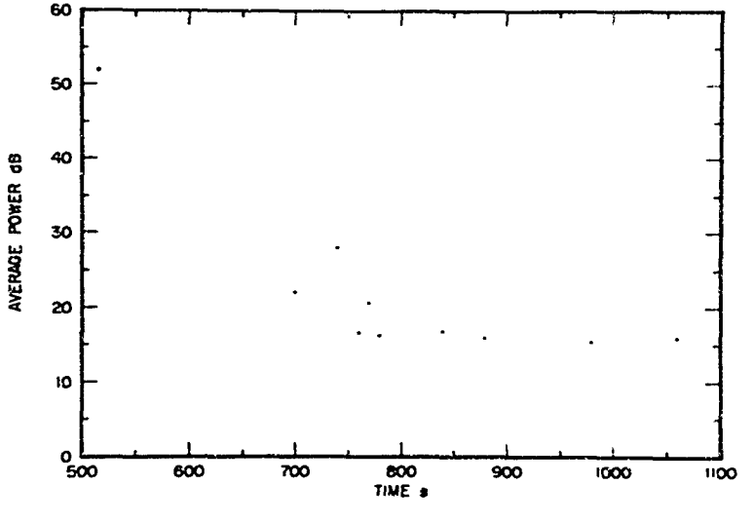


KODIAK GUM FREQUENCY= 45 MHz

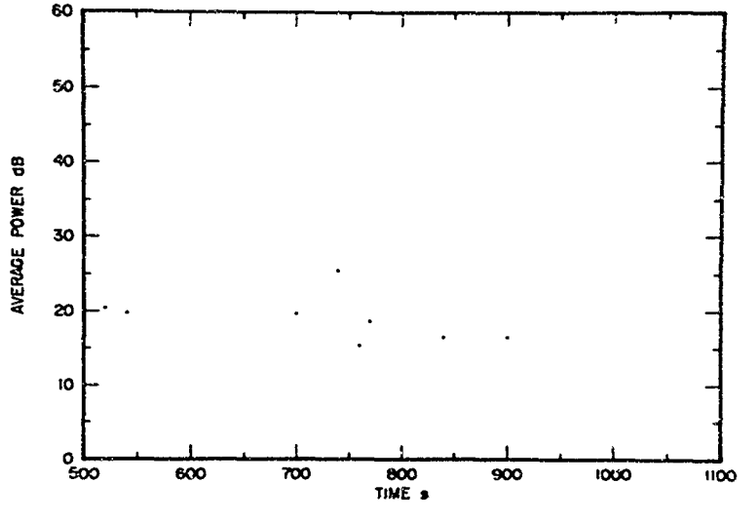


KODIAK GUM FREQUENCY= 47 MHz

UNCLASSIFIED
Security Classification

## DOCUMENT CONTROL DATA - R & D

(Security classification of title, body of abstract and indexing annotation must be entered when the overall report is classified)

| | |
|---|---|
| 1. ORIGINATING ACTIVITY (Corporate author)<br>Stanford Research Institute<br>Menlo Park, California 94025 | 2a. REPORT SECURITY CLASSIFICATION<br>UNCLASSIFIED<br>2b. GROUP<br>N/A |

3. REPORT TITLE

STEP FREQUENCY RADAR STUDY OF SECEDE III BARIUM RELEASES

4. DESCRIPTIVE NOTES (Type of report and inclusive dates)

Final Report Covering the period November 1968 through March 1970

5. AUTHOR(S) (First name, middle initial, last name)

Howard F. Bates

| | | |
|---|---|---|
| 6. REPORT DATE<br>March 1970 | 7a. TOTAL NO. OF PAGES<br>120 | 7b. NO. OF REFS<br>11 |
| 8a. CONTRACT OR GRANT NO.<br>DASA01-69-C-0032-P001<br>b. PROJECT NO.<br>K 43 AAXHX 607<br>c.<br>d. Work Unit: 021 | 9a. ORIGINATOR'S REPORT NUMBER(S)<br>Final Report<br>SRI Project 7784<br>9b. OTHER REPORT NO(S) (Any other numbers that may be assigned this report)<br>DASA 2409 | |

10. DISTRIBUTION STATEMENT

This document has been approved for public release and sale; its distribution is unlimited.

| | |
|---|---|
| 11. SUPPLEMENTARY NOTES | 12. SPONSORING MILITARY ACTIVITY<br>Director<br>Defense Atomic Support Agency<br>Washington, D. C. |

13. ABSTRACT

Step-frequency radars were installed near Kodiak and Homer, Alaska, to view the barium releases made into the lower F region near Fairbanks in March 1969. Echoes were obtained from four of the six releases; good echoes were obtained from two, but quantitative results can only be obtained from one. Backscatter cross sections of $10^4$ km$^2$ were found at early times for two of the releases, whereas photographs indicate cloud sizes were less than $10^2$ km$^2$. The echo amplitudes observed at Homer (line-of-sight 725 km range and 5° off-perpendicular from magnetic field at cloud) were 10 to 15 dB less than those at Kodiak (925 km and 3°). The frequency range covered by the Kodiak echoes was higher than that at Homer. These factors taken together indicate that the echoes were produced by highly aspect-sensitive field-aligned irregularities; the aspect sensitivity is estimated to be about 10 to 20 dB per degree of off-perpendicularity. Strong, persistent echoes observed near 18 MHz at Kodiak and 13 MHz at Homer during the one release for which quantitative data can be computed are interpreted as resulting from exact normality between RF wave and magnetic field; the aspect sensitivity of these echoes was about 20 dB per degree. The backscatter cross section apparently had a maximum near 30 MHz; this is interpreted as showing that the irregularities in the cloud had a dominant transverse size near 5 m. A diffraction argument utilizing the observed aspect sensitivity indicates that the length of the structure before striation was of the order of a kilometer. At the onset of pronounced striations the aspect sensitivity abruptly decreased,

(Continued on attached sheet)

DD FORM 1 NOV 65 1473 (PAGE 1)

S/N 0101-807-6801

UNCLASSIFIED
Security Classification

UNCLASSIFIED

13. Abstract (Continued)

indicating that the length of the irregularities decreased, or, alternatively, the angular spectrum of the irregularity distribution increased in width. With the exception of this change, no correspondence between optical and radio effects could be found, suggesting that the changes observed by the radars were invisible changes within the cloud. All of the results of the various radio experiments suggest that the ion cloud was either (1) an overdense ball of field-aligned irregularities, or (2) a smooth, overdense ball immersed within a field-aligned cloud of weak-scattering irregularities. Both models have drawbacks, but the second appears the most likely at this point. Further experimental work is needed to clarify this problem.

UNCLASSIFIED
Security Classification

| 14 KEY WORDS | LINK A ROLE | LINK A WT | LINK B ROLE | LINK B WT | LINK C ROLE | LINK C WT |
|---|---|---|---|---|---|---|
| Barium Releases | | | | | | |
| F Layer | | | | | | |
| HF Backscatter | | | | | | |
| High Latitude Ionosphere | | | | | | |
| HF Aspect Sensitivity | | | | | | |
| HF Backscatter Cross-section | | | | | | |

DD FORM 1 NOV 65 1473 (BACK)
(PAGE 2)

UNCLASSIFIED
Security Classification